MOLECULAR GENETICS OF GYNECOLOGIC CANCERS

by
Ren-Chin Wu

A dissertation submitted to Johns Hopkins University in conformity with the requirements for the degree of Doctor of Philosophy

Baltimore, Maryland
July 2014

Abstract

The thesis is focused on the molecular genetics of gynecologic cancers, specifically uterine serous carcinoma (USC) and ovarian clear cell carcinoma (OCCC), two relatively uncommon cancer types with aggressive clinical behavior. In the first project, we sequenced 10 exomes of USCs and validated the most frequent somatic mutations in 66 additional USCs. In addition, gene copy number was characterized by single-nucleotide polymorphism (SNP) arrays in 23 USCs. Frequent somatic mutations were identified in *TP53* (81.6%), *PIK3CA* (23.7%), *FBXW7* (19.7%), and *PPP2R1A* (18.4%) in USCs. Concordant *PIK3CA*, *PPP2R1A*, and *TP53* mutation status between USC and the its precursor lesion, serous endometrial intraepithelial carcinoma (SEIC), were recognized in all SEICs examined. DNA copy number analysis revealed frequent genomic amplification of the *CCNE1* locus and deletion of the *FBXW7* locus. Among 23 uterine serous carcinomas that were subjected to SNP array analysis, seven tumors with *FBXW7* mutations did not have *CCNE1* amplification, and 13 (57%) tumors had either a molecular genetic alteration in *FBXW7* or *CCNE1* amplification. Nearly half of these uterine serous carcinomas harbored *PIK3CA* mutation and/or *PIK3CA* amplification. This study implicated genetic aberrations of the p53, cyclin E–FBXW7, and PI3K pathways as major mechanisms in the development of USC. In the second project, I evaluated in 525 gynecologic cancers the prevalence of gain-of-function *TERT* promoter mutations, which have been shown to promote transcriptional activation of *TERT* and likely play a key role in immortalization of some cancer types. With the exception of ovarian clear cell

carcinomas (OCCC), of which 15.9% harbored the mutations, the majority of gynecological malignancies were wild-type. *TERT* promoter mutation does not appear to be an early event during oncogenesis, as it was not detected in the contiguous endometriosis associated with OCCC. OCCC cell lines with *TERT* promoter mutations exhibited higher TERT mRNA expression than those with wild-type sequences. *TERT* promoter mutation tended to be mutually exclusive with loss of ARID1A protein expression and *PIK3CA* mutation in ovarian clear cell carcinomas. These results suggest that aberrations in telomere biology may play an important role in the pathogenesis of OCCC.

Thesis advisors: Dr. Ie-Ming Shih, Dr. Tian-Li Wang, and Dr. Alan K. Meeker

Thesis readers: Dr. Ie-Ming Shih and Dr. Tian-Li Wang

Preface & Acknowledgements

I could not have made a better decision four years ago, when I chose to pursue my thesis research in the Molecular Genetics Laboratory of Female Reproductive Cancer led by Dr. Ie-Ming Shih and Dr. Tian-Li Wang. For a long time, the Shih & Wang laboratory has been tackling gynecologic malignancies by studying their genetic aberrations to identify potential therapeutic targets. I acknowledge Dr. Shih and Dr. Wang for giving me the opportunity to lead two research projects on determining the genetic anomalies of gynecologic cancers, which culminates in this dissertation. I would also like to thank Dr. Alan K. Meeker, who has offered me countless helpful suggestions and advice for my research projects. The guidance they have provided, both theoretical and practical, has been instrumental for this work. Their strong dedication to biomedical research and infectious enthusiasm for everything scientific have greatly influenced my career.

These research projects were highly collaborative and could not have been completed without the kind provision of precious tissue samples from our collaborators all over the world. For this I would like to express my gratitude to Dr. Ayse Ayhan, Dr. Daichi Maeda, Dr. Kyu-Rae Kim, Dr. Blaise A. Clarke, Dr. Patricia Shaw, Dr. Michael Herman Chui, Dr. Barry Rosen, Dr. Kuan-Tin Kuo, Dr. Tsui-Lien Mao, Dr. Douglas A. Levine, and Dr. Robert J. Kurman. I also want to thank Dr. Gang Wu, Dr. Jinghui Zhang, and Dr. Yue Wang, who have provided tremendous help on the bioinformatics analysis of my thesis work.

My dear labmates have made my graduate school career a pleasurable experience. They have not only taught me so much about science and life but also provided me companionship in this long journey. I am grateful for Dr. Elisabetta Kuhn's collaboration, without which I could not have finished the project. I am also deeply indebted to previous and current postdoctoral fellows and graduate students, Dr. Bin Guan, Dr. Alex Stoeck, Dr. Kai Lee Yap, Dr. Jin Jung, Dr. Yohan Suryo Rahmanto, and Dr. Yu Yu, for always being so willing to guide me when I needed help and advice. A big thank goes to the laboratory manager, Ms. Asli Bahadirli-Talbott, who makes the life in the laboratory much easier for me.

I would also like to acknowledge my first-year graduate school advisor Dr. James R. Eshleman, who has been helping me in the development of my career and given me so much support, and also my rotation advisors Dr. Saraswati Sukumar and Dr. Alan K. Meeker, who have played an important role in my training. I am grateful for the Pathobiology Graduate Program support during my graduate school career, especially Dr. Noel Rose, our caring program director and Ms. Wihelmena Braswell, Nancy Nath, and Tracie McElroy, our program coordinators, whom I can't thank enough for taking care of us and making sure everything was in order.

My graduate school career at Hopkins would not have begun if not for the generous support from Chang Gung Memorial Hospital. I want to thank them deeply for investing in the education of junior physician scientists. My gratitude also goes to Dr. Ralph Hruban, Dr. Edward Gabrielson, and Dr. Tzyy-Choou Wu, for their kindness and

help in enabling me to begin my study at Hopkins.

Much gratitude goes to my friends at Hopkins for their relentless support during this journey. I especially thank my classmate, Wei Wen Teo, from whom I learned a great deal ranging from experimental techniques to scientific thinking during our countless lunch meetings. Last but not least, I would like to thank my family: my wife, Portia, for her love, care, and encouragement, my son, James, for his cuteness that delights me every day, and my parents and sisters, who are always on my side.

Thank you.

Table of Contents

Abstract ii

Preface & Acknowledgements iv

Table of Contents vii

List of Tables x

List of Figures xi

1 Introduction 1

2 Integrative Genomic Analysis of Uterine Serous Carcinoma 5

2.1 Methods 7

2.1.1 Tissue Specimens and Genomic DNA Preparation 7

2.1.2 Whole-Exome Sequencing of the Discovery Set 8

2.1.3 Detection of Somatic Sequence Mutations 9

2.1.4 Analysis of Background Mutation Frequency 10

2.1.5 Sanger Sequencing for Validation of Putative Mutations 11

2.1.6 Single-Nucleotide Polymorphism Array and DNA Copy Number Analysis 12

2.1.7 Immunohistochemistry 14

2.1.8 Chromosomal Instability Index Analysis 14

2.1.9 Statistical Analysis 15

2.2 Results 17

2.2.1 Paired-End Whole-Exome Sequencing of Uterine Serous Carcinoma 17

2.2.2 Prevalence Screening of Mutations in Selected Genes 24

2.2.3 DNA Copy Number Alterations in Uterine Serous Carcinoma and Other Gynecological Cancers 27

2.2.4 DNA Copy Number Alterations in Uterine Serous Carcinoma 30

2.2.5 FBXW7, PIK3CA, PPP2R1A, and TP53 Mutations in Serous Endometrial Intraepithelial Carcinoma 36

2.3 Discussion 41

2.4 Acknowledgements 46

3 *TERT* Promoter Mutation in Gynecological Malignancies 47

3.1 Methods 49

3.1.1 Screening *TERT* promoter mutations in gynecological 49

3.1.2 *TERT* promoter mutation in precursor lesions of ovarian clear cell carcinoma 51

3.1.3 *TERT* promoter mutation and mRNA expression in ovarian clear cell carcinoma 51

3.1.4 Telomere length evaluation in ovarian clear cell carcinoma 52

3.1.5 Immunohistochemical staining for ARID1A in ovarian 52

3.1.6 Sequencing of *PIK3CA* in ovarian clear cell carcinoma 53

3.1.7 Statistical analysis 54

3.2 Results 56

3.2.1 *TERT* promoter mutations in gynecological malignancies 56

3.2.2 *TERT* promoter mutations are not present in endometriotic cyst epithelium adjacent to ovarian clear cell carcinoma 59

3.2.3 *TERT* promoter mutation is associated with elevated mRNA expression in ovarian clear cell carcinoma cell lines 60

3.2.4 Ovarian clear cell carcinomas with *TERT* promoter mutation tend to have longer telomere length..... 61

3.2.5 *TERT* promoter mutation is inversely associated with loss of ARID1A protein expression in ovarian clear cell carcinomas..... 62

3.2.6 *TERT* promoter mutation and *PIK3CA* mutation tend to be mutually exclusive in ovarian clear cell carcinoma..... 63

3.2.7 *TERT* promoter mutation has no impact on prognosis in ovarian clear cell carcinoma 65

3.3 Discussion 67

3.4 Acknowledgements 72

4 Conclusions 73

Appendix 1 76

Appendix 2 87

Appendix 3 90

Bibliography 102

Curriculum Vitae 110

List of Tables

Table 2-1. Mapping statistics and the coverage of whole-exome sequencing of 10 uterine serous carcinomas 18

Table 2-2. Detailed mutation profiles in the discovery set of uterine serous carcinomas ..20

Table 2-3. Detailed Recurrently mutated genes in 10 uterine serous carcinomas of the discovery set.....23

Table 2-4. The prevalence of most common somatic mutations in uterine serous carcinoma.....25

Table 2-5. Mutation rate comparison of *PIK3CA*, *FBXW7*, and *PPP2R1A* between uterine serous carcinoma and ovarian high-grade serous carcinoma 26

Table 2-6. Chromosomal instability index of gynecologic cancers 29

Table 3-1. Prevalence of *TERT* promoter mutation in gynecologic malignancies 57

Table 3-2. Correlation between *TERT* promoter mutation and ARID1A immunoreactivity in ovarian clear cell carcinomas.....62

Table 3-3. Correlation between *TERT* promoter mutation and *PIK3CA* mutation in ovarian clear cell carcinomas.....63

Table 3-4. Clinicopathological features of ovarian clear cell carcinoma 65

List of Figures

Figure 2-1. The mutation spectrum in 10 USC samples 21

Figure 2-2. Copy number alteration in uterine serous carcinoma and other types of gynecological neoplasia 28

Figure 2-3. Genome-wide chromosome instability index for individual tumors..... 29

Figure 2-4. Overall view of DNA copy number gain and loss in uterine serous carcinoma 31

Figure 2-5: Heat map of DNA copy number ratio along the chromosome 19 32

Figure 2-6. Heat map of the cancer-associated genes in COSMIC database with statistically significant DNA copy number variations (CNVs) from 23 uterine serous carcinomas..... 34

Figure 2-7. Molecular genetic alterations involving the FBXW7–cyclin E and phosphatidylinositol 3-kinase (PI3K) pathways in uterine serous carcinoma 35

Figure 2-8. Mutation profiles of *FBXW7*, *PIK3CA*, *PPP2R1A*, and *TP53* in nine uterine serous carcinomas (USC) with a concurrent serous endometrial intraepithelial carcinoma (SEIC) component 37

Figure 2-9. A uterine serous carcinoma (USC) with a serous endometrial carcinoma (SEIC) component..... 39

Figure 2-10. Locations of *FBXW7* mutations identified among the 76 uterine serous carcinomas..... 40

Figure 2-11. Schematic presentation of possible mechanisms involving the FBXW7–

cyclin E and PI3K pathways in the development of uterine serous carcinoma 42

Figure 3-1. *TERT* promoter mutations in ovarian clear cell carcinoma..... 58

Figure 3-2. An example of ovarian clear cell carcinoma arising from an endometriotic cyst 59

Figure 3-3. Comparison of TERT mRNA expression between ovarian clear cell carcinoma cell lines with and without mutated *TERT* promoter..... 60

Figure 3-4. Comparison of telomere length between ovarian clear cell carcinomas with and without *TERT* promoter mutation..... 61

Figure 3-5. Mutation status of *TERT* promoter and *PIK3CA,* and immunostaining result of ARID1A in 71 clear cell carcinoma tissues..... 64

Figure 3-6. Kaplan-Meier survival curves of ovarian clear cell carcinoma patients..... 66

For Portia and James

1 Introduction

Gynecologic cancer is complex and heterogeneous, encompassing a huge family of neoplasms with different histopathologic and molecular genetic features. On the one hand, a myriad of cancer subtypes can arise in each of the organs in the female reproductive system (1). For example, the epithelial cancer affecting the ovary comprises of at least four major carcinoma subtypes defined by their histopathologic attributes, including serous carcinoma, endometrioid carcinoma, clear cell carcinoma, and mucinous carcinoma (1,2). At times, it can be a challenging task to classify ovarian carcinomas by histopathology alone, as they occasionally develop with mixed or borderline histologic features. On the other hand, cancers of similar histopathology can affect different parts of female reproductive system. For instance, clear cell carcinoma, high grade serous carcinoma, and endometrioid carcinoma can develop in either uterine endometrium or ovary (1,2). Though showing similar histomorphology, these cancers arising in different parts of female genital organs likely feature distinct molecular genetic aberrations. Hence, careful study of molecular genetics of cancer subtypes will help fine tune the classification of cancers and provide a guidance for risk prognostication and personalized treatment. In this thesis research, we set out to study the genetic alterations of gynecologic cancers, focusing on serous carcinoma arising from the uterine endometrium and ovarian clear cell carcinoma.

Endometrial carcinoma is the most frequently diagnosed gynecological cancer

and the fourth most common malignant neoplasm among women in the United States (3). The incidence rate of endometrial cancer has been steadily increasing after the precipitous decline in menopausal hormone replacement therapy since 2002 (4). It is estimated that in 2014, about 52,630 new cancers in the uterine corpus, most of them endometrial cancers, will be diagnosed in the United States, and 8,590 will die from cancers in the uterine corpus (5). Endometrial carcinoma is traditionally classified as type I and type II, based on the epidemiological and clinical findings (6). Type I endometrial carcinomas are estrogen dependent and develop from endometrial hyperplasia, whereas type II carcinomas are estrogen independent and arise in atrophic endometrium or endometrial polyps. Histologically, type I carcinomas are generally of endometrioid subtype, and type II are composed mainly of serous carcinoma, which resembles ovarian high grade serous carcinoma histologically and clinically. Uterine serous carcinoma tends to occur in older women and often presents at an advanced stage. Although uterine serous carcinomas constitute only 10% of all endometrial cancers, they account for a disproportionately high number of deaths (7). This highly aggressive behavior can be attributable to the unique tendency of uterine serous carcinomas to disseminate to peritoneal cavity even when the primary tumor is small; in addition, uterine serous carcinoma is highly resistant to conventional chemotherapy, and recurrence is inevitable in most patients with advanced-stage disease.

The first half of the thesis is focused on delineating the genetic landscapes of uterine serous carcinoma. In this project, we performed whole exome sequencing on pairs of uterine serous carcinoma and non-tumor tissue and validated the most frequent somatic mutations in additional samples. We also examined the gene copy number aberration in

uterine serous carcinoma with single-nucleotide polymorphism (SNP) arrays. Moreover, we interrogated which gene mutations were early events during the oncogenesis of serous carcinoma by sequencing serous endometrial intraepithelial carcinoma, the pre-invasive lesions of uterine serous carcinoma. This study identified genetic aberrations of the p53, cyclin E–FBXW7, and PI3K pathways as major mechanisms in the development of uterine serous carcinoma. The details and implications of this study will be elaborated in Chapter 2.

The second half of the thesis is devoted to a study on the genetic alteration of telomerase reverse transcriptase (*TERT*) in gynecologic malignancies. Telomeres protect the ends of eukaryotic chromosomes from inappropriate triggering of DNA repair machinery that may cause chromosome end to end fusion (8). Telomere dysfunction, either through shortening of telomeric DNA or loss of function of telomere-capping proteins, results in a DNA damage response that activates p53 tumor suppressor gene, which induces replicative senescence or apoptosis. If p53 function is lost, these responses to telomere dysfunction are mitigated and chromosomal fusion ensues (9). The fused chromosomes are di-centric and may be broken during mitosis (10). These broken ends serve as catalysts for further chromosome structural aberrations if telomere function is not restored (11). To maintain unlimited replication potential, cancer cells evolve mechanisms to maintain telomere length (11). Most cancers, especially carcinomas, maintain their telomere length by increasing the activity of telomerase reverse transcriptase, the catalytic unit of the telomerase that extend the telomeric nucleotide repeats to the end of chromosomes (12). This is achieved through a variety of mechanisms, including amplification of the *TERT* gene (13), expression of transcriptional

activators of TERT (14) and CpG methylation at the *TERT* promoter (15).

Recently, somatic mutations at the *TERT* promoter in human cancer have been reported in several cancer subtypes , including malignant melanoma, glioma, urinary bladder carcinoma, tongue squamous cell carcinoma and hepatocellular carcinoma (16-20). Such mutations were thought to promote the transcription of TERT (16,17). The prevalence and clinical significance of *TERT* promoter mutations in gynecological malignancies remains largely unclear because noncoding regions, including promoter sequences, were not routinely included in large-scale genomic analyses. In this study, we performed mutational analysis in a total of 525 gynecological malignancies, and correlated *TERT* promoter mutations with clinicopathological features. We found that *TERT* promoter mutation is most prevalent in ovarian clear cell carcinoma. *TERT* promoter mutation is associated with higher TERT mRNA expression in cell lines derived from ovarian clear cell carcinomas. Furthermore, *TERT* promoter mutation is mutually exclusive with ARID1A loss and PIK3CA mutation, the most common genetic aberrations in ovarian clear cell carcinoma. The results of this study will be detailed in Chapter 3.

2 Integrative Genomic Analysis of Uterine Serous Carcinoma

Endometrial carcinoma is the most frequently diagnosed gynecological cancer and the fourth most common malignant neoplasm among women in the United States (3). Traditionally, endometrial carcinoma is classified into two main groups: type I and type II (6). Type I endometrial carcinoma is composed of low-grade endometrioid carcinoma, and type II is composed mainly of uterine serous carcinoma. Uterine serous carcinoma occurs in older women and often presents at an advanced stage. Low-grade endometrioid carcinomas are estrogen dependent and develop from endometrial hyperplasia, whereas uterine serous carcinomas are estrogen independent and arise in atrophic endometrium and endometrial polyps from pre-invasive lesions known as serous endometrial intraepithelial carcinoma. Although uterine serous carcinomas constitute only 10% of all endometrial cancers, they account for a disproportionately high number of deaths (7). This highly aggressive behavior is related mainly to the unique tendency of uterine serous carcinomas to metastasize even when the primary tumor is small; as a result, most patients with uterine serous carcinoma have metastatic disease, which is not curable, at the time of diagnosis. Moreover, uterine serous carcinoma is highly resistant to conventional chemotherapy, and recurrence is inevitable in most patients with advanced-stage disease. Until the molecular pathogenesis of uterine serous carcinoma is better

understood, therapeutic interventions to improve the clinical outcomes of these patients remain empirical.

Previous molecular genetic studies of endometrial carcinoma have focused on low-grade endometrioid carcinoma (21,22). More recently, the genome-wide molecular changes in endometrioid carcinomas, especially those of low grade, have been revealed through the efforts of The Cancer Genome Atlas. By contrast, the molecular genetic changes that account for the malignant behavior of uterine serous carcinoma are largely unknown. Thus, the purpose of this study is to elucidate the molecular genetic characteristics of uterine serous carcinoma by cataloguing the genetic alterations detected by whole-exome sequencing and gene copy number analysis, with emphasis on identifying the aberrant molecular pathways that may be targetable for therapeutic intervention.

2.1 Methods

2.1.1 Tissue Specimens and Genomic DNA Preparation

A total of 76 uterine serous carcinomas were studied in this report: six fresh tumors from which we affinity purified tumor cells (designated by the suffix "TS" or "S") and four frozen tumors (designated by the suffix "T") were used for discovery, and 66 tumors including 34 frozen tumors and 32 paraffin-embedded tumors were used for validation. Normal tissues were designated with the suffix "N." The diagnosis of uterine serous carcinoma was confirmed in all tumors according to previously described diagnostic criteria (1,2) by three gynecological pathologists based on review of the hematoxylin and eosin–stained slides. The tumor cells from the six of the 10 specimens in the discovery set were isolated by digestion with collagenase I (Roche, Indianapolis, IN), followed by epithelial cell enrichment using Dynabeads coated with EPCAM antibodies (Invitrogen Inc., Carlsbad, CA). We performed immunocytochemistry using an anti-cytokeratin antibody (prediluted, CAM5.2; Becton Dickinson, Franklin Lakes, NJ) to ensure that more than 90% of cells in the purified samples were epithelial cells. Affinity purification of tumor cells and immunocytochemistry were performed as previously described (23,24). Genomic DNA was extracted from both tumor and normal cells with the use of a DNeasy Blood and tissue kit (Qiagen, Inc., Valencia, CA) according to the manufacturer's protocol.

The validation set comprising 66 uterine serous carcinomas was obtained from the Johns Hopkins Hospital (Baltimore, MD), Memorial Sloan-Kettering Cancer Center

(New york, NY), and University of Toronto Health System (Toronto, NN, Canada). Among tumors from discovery and validation sets, nine contained serous intraepithelial carcinoma, a preinvasive (in situ) uterine serous carcinoma component, which was isolated by laser-capture microdissection. Genomic DNA was isolated from all validation set samples as described above and was subjected to Sanger sequencing analysis. Patient consent information was not available because we used anonymous tissue materials that lacked patient's identification. The use of de-identified tissue material was approved by the Institutional Review Boards of Johns Hopkins Hospital, Memorial Sloan-Kettering Cancer Center, University of Toronto Health System, and the National Taiwan University Hospital.

2.1.2 Whole-Exome Sequencing of the Discovery Set

Exome DNA capture was performed with the use of a TruSeq exome enrichment Kit (Illumina, San Diego, CA), and paired-end libraries were constructed with the use of a TrueSeq DNA Sample Prep Kit (Illumina) as previously described (23). Paired-end sequencing (100-bp reads × 2) was performed with the use of a HiSeq Analyzer (Illumina) provided by Illumina's fast track genetic analysis service. Whole-exome sequencing was also performed on DNA isolated from the matched normal tissues (peripheral mononucleated blood cells or myometrium) from each of the 10 patients who had tumor tissue in the discovery set.

All Illumina paired-end reads from both tumor and matched normal DNA were

aligned to the human reference sequence known as the National Center for Biotechnology Information (NCBI) Build 36 (ftp://ftp.ncbi.nih.gov/genomes/h_sapiens/ArChIVe/ BuILD.36.3/) using the Burrows–Wheeler Aligner (version 0.5.5) (25), and reads were removed using the Picard package 1.29 (http:// picard.sourceforge.net). The total number of sequencing reads and mapping statistics were assessed by using the flagstat function of Samtools (version 0.1.7) (25).

The effective coverage of the whole exome was obtained by summarizing the coverage of aligned bases using the Coverage module of Bambino. We only included sequencing reads with a quality score of 15 or higher so that the expected error rate was less than 5% at each position of the reference human exome (26). We considered a base as covered if the effective coverage was at least 10-fold. We also excluded all ambiguous bases and sequencing gaps in the human reference sequence from our coverage analysis. The exome annotation was based on NCBI RefSeq (27).

2.1.3 Detection of Somatic Sequence Mutations

Putative sequence mutations, including single-nucleotide variations, insertions, or deletions, were initially detected by using the variation detection module of Bambino (26). Specifically, the analysis was run using three different parameters as previously described (28,29): a) a high-quality threshold (minimum quality score set to 20) for pooled tumor and matching normal tissue BAM files; b) a low-quality threshold (minimum quality score set to 10) for pooled tumor and matching normal tissue BAM

files; and c) a high-quality threshold (minimum quality score set to 20) for normal tissue–only analysis (see definition of minimum quality score at https://cgwb.nci.nih.gov/goldenPath/bamview/ documentation/index.html). The pooled tumor–normal tissue analysis reduces the possibility of misclassifying germline variations with poor coverage in matching normal tissue samples as somatic mutations. Variants identified by normal tissue–only analysis were removed for further consideration, whereas those only identified by paired tumor and normal tissue analysis were subjected to an automated review process to remove additional false-positive calls caused by misalignment or mismapping of whole-exome sequencing reads. Specifically, the automated review process firstly used the Smith–Waterman algorithm to realign all reads that harbored the mutant allele, followed by quality and alignment trimming, then a double-strand coverage check for the variant allele, and a final remapping of reads that harbored the minor allele to the reference genome to ensure uniqueness.

Transcripts from NCBI RefSeq (build download may 21, 2009) (27) were used for annotation. Variants were classified as coding synonymous ("silent"), missense, nonsense, intronic, regions within 10bp of a canonical splice site, splice site, or noncoding RNA variants, as well as those that occurred in 3′ and 5′ untranslated regions. The insertions and deletions were further classified as frameshifts or in-frame insertions or deletions.

2.1.4 Analysis of Background Mutation Frequency

Assuming that the silent codon position is selectively neutral, we used the

mutation rate at this position to approximate the background mutation frequency. Specifically, the background mutation frequency (μ) can be calculated by the following equation:

$$\mu = \frac{M}{\beta * Ne}$$

where M is the total number of validated silent somatic mutations in each tumor sample (ie, the nonfunctional background mutations), N_e is the total number of effectively covered coding bases (ie, simultaneously covered by ≥10-fold in both tumor and matching normal tissue) in all RefSeq protein coding genes, and β is the silent-to-nonsilent ratio [estimated to be 0.350 by the TCGA Consortium (30) across the coding regions.

2.1.5 Sanger Sequencing for Validation of Putative Mutations

Putative mutations identified by whole-exome sequencing were validated by conventional Sanger sequencing of both tumor and normal DNA (from peripheral blood mononucleated cells or myometrium) samples in the discovery set. Before Sanger sequencing, genomic DNA containing the putative mutations was amplified by polymerase chain reaction (PCR) with the use of primers that flanked the putative mutations. We also used the Sanger method to sequence DNA isolated from the 66 uterine serous carcinomas and matched normal tissue in the validation set to identify the prevalence of somatic mutations in selected genes. The results of Sanger sequencing were

analyzed using Mutation Surveyor software (version 4.0; SoftGenetics, State College, PA).

2.1.6 Single-Nucleotide Polymorphism Array and DNA Copy Number Analysis

We analyzed 23 uterine serous carcinomas for which there was sufficient material to examine DNA copy number changes by single-nucleotide polymorphism (SNP) arrays. These included 10 samples from the discovery set and 13 frozen tumors from the validation set. SNPs were genotyped using 250K StyI arrays (seven tumors) or SNP Array 6.0 (16 tumors; both arrays from Affymetrix, Santa Clara, CA) at the microarray core facility at the Johns Hopkins University according to manufacturer's instructions. In addition, 13 uterine endometrioid carcinomas from the National Taiwan University Hospital were analyzed for copy number alterations using the 250K StyI arrays. The SNP array data for 25 normal tissues, 12 ovarian serous borderline tumors, 12 ovarian low-grade serous carcinomas, seven ovarian endometrioid carcinomas, 12 ovarian clear cell carcinomas, and 33 ovarian high-grade serous carcinomas were previously reported (31,32).

The analysis of SNP array data was performed using the dChip software (2006 version) as previously described (31,32). Only data corresponding to probes present in both SNP Array 6.0 and 250K StyI array were analyzed. To quantify the relative levels of somatic DNA copy number alterations, we used a previously described method (32) to

calculate the genome-wide chromosomal instability index based on dChip analysis to infer the copy number. To identify the genes and regions with somatic copy number alterations (DNA copy number gain or loss as compared with matched normal tissue samples), the intensity of each probe was inferred with the use of Genotyping Console software (version 4.1.3; Affymetrix). To detect somatically altered chromosomal regions in the 23 uterine serous carcinomas, we used R package DNAcopy (http://www.bioconductor.org/packages/2.3/bioc/html/ DNAcopy.html) to perform circular binary segmentation analysis (33,34) and combined the segmentation results for all 23 uterine serous carcinomas. To identify the genes with statistically significant DNA copy number alterations, we used cghMCR (http://www.bioconductor.org/packages/release/bioc/html/cghMCR.html), an R implementation of a modified version of GISTIC analysis (35), because the original GISTIC algorithm only works for segmentation results from the same platform. Instead of the G score, which is reported by GISTIC algorithm, the cghMCR package uses a Segments-of-Gain-or-Loss (SGOL) score to indicate the frequency and degree of copy number changes in each gene or segment. Here, we selected three standard deviations (SDs) from the mean SGOL score as the cutoff because 99.7% of genes had SGOL scores within this range. In particular, we defined amplified genes as the genes with SGOL scores greater than 3 SDs of the mean SGOL scores and deleted genes as those with SGOL scores less than 3 SDs of the mean SGOL scores.

2.1.7 Immunohistochemistry

Immunohistochemistry for p53 and cyclin E1 expression was performed on paraffin-embedded sections of 41 and 37 uterine serous carcinomas, respectively, from both the validation and discovery sets. The detailed protocol for p53 immunohistochemistry has been reported previously (36). Briefly, after antigen retrieval was carried out with Cell Conditioning 1 solution (Ventana Medical Systems, Tucson, AZ), the sections were incubated with a mouse monoclonal p53 antibody (clone Bp53-11, prediluted; Ventana Medical Systems) for 16 minutes at 37°C. Staining was detected with the use of an iView DAB detection system (Ventana Medical Systems). For cyclin E1 staining, heat-induced epitope retrieval was performed with the use of Target Retrieval Solution (Dako, Carpinteria, CA), and nonspecific endogenous peroxidase activity was blocked by treatment with 3% hydrogen peroxide. The sections were then incubated with a polyclonal rabbit cyclin E antibody (1:250 dilution; Sigma-Aldrich, St Louis, MO) at room temperature for 65 minutes, followed by antibody detection with the use of an LSAB kit (catalog # K0690; Dako). Cyclin E1 immunoreactivity was visualized by a peroxidase reaction (Dako), and the sections were counterstained with hematoxylin (Dako).

2.1.8 Chromosomal Instability Index Analysis

We used the genome-wide chromosomal instability index to quantify the degree of somatic DNA copy number alterations according to a previously described method

(32). the genome-wide chromosomal instability index was defined as log(C1 + 1) + ... + log(Ci + 1) + ... + log(C23 + 1), where C1, Ci, and C23 are the chromosomal instability indices for chromosomes 1, i, and 23 (X chromosome), respectively. the chromosomal instability index for each chromosome was calculated as the sum of magnitudes of all subchromosomal segments whose copy numbers were amplified or deleted. The magnitude of an amplified copy number segment was the average intensity of SNP signals within the segment. The magnitude of a deleted copy number segment was normalized by the transformation 2.5 + (R − 2.5)(1.5 − x)/1.5, where x was the average intensity of SNP signals within the segment and R was the maximum magnitude of amplified copy number segments across all samples.

2.1.9 Statistical Analysis

We used one-way analysis of variance (ANOVA) followed by the Tukey–Kramer test for multiple comparisons to examine whether the chromosomal instability index for uterine serous carcinoma was statistically significantly higher than that for other types of gynecological neoplastic diseases based on our previous report (32). The Fisher exact test was used to compare the frequency of somatic mutations of several candidate genes in uterine serous carcinoma with the previously reported frequency in high-grade serous carcinoma of the ovary (37); P values were adjusted using the Bonferroni method. The association between p53 immunopositivity and *TP53* mutation status was evaluated by a two-tailed Fisher exact test. All statistical tests were two-sided, and a P value less than

.05 was considered statistically significant.

2.2 Results

2.2.1 Paired-End Whole-Exome Sequencing of Uterine Serous Carcinoma

To gain new insight into the genetic basis of uterine serous carcinoma, we determined the sequences of approximately 18,000 protein encoding genes in tumor and normal tissue samples from 10 uterine serous carcinomas by paired-end sequencing. To increase the sensitivity of somatic mutation detection, we used DNA extracted from epithelial tumor cells that were affinity-purified from six fresh tumor specimens with the use of EpCAM antibody–conjugated beads. Immunohistochemical staining of the purified cells with a cytokeratin antibody verified that more than 90% of each tumor was of epithelial origin. Our use of a high-throughput, paired-end sequencing system resulted in more than 75 million reads per DNA sample. The mean mapping rate for total reads was 98.4% (SD = 0.4%), and the mean percentage of targeted bases that were covered by at least 10 reads was 89.9% (SD = 2.5%; Table 2-1).

Table 2-1. Mapping statistics and the coverage of whole-exome sequencing of 10 uterine serous carcinomas (discovery set)

Sample*	Total reads	Read mapping rate (%)	Mean no. of reads	Median no. of reads	% of coding bases with coverage of ≥10×	≥20×	≥30×
900T	115,779,238	98.53	61.9	52	89.8	80.2	69.9
900N	111,798,422	98.27	60.2	56	90.8	82.4	73
366TS	125,512,762	98.65	64.1	58	91	82.7	73.7
366N	151,883,024	97.74	74.4	65	92.4	85.5	77.4
702TS	199,251,410	97.86	99.4	85	94.1	89.6	84.2
702N	76,933,210	98.02	35.9	33	85.2	69.6	52.8
863TCS	108,667,726	98.27	54.6	50	90.3	80.9	70.1
863N	113,439,292	98.03	61.5	58	91.8	84.5	75.7
340TS	111,431,136	98.64	52.1	46	89.8	79.6	67.9
340N	84,684,952	98.79	41.7	38	88.3	75.3	60.3
993TCS	110,439,740	98.84	53.3	45	84.7	72.9	62
993N	105,576,046	98.75	54.6	50	88.5	78.3	67.6
FM403T	107,195,624	98.83	51.9	43	87.5	75.4	63
FM403N	121,779,982	98.60	63.6	59	90.7	82.6	73.7
DM851T	115,971,750	98.59	61.9	56	89.2	80.1	70.8
DM851N	116,959,022	98.57	60.1	56	90	81.2	71.7
FM474T	106,664,394	98.55	50.9	47	89	79.1	67.9
FM474N	106,243,310	98.76	58.3	53	90.7	81.8	71.6
555TS	212,645,988	97.91	101.9	92	94.9	91.4	87
555N	106,972,698	98.06	44.3	43	89.8	79	65.9

*TS and TCS = fresh tumor with affinity-purified tumor cells; T= frozen tumor samples without affinity purification; N = normal tissue.

We identified 946 somatic mutations in 874 genes among 10 uterine serous carcinomas using the method reported in the analysis of whole genome sequencing data of T-cell precursor acute lymphoblastic leukemia and retinoblastoma (28,29). To ensure that our method could reliably detect somatic mutations, we re-sequenced 331 randomly selected mutated regions (mainly those containing non-silent mutations) by Sanger sequencing and verified that 303 (91.5%) contained the originally identified mutation (Appendix 1).

The median number of somatic sequence mutations for uterine serous carcinomas in the discovery set, including synonymous and nonsynonymous changes, alterations in 5′ and 3′ untranslated regions, and alterations in noncoding RNA, was 96 (range = 38–156) (Table 2-2). The median number of somatic nonsynonymous and splice site mutations for uterine serous carcinomas in the discovery set was 38 (range = 10–64). The most common sequence mutation in these 10 uterine serous carcinomas was a C to T or G to A transition (Figure 2-1). Specifically, there were 454 nonsynonymous and splice site mutations in 425 genes (Appendix 1), and the average nonsilent-to-silent mutation ratio was 3:2 (Table 2-2).

Table 2-2. Detailed mutation profiles in the discovery set of uterine serous carcinomas*

Mutation type or location	900T	366TS	702TS	863TCS	340TS	993TCS	FM403T	DM851T	FM474T	555TS
CDS SNV										
Missense	35	17	58	42	6	23	56	32	57	18
Nonsense	6	0	3	3	3	2	3	2	5	0
Silent	17	5	14	16	5	9	30	12	17	9
Splice site SNV	7	3	6	9	2	2	3	3	11	6
Non-silent SNV	48	20	67	54	11	27	62	37	73	24
Indels										
Frameshift	4	1	1	4	1	2	3	4	3	1
In-frame	1	0	3	1	0	0	1	0	1	0
3′ UTR	17	8	37	27	12	24	44	26	39	15
5′ UTR	3	5	6	4	7	3	7	8	5	7
Non-coding RNA	4	1	8	1	2	5	8	8	6	4
Intron	2	0	0	0	0	1	1	1	1	1
Total no. of somatic alterations	96	40	136	107	38	71	156	96	145	61
No. of CDS bases covered ≥10×	29,190,215	29,650,859	30,857,945	29,360,631	29,198,448	27,407,447	28,377,912	28,990,451	28,947,907	31,121,142
Background mutation rate†	1.7×10^{-06}	5.1×10^{-07}	1.4×10^{-06}	1.6×10^{-06}	5.1×10^{-07}	9.9×10^{-07}	3.2×10^{-06}	1.2×10^{-06}	1.8×10^{-06}	8.7×10^{-07}

*CDS = coding sequence; SNV = single nucleotide variation; indels = insertions and deletions; UTR = untranslated region.
†Background mutation rate = the total number of silent mutations normalized to the number of "covered" synonymous sites (approximately one-third of "covered" CDS bases).

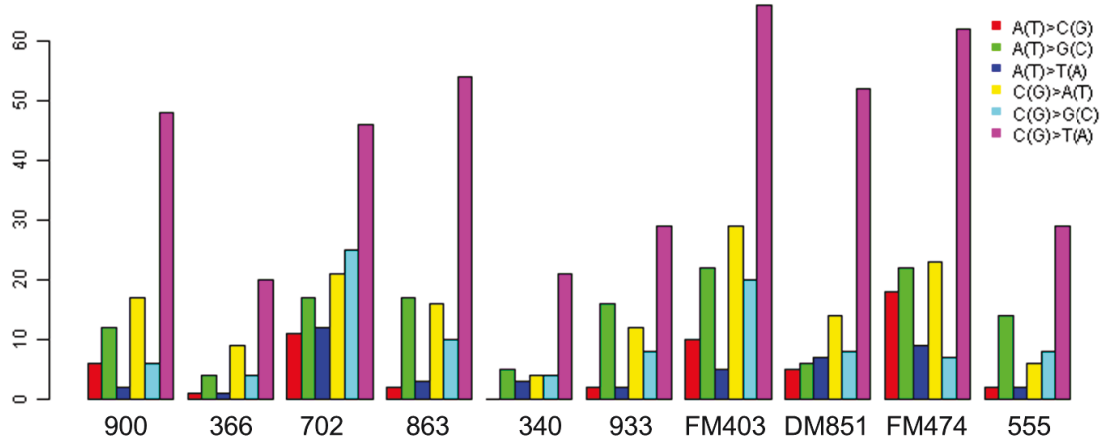

Figure 2-1. The mutation spectrum in 10 USC samples. The most common point mutation in those 10 USCs was from C(G) to T(A) transition.

Among the 425 somatically mutated genes, 14 were mutated in two or more of the 10 uterine serous carcinomas: *TP53, PIK3CA, FBXW7, PPP2R1A, BSN, DNAH11, NEB, OBSCN, ORAI2, RNF19B, SLC28A1, SPTA1, UBA2,* and *UTRN* (Table 2-3). To identify other cancer-related genes that are less commonly mutated in uterine serous carcinoma, we compared all genes harboring mutations from this study with the cancer-related mutations reported in the Cancer Gene Census database (http://www.sanger.ac.uk/genetics/CGP/Census/). This comparison yielded 16 genes: four genes (*FBXW7, PIK3CA, PPP2R1A,* and *TP53*) were mutated in more than one of the 10 uterine serous carcinomas, whereas 12 cancer-associated genes occurring in Cancer Gene Census database were mutated only once in these 10 tumors (*AKAP9,*

BCL9, BRCA2, ERCC5, KRAS, LHFP, MLL3, MYH11, NCOA2, NSD1, PDGFRA, and *USP6*). Of note, all three missense mutations detected in *FBXW7* occurred at the Arg465 hotspot (COSMIC database, http://www.sanger.ac.uk/perl/genetics/CGP/cosmic?action=bygene&ln=FBXW7&start=1&end=708&coords=AA:AA), whereas none of the four *PIK3CA* mutations were located at previously reported exons containing hotspots. We found no mutations in mismatch repair genes in any of the 10 tumors in the discovery set.

Table 2-3. Recurrently mutated genes in 10 uterine serous carcinomas of the discovery set*

Gene	Transcript	900T	366TS	702TS	863TCS	340TS	993TCS	FM403T	DM851T	FM474T	555TS	Total
TP53	NM_000546.4	c.677del p.G226Afs		c.742C>T p.R248W	c.722C>T p.S241F	c.481G>A p.A161T	c.832C>A p.P278T	c.647_672+3del p.V216Gfs	c.713G>A p.C238Y	c.742C>T p.R248W	c.730G>C p.G244R	9
PIK3CA	NM_006218.2			c.1252G>A p.E418K	c.353G>A p.G118D			c.1093G>A p.E365K		c.1031T>G p.V344G		4
FBXW7	NM_033632.2	c.1393C>T p.R465C	c.1394G>A p.R465H						c.1394G>T p.R465L			3
PPP2R1A	NM_014225.3			c.767C>A p.S256Y							c.536C>G* p.P179R*	2
BSN	NM_003458.3		c.8374C>G p.Q2792E		c.2687G>A p.R896H							2
DNAH11	NM_003777.3	c.3925G>A p.A1309T						c.6536T>C p.V2179A				2
NEB	NM_001164508.1				c.20330T>C p.V6777A			c.23491A>T p.I7831F				2
OBSCN	NM_001098623.1				c.11274_11275del p.H3758Qfs						c.22967A>T p.E7656V	2
ORAI2	NM_001126340.1								c.214G>A p.G72S	c.397T>G p.S133A		2
RNF19B	NM_153341.2			c.842-5C>G ex3_splice				c.1264G>T p.G422C				2
SLC28A1	NM_004213.3							c.1754G>A p.C585Y	c.-16-1G>T ex3_splice			2
SPTA1	NM_003126.2	c.610del p.Q204Kfs							c.3697G>A p.V1233I			2
UBA2	NM_005499.2			c.347T>C p.L116S						c.223-2A>T ex3_splice		2
UTRN	NM_007124.2				c.8782G>A p.V2928I					c.5074-1G>A ex36_splice		2

- Sanger sequencing discovered an additional *PPP2R1A* mutation that was not originally recorded in the Illumina HiSeq platform.

2.2.2 Prevalence Screening of Mutations in Selected Genes

We performed Sanger sequencing to determine prevalence of mutations in *FBXW7, FBXW8, PIK3CA, PPP2R1A, PIK3C2B, PIK3R4, RNF19B,* and *TP53* in 34 frozen tumors from the validation set with sufficient DNA. In addition, we sequenced known mutational hotspots in *FBXW7* [coding exons 8 and 9; (38)], *PIK3CA* [coding exons 1, 9, and 20; (39)], *PPP2R1A* [coding exons 5 and 6; (23)], and *TP53* (coding exons 4–9; COSMIC database, http://www.sanger.ac.uk/perl/genetics/CGP/cosmic?action=byg ene&ln=tP53&start=1&end=394&coords=AA:AA) in an additional 32 paraffin-embedded uterine serous carcinomas from the validation set. We also sequenced exon 9 of *FBXW8* in the 32 uterine serous carcinomas because a somatic mutation in this exon was identified in our discovery screen. *RNF19B* was selected for validation because it was somatically mutated in two of the 10 uterine serous carcinomas in the discovery set and it encodes an E3 ligase that ubiquitinates uridine-cytidine kinase-like 1 (UCKL1), a tumor survival factor (40-42). Although only one somatic mutation was found in the discovery set for *FBXW8*, *PIK3C2B*, and *PIK3R4*, these genes were chosen for validation because, similar to FBXW7, FBXW8 also contains F-box and WD-40 domains and functions as E3 ubiquitin ligase (43), and both PIK3C2B and PIK3R4 are involved in the phosphatidylinositol 3-kinase (PI3K) signaling pathway (44). The prevalence of somatic mutations in *TP53, PIK3CA, FBXW7,* and *PPP2R1A* in the validation set (n = 66) was 80.3%, 21.2%, 18.2%, and 18.2%, respectively. When we combined all uterine serous

carcinomas from the discovery and validation sets (n = 76), the prevalence of somatic mutations in *TP53*, *PIK3CA*, *FBXW7*, and *PPP2R1A* was 81.6%, 23.7%, 19.7%, and 18.4%, respectively (Table 2-4); all mutations in these four genes in all 76 tumors are listed in Appendix 2. For *FBXW7*, there were 16 somatic mutations (15 mutations involved the coding region and one involved the noncoding region at the splice site) detected in 15 tumors among all 76 tested tumors; all *FBXW7* somatic mutations involving the coding region occurred in the WD40 domain, whose function in E3 ubiquitin ligases is to recognize phosphorylated ubiquitination signals (45). However, we did not detect any somatic mutations in *FBXW8*, *PIK3C2B*, *PIK3R4*, or *RNF19B* in the validation set. It should be noted that the higher mutation frequency of *TP53* in the discovery set than in the validation set (90% vs 80%) may reflect the fact that we used affinity-purified tumor cells in some of the discovery samples. Accordingly, the actual prevalence of mutations in all the genes analyzed could be slightly higher than that reported in this study.

Table 2-4. The prevalence of most common somatic mutations (frequency >10%) in uterine serous carcinoma in all 76 tumors analyzed

Sample set	No. of tumors analyzed	*FBXW7* mutation	*PIK3CA* mutation	*PPP2R1A* mutation	*TP53* mutation
Discovery set	10	3	4	2	9
Validation set (paraffin-embedded)	32	8	5	4	24
Validation set (fresh frozen)	34	4	9	8	29
Total (%)	76 (100.0)	15 (19.7)	18 (23.7)	14 (18.4)	62 (81.6)

To examine whether the *TP53* mutation pattern was associated with p53 protein expression in carcinoma tissues, we performed p53 immunohistochemistry on 41 uterine serous carcinomas from both discovery and validation sets for which paraffin-embedded tissues were available. We found that 27 of 28 tumors bearing *TP53* missense mutations or in-frame deletion had diffuse p53 staining. The frequency of diffuse staining in tumors with TP53 missense mutation or in-frame deletion was statistically significantly higher than in those with a null mutation or wildtype TP53 (96.4% vs 46.2%, P < .001, two-tailed Fisher exact test). These findings are consistent with our previous report showing a similar association between p53 immunostaining pattern and *TP53* mutation type in ovarian high-grade serous carcinomas and serous tubal intraepithelial carcinomas (36).

In contrast, by analyzing 316 ovarian high-grade serous carcinomas from the ovarian cancer dataset of TCGA (37), we found somatic mutations of *PIK3CA*, *FBXW7*, and *PPP2R1A* in only 0.63%, 0.95%, and 1.27%, respectively (Table 2-4). The mutation frequencies of those genes were statistically significantly higher in uterine serous carcinoma than in ovarian high-grade serous carcinoma (P < .001, Fisher exact test; Table 2-5).

Table 2-5. Mutation rate comparison of *PIK3CA*, *FBXW7*, and *PPP2R1A* between uterine serous carcinoma and ovarian high-grade serous carcinoma

	Somatic mutation rate		
Tumor type	*PIK3CA*	*FBXW7*	*PPP2R1A*
Uterine serous carcinoma	18/76	15/76	14/76
Ovarian high-grade serous carcinoma	2/316	3/316	4/316
Fisher exact test *P* value	<.001	<.001	<.001
Bonferroni corrected *P* value	<.001	<.001	<.001

2.2.3 DNA Copy Number Alterations in Uterine Serous Carcinoma and Other Gynecological Cancers

Because DNA copy number alterations are commonly associated with tumorigenesis (46), we also used the SNP arrays for copy number analysis of 23 uterine serous carcinomas (10 from discovery set and 13 from validation set) for which the genomic DNA was available for analysis. By using the chromosomal instability index, a quantitative measure of the genome-wide level of DNA copy number changes (32), we found that among a panel of gynecological tumors, uterine serous carcinoma displayed a mean chromosomal instability index comparable to that of ovarian high-grade serous carcinoma, a fatal subtype of ovarian cancer with known prominent genomic alterations (Table 2-6) (32,37). The mean chromosomal instability index for both uterine serous carcinoma (mean = 1.129) and ovarian high-grade serous carcinomas (mean = 1.475) was statistically significantly higher than that in other types of gynecological cancers, including uterine endometrioid carcinoma (mean = 0.298), ovarian serous borderline tumor (mean = 0.134), ovarian low-grade serous carcinoma (mean = 0.386), ovarian endometrioid carcinoma (mean = 0.228), and ovarian clear cell carcinoma (mean = 0.302) ($P < .001$, one-way ANOVA followed by Tukey–Kramer test) (Figure 2-2 and 2-3). The details of the chromosome instability index for each type of gynecological cancer and P values for all pair-wise comparisons are shown in Table 2-6.

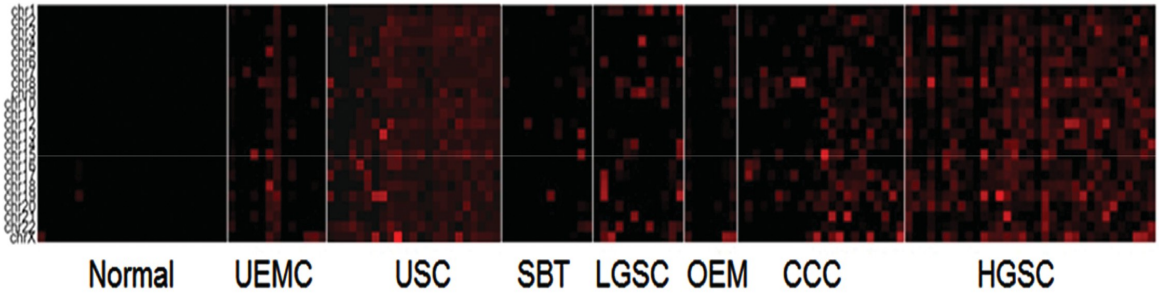

Figure 2-2. Copy number alteration in uterine serous carcinoma and other types of gynecological neoplasia. Individual chromosomes (vertical axis) of each tumor (horizontal axis) are plotted using a pseudo-color gradient indicating the overall level of copy number alteration (low [**black**] to high [**red**]). Normal = normal tissue (n = 25); UEMC = uterine endometrioid carcinoma (n = 13); USC = uterine serous carcinoma (n = 23); SBT = ovarian serous borderline tumor (n = 12); LGSC = ovarian low-grade serous carcinoma (n = 12); OEM = ovarian endometrioid carcinoma (n = 7); CCC = ovarian clear cell carcinoma (n = 12); HGSC = ovarian high-grade serous carcinoma (n = 33).

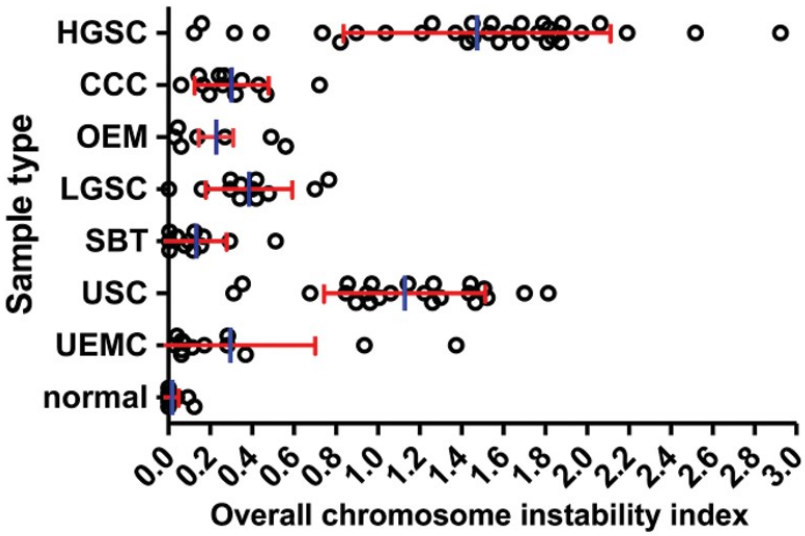

Figure 2-3. Scatter plot of genome-wide chromosome instability index for individual tumors (open circles). Vertical blue lines indicate mean values; horizontal red lines indicate plus or minus one SD.

Table 2-6. Chromosomal instability index of gynecological cancers*

Cancer type	Chromosomal Instability Index		Pair-wise comparison *P* values†	
	Mean	SD	USC	HGSC
USC	1.129	0.385	–	.03
HGSC	1.475	0.638	.03	–
CCC	0.302	0.176	<.001	<.001
LGSC	0.386	0.207	<.001	<.001
OEM	0.228	0.220	<.001	<.001
SBT	0.134	0.146	<.001	<.001
UEMC	0.298	0.405	<.001	<.001

*USC = uterine serous carcinoma; – = not applicable; HGSC = ovarian high-grade serous carcinoma; CCC = ovarian clear cell carcinoma; LGSC = ovarian low-grade serous carcinoma; OEM = ovarian endometrioid carcinoma; SBT = ovarian serous borderline tumor; UEMC = uterine endometrioid carcinoma.

† Tukey–Kramer test (two-sided).

2.2.4 DNA Copy Number Alterations in Uterine Serous Carcinoma

We used DNAcopy and cghMCR software to identify genomic regions of uterine serous carcinomas that displayed a statistically significant copy number gain or loss compared with normal tissues. By using the mean SGOL score plus or minus 3 SDs to define amplified and deleted genes, respectively, we found 13 discrete amplified regions containing 307 genes and 25 discrete deleted regions containing 520 genes, including 25 regions that harbored six or fewer genes. Frequently amplified genes (and the corresponding chromosomal locations) included *BCL9* (1q21.1), *EVI1* (3q26.2), *KRAS* (12p12.1), *ADAM6* (14q32.33), and *CCNE1* (19q12); the percentage of samples that exhibited an inferred gene copy number greater than three for *BCL9*, *EVI1*, *KRAS*, *ADAM6*, and *CCNE1* were 13%, 21.7%, 4.4%, 30.4%, and 26.1%, respectively. Among these frequently amplified genes, the *CCNE1* locus (chromosome 19: nucleotide 34,995,401–35,007,059) demonstrated a very high SGOL score (9.1) and was amplified in six of the 23 uterine serous carcinoma samples examined (Figure 2-4 and 2-5). The most commonly deleted regions harbored *LCE3C* (1q21.3), *MGAM* (7q34), *CSMD1* (8p23.2), and *CDH13* (16q23.3); these deletions occurred in 17.4%, 34.8%, 26.1%, and 34.8%, respectively, of the 23 uterine serous carcinomas.

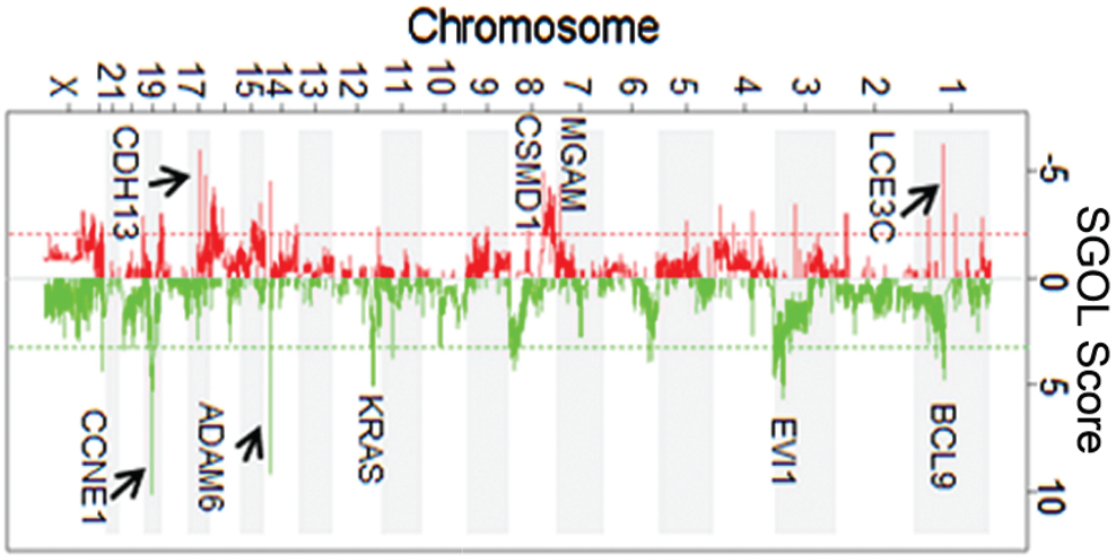

Figure 2-4. Overall view of DNA copy number gain and loss in uterine serous carcinoma. To generate an overview of DNA copy number alterations, we performed circular binary segmentation analysis and combined the segmentation results for all 23 uterine serous carcinomas. Based on the Segments-of-Gain-Or-Loss (SGOL) scores (horizontal axis), DNA copy number gains (green) and losses (red) are plotted as a function of distance along the normal genome (vertical axis). Dashed vertical lines are generated based on the values of 3 SDs of the SGOL scores of gains or losses. Tumor-associated genes located in representative amplified and deleted regions are annotated.

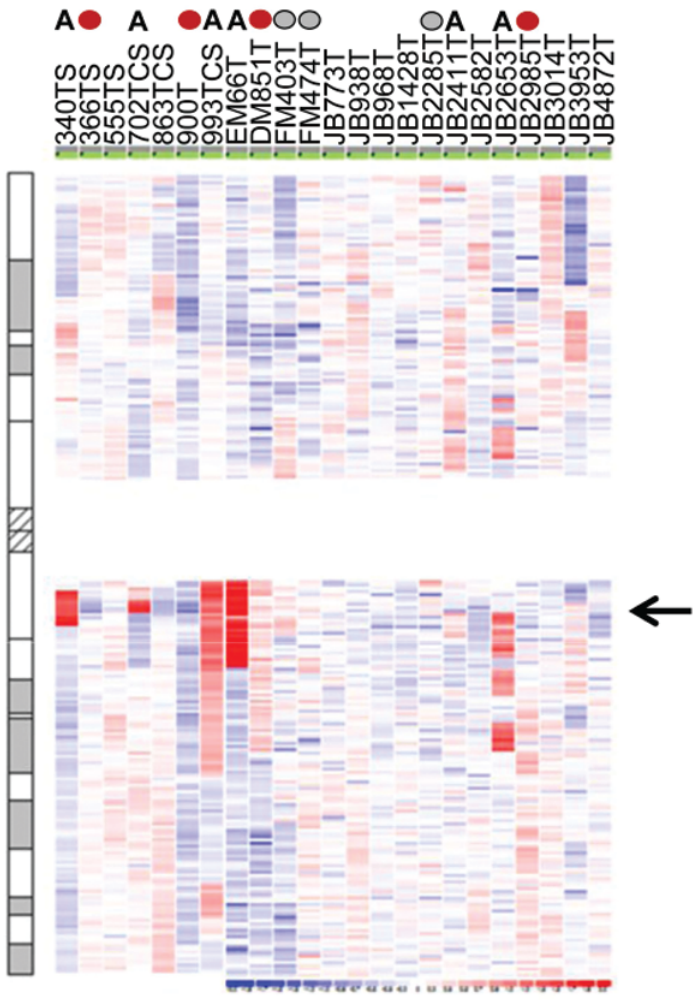

Figure 2-5: Heat map of DNA copy number ratio along the chromosome 19. Arrow shows amplification in the *CCNE1* locus in 23 uterine serous carcinoma samples. A = *CCNE1* amplification; red circles = *FBXW7* mutation; gray circle = *FBXW7* hemizygous deletion. Suffix of the tumor numbers: TS and TCS = fresh tumor with affinity-purified tumor cells; T = tumor samples without affinity purification; N = normal control.

To discover cancer-associated genes whose function was affected by somatic point mutation and DNA copy number change, we compared the genes that harbored nonsynonymous and splice site mutations (Appendix 1) with those that are amplified or deleted. This comparison yielded 11 genes, including *BCL9*, *DAZAP1*, and *KRAS*. In addition, close examination of copy number at the *FBXW7* locus revealed that *FBXW7* was deleted in a hemizygous fashion in three tumors (Figure 2-6). This is interesting because *FBXW7* encodes a substrate recognition component of a SKP1-cullin-F-box (SCF)–type E3 ubiquitin ligase, which is responsible for ubiquitin-dependent degradation of cyclin E (encoded by *CCNE1*). Thus, we examined the co-occurrence of somatic mutations and/or *FBXW7* deletion and *CCNE1* amplification in the 23 uterine serous carcinomas that were subjected to SNP array analysis. We found that seven tumors with *FBXW7* mutations (four tumors with sequence mutations, three tumors with hemizygous deletions) did not have *CCNE1* amplification, and six tumors with *CCNE1* amplification did not have *FBXW7* mutations; therefore, 13 (57%) of 23 tumors had either a molecular genetic alteration in *FBXW7* or *CCNE1* amplification (Figure 2-7). We also found that *PIK3CA* mutation and gene amplification were mutually exclusive except for one tumor (case ID: JB2411), which showed both genetic alterations. Integrated analysis demonstrated that 48% of the 23 uterine serous carcinomas harbored a *PIK3CA* mutation and/or *PIK3CA* amplification (Figure 2-7). Taken together, these findings suggest that the cyclin E–FBXW7 and PI3K pathways are involved in the development of uterine serous carcinoma.

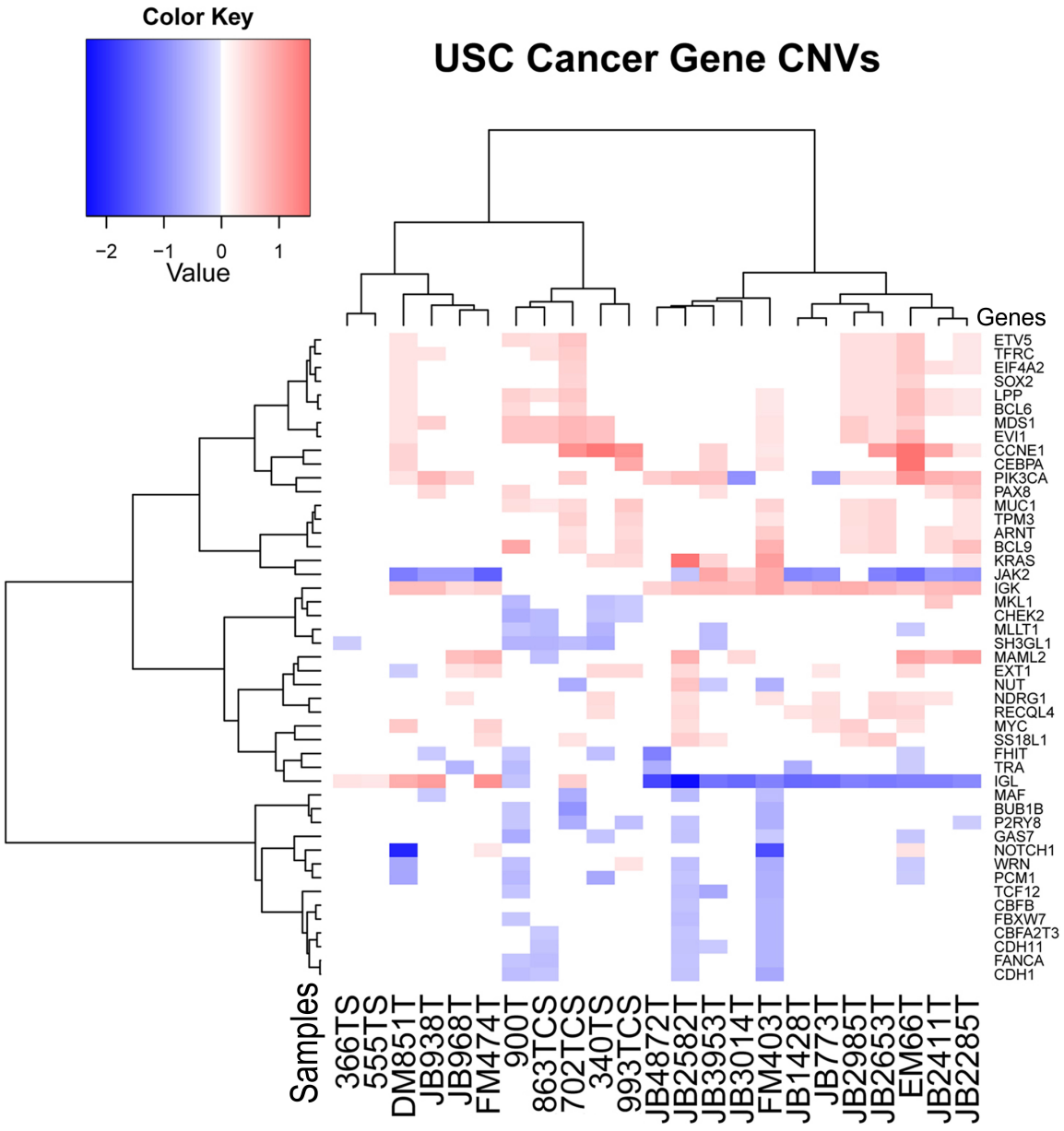

Figure 2-6. Heat map of the cancer-associated genes in COSMIC database with statistically significant DNA copy number variations (CNVs) from 23 uterine serous carcinomas. Pseudocolor gradient indicates the level of amplification (red) and deletion (blue). Genes and samples are grouped by unsupervised clustering.

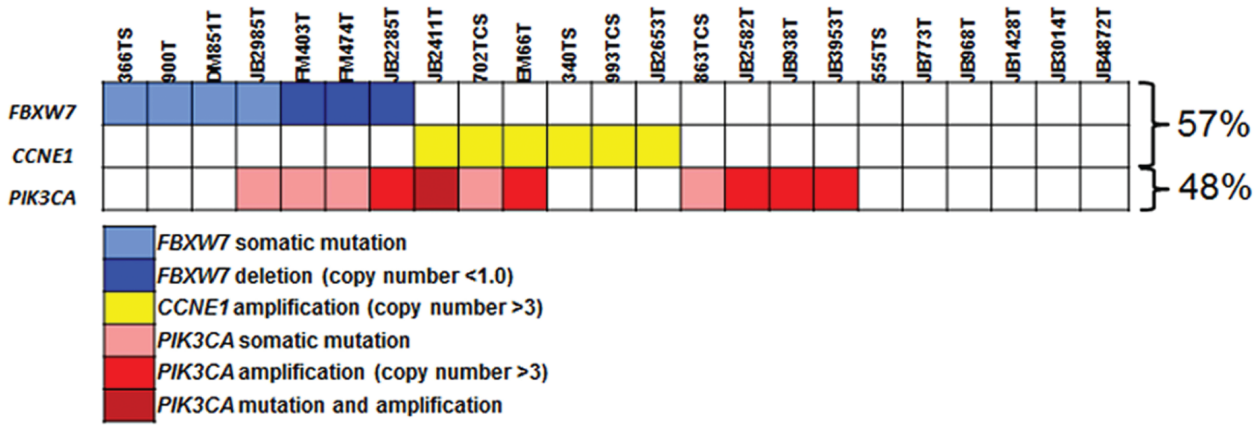

Figure 2-7. Molecular genetic alterations involving the FBXW7–cyclin E and phosphatidylinositol 3-kinase (PI3K) pathways in uterine serous carcinoma.A) Summary of sequence mutations and DNA copy number changes in *FBXW7*, *CCNE1*, and *PIK3CA*.

2.2.5 FBXW7, PIK3CA, PPP2R1A, and TP53 Mutations in Serous Endometrial Intraepithelial Carcinoma

It has been proposed that serous endometrial intraepithelial carcinoma is the pre-invasive precursor of uterine serous carcinoma (2,47,48). We, therefore, examined whether somatic mutations of the frequently mutated genes in uterine serous carcinoma identified in this study, including *FBXW7*, *PIK3CA*, *PPP2R1A*, and *TP53*, occurred in serous endometrial intraepithelial carcinoma. We identified nine uterine serous carcinomas that had a concurrent serous endometrial intraepithelial carcinoma component; we laser-capture microdissected nine serous endometrial intraepithelial carcinomas for mutation analysis. As summarized in Figure 2-8, all nine pairs of serous carcinoma and associated serous endometrial intraepithelial carcinoma had concordant *PIK3CA*, *PPP2R1A*, and *TP53* mutation status between uterine serous carcinoma and its concurrent serous endometrial intraepithelial carcinoma component, whereas eight of the nine pairs had concordant *FBXW7* mutation status between these two components. the only discordant pair (case ID: 1FFPE) contained a *FBXW7* p.Asp440Asn mutation in the uterine serous carcinoma component, but this mutation was not detected in the serous endometrial intraepithelial carcinoma.

		FBXW7	*PIK3CA*	*PPP2R1A*	*TP53*
1 FFPE	SEIC	wt	ND	W257G	P278A
	USC	D440N	wt	W257G	P278A
3 FFPE	SEIC	ND	H1047R	S256F	N179H
	USC	wt	H1047R	S256F	N179H
5 FFPE	SEIC	ND	E545A*	ND	Y163H
	USC	wt	E545A*	wt	Y163H
10 FFPE	SEIC	ND	P104L#	ND	ND
	USC	wt	P104L#	wt	wt
16 FFPE	SEIC	R465C	ND	ND	NA
	USC	R465C	wt	wt	N131S
366TS	SEIC	R465H	ND	ND	ND
	USC	R465H	wt	wt	wt
702TS	SEIC	ND	E418K	S256Y	R248W
	USC	wt	E418K	S256Y	R248W
19 FFPE	SEIC	R465C	H1047R	ND	R248W
	USC	R465C	H1047R	wt	R248W
32FFPE	SEIC	R465H	ND	ND	L194P
	USC	R465H	wt	wt	L194P

Figure 2-8. Mutation profiles of *FBXW7*, *PIK3CA*, *PPP2R1A*, and *TP53* in nine uterine serous carcinomas (USC) and with a concurrent serous endometrial intraepithelial carcinoma (SEIC) component. Manual microdissection and laser-capture microdissection were used to isolate USC and SEIC, respectively, for DNA analysis. Mutations are highlighted in different colors for each gene. ND = not done; wt = wildtype; NA = not available for analysis; *tumor (5FFPE) has two additional mutations in *PIK3CA*: S553Ifs, H1047R; #tumor (10FFPE) has one additional mutation in *PIK3CA*: G1007R.

We also examined whether cyclin E protein expression, as detected by immunohistochemistry, was increased in *FBXW7* mutated serous endometrial intraepithelial carcinomas. We found that all four pairs of serous endometrial intraepithelial carcinomas and concurrent serous carcinomas with a *FBXW7* mutation had increased cyclin E expression compared with normal endometrial epithelium. The expression of cyclin E and *FBXW7* mutation status in one of the cases are shown in Figure 2-9. The locations of *FBXW7* mutations, including those found in five serous endometrial intraepithelial carcinomas and in 15 uterine serous carcinomas, are shown in Figure 2-10. All mutations were missense mutations except one (a splice site mutation) and were located in the WD40 domain. Our finding that most uterine serous carcinomas and their in situ counterparts have identical mutations, when taken together with previous reports (49,50) showing *TP53* mutations in serous endometrial intraepithelial carcinoma, indicates that mutations in *FBXW7*, *PIK3CA*, *PPP2R1A*, and *TP53* occur early during tumor progression of uterine serous carcinoma.

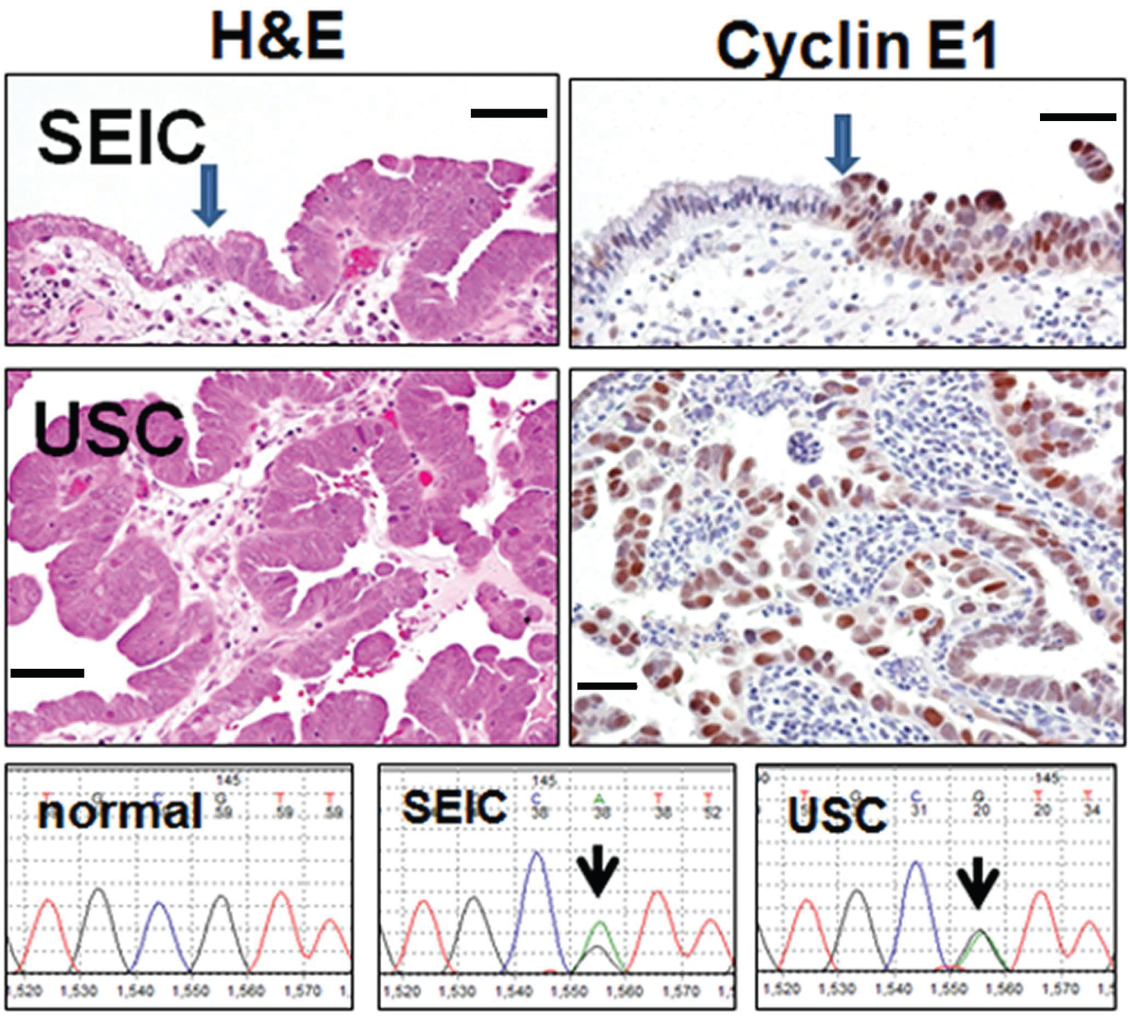

Figure 2-9. A uterine serous carcinoma (USC) with a serous endometrial carcinoma (SEIC) component. Top panel, SEIC; middle panel, USC. The tumor cells in both lesions show highly atypical and enlarged nuclei. The arrow indicates the junction between normal-appearing uterine surface epithelium (left) and SEIC (right). Cyclin E immunoreactivity (brown) was detected in both USC and SEIC cells but not in adjacent normal epithelium or stromal cells (scale bar = 100 um). Bottom panels: Mutational analysis showing an identical somatic mutation of *FBXW7*, from CGT to CAT (arrows), leading to the amino acid change R465H in both SEIC and USC.

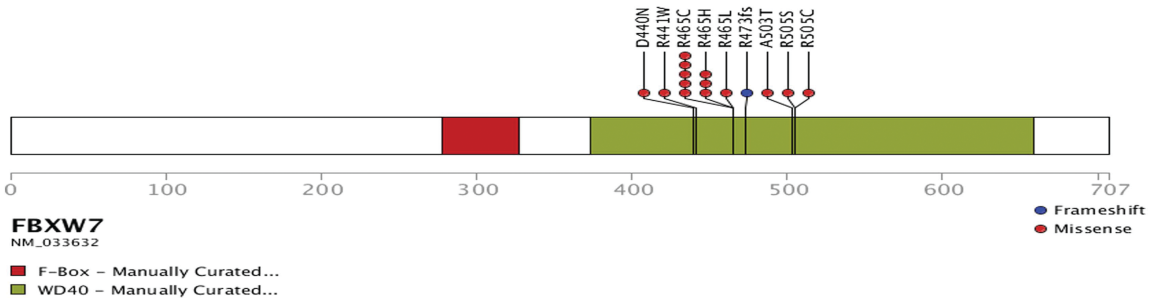

Figure 2-10. Locations of *FBXW7* mutations identified among the 76 uterine serous carcinomas. Each circle represents an individual mutation.

2.3 Discussion

This is the first study to our knowledge to characterize the genomic landscape of uterine serous carcinoma, a highly aggressive neoplastic disease in women. Whole-exome sequencing and DNA copy number analysis demonstrated that mutations in *TP53*, *PIK3CA*, and *FBXW7*, as well as amplification of *CCNE1*, are the most common genetic alterations in this type of tumor. The presence of *FBXW7* mutations and *CCNE1* amplification increased the levels of cyclin E protein, which facilitates cell cycle progression through cdk2, Rb phosphorylation, and E2F-1 (Figure 2-11). Conversely, an activating mutation and/or gene amplification of *PIK3CA* would enhance PI3K signaling and, subsequently, Akt activity, which promotes cellular proliferation and survival (Figure 2-11). Therefore, both signaling pathways may work in concert to promote tumorigenesis in uterine serous carcinoma. Because patients with uterine serous carcinoma are often diagnosed at late clinical stages when conventional chemotherapy is not effective, there is an unmet need to develop new therapeutics for those patients. The results as reported here suggest that PI3K inhibitors and inhibitors targeting the cyclin E pathway may represent new therapeutic interventions in advanced-stage uterine serous carcinoma.

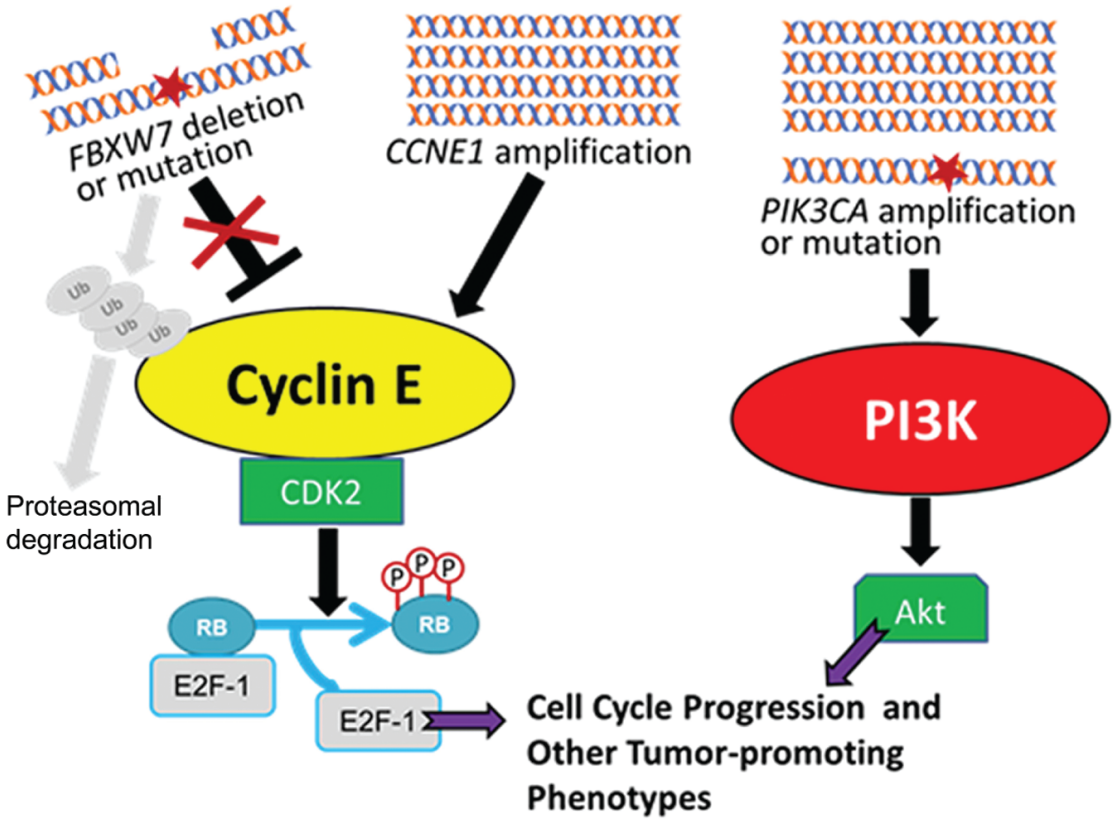

Figure 2-11. Schematic presentation of possible mechanisms involving the FBXW7–cyclin E and PI3K pathways in the development of uterine serous carcinoma. *FBXW7* gene deletion or mutation results in an increased level of cyclin E because of the suppression of FBXW7-mediated ubiqutination and subsequent proteasome-mediated degradation of cyclin E proteins. Alternatively, activation of PI3K can be a result of increased DNA copy number of *PIK3CA* and activating mutation of the gene. Increased E2F-1 and PI3K activity leads to activation of their downstream targets that promote cell cycle progression and other tumor-promoting phenotypes. Ub = ubiquitin; P = phosphate.

Our results also have several biological implications regarding the molecular genetics of uterine serous carcinoma. First, this study not only confirmed frequent *PIK3CA*, *PPP2R1A*, and *TP53* mutations in uterine serous carcinoma as previously reported (49,51-54) but also identified novel recurrent somatic mutations of *FBXW7*, which occurred in approximately 20% of tumors. Although *FBXW7* mutations have been reported in several types of human cancers, including those of hematopoietic, gastrointestinal tract, pancreatic, uterine, and cervical origins (55), to our knowledge, this gene has not been sequenced in uterine serous carcinoma. FBXW7, also known as hCDC4, is a member of the F-box family of proteins that serves as a substrate recognition component of the ubiquitin ligase SCF complex (55,56). FBXW7 functions as a haploinsufficient tumor suppressor gene (57), and the protein is responsible for the ubiquitin-dependent proteolysis of several tumor-promoting proteins, including cyclin E, c-Jun, c-Myc, MCL1, and Notch (56,58-62). It is interesting that our DNA copy number analysis revealed that the *CCNE1* locus is one of the most frequently amplified chromosomal regions in uterine serous carcinoma and that *CCNE1* amplification occurs mutually exclusively with *FBXW7* mutations (including point mutation and deletion), suggesting that CCNE1 and FBXW7 participate in the same signaling pathway. In fact, we found that molecular genetic aberrations in the cyclin E pathway due to *FBXW7* point mutations, *FBXW7* deletions, or *CCNE1* amplification, when considered together, occurred in more than half of uterine serous carcinomas. Thus, activation of cyclin E, either by inhibiting its ubiquitin-dependent protein degradation due to *FBXW7* mutations or by increased expression as a result of gene amplification, may play a major role in driving the tumorigenesis of uterine serous carcinoma.

Second, we observed that concordant mutation status in *PIK3CA*, *PPP2R1A*, and *TP53* occurred in all nine pairs of tumors containing uterine serous carcinoma and concurrent serous endometrial intraepithelial carcinoma, whereas concordant *FBXW7* mutation status was found in eight of nine pairs. This result suggests that mutations of the above genes occurred in the pre-invasive stage of uterine serous carcinoma and, if confirmed in a larger number of tumors, may have translational implications. For example, detection of those mutations may be helpful for screening for uterine serous carcinoma at a preinvasive stage in endometrial curettage or cervical lavage specimens using emerging highly sensitive molecular techniques.

Third, our results may clarify the relationship between uterine serous carcinoma and ovarian high-grade serous carcinoma, another highly aggressive gynecologic neoplasm. these two tumors have different clinicopathologic features, such as older age at diagnosis for uterine serous carcinoma compared with ovarian high-grade serous carcinoma [68 years for uterine serous carcinoma vs. 55 years for ovarian high-grade serous carcinoma (2)] and a genetic predisposition for some cases of ovarian serous carcinoma due to germline *BRCA1* and *BRCA2* mutations (2) but not for uterine serous carcinoma. however, uterine serous carcinoma and ovarian high-grade serous carcinoma have some similar features, including an aggressive clinical course, certain morphological features, and a similar relationship to intraepithelial carcinoma precursors (2). Molecularly, both are characterized by a high prevalence of *TP53* mutations, a similar overall number of somatic mutations, and a high level of genome-wide DNA copy number alterations. In fact, in the World health organization histopathologic classification (1,63), the term "serous carcinoma" is used to describe both tumors, implying that they

share similar morphological features. However, in this study, we found a higher frequency of somatic mutations in *FBXW7*, *PIK3CA*, and *PPP2R1A* in uterine serous carcinoma compared with ovarian high-grade serous carcinoma, providing evidence for molecular genetic alterations that are unique to uterine serous carcinoma.

There are two major limitations in this study. First, we focused on only 10 uterine serous carcinomas in the discovery set, and it is possible that other somatic genetic changes will be identified in studies using a larger cohort. Second, we did not investigate whether the molecular changes reported here are associated with any clinical features. Therefore, it will be interesting to determine whether mutations in *FBXW7*, *PIK3CA*, *PPP2R1A*, or *TP53* are associated with clinical stage, disease-free or overall survival, or response to treatment.

In summary, genome-wide analyses identified aberrations involving three pathways, the p53, PI3K, and cyclin E–FBXW7 pathways, in uterine serous carcinomas. Our findings have important implications not only for understanding the pathogenesis of uterine serous carcinoma but possibly also for developing more effective target-based therapy. Moreover, the presence of these changes in the preinvasive stage of uterine serous carcinoma suggests that these molecular alterations occur relatively early in tumor progression and may serve as molecular markers for early detection of uterine serous carcinoma.

2.4 Acknowledgements

This work was supported by the National Cancer Institute at the National Institutes of health (RO1 CA103937, RO1 CA129080, RO1 CA148826, RO1 CA122581, P50 CA098252), the National Taiwan university hospital (NTUH98-1265), and the National Science Council in Taiwan (NSC99-2320-B-002-056-MY2).

3 *TERT* Promoter Mutation in Gynecological Malignancies

Telomeres are DNA–protein complexes that protect the ends of eukaryotic chromosomes by preventing them from being recognized as DNA double-strand breaks, which inappropriately trigger DNA damage response pathways and may lead to cellular senescence or illegitimate fusion of chromosomal ends (64). The termini of a linear DNA template cannot be completely replicated by conventional DNA-dependent DNA polymerases and thus, in the absence of mechanisms to counter this effect, telomeres of eukaryotic cells shorten every round of DNA replication. Telomere shortening in somatic cells limits the life span of somatic cells and acts as a natural barrier to oncogenic transformation (65). To maintain unlimited replication potential, cancer cells evolve mechanisms to maintain telomere length (11). Most cancers, especially carcinomas, maintain their telomere length by increasing the activity of telomerase reverse transcriptase (TERT), the catalytic unit of the telomerase that adds the six-nucleotide telomere sequences to the end of chromosomes (12). This is made possible through a variety of mechanisms, including amplification of the *TERT* gene (13), expression of transcriptional activators of TERT (14) and CpG methylation at the *TERT* promoter (15). Some cancers maintain telomere length through a telomerase-independent mechanism called alternative lengthening of telomeres (66), which is thought to be dependent on

homologous recombination (67).

Recently, somatic mutations at the *TERT* promoter in human cancer have been reported in two independent studies, using whole-genome sequencing on sporadic melanomas and multipoint linkage analysis in melanoma-prone families (16,17). Both studies demonstrated an unusually high frequency of *TERT* promoter mutations in sporadic melanomas; >70% of cases studied harboured such mutations (16,17). Subsequent studies reported *TERT* promoter mutations in other malignancies, including glioma, urinary bladder carcinoma, tongue squamous cell carcinoma and hepatocellular carcinoma (18-20). The majority of reported mutations are located at two hot-spots, both of which create an 11 bp sequence, resembling the binding motif for ETS-domain transcription factors (16,17). Mutations in these hot-spots were shown to enhance transcriptional activity of the *TERT* promoter in vitro, and were thought to increase the expression of TERT in cancer cells (17).

Cancer genomes have been recently sequenced in a number of gynecological neoplasms, including high-grade ovarian serous carcinoma, low-grade ovarian serous carcinoma, ovarian clear cell carcinoma, uterine endometrioid carcinoma and uterine serous carcinoma (23,24,37,68,69). However, the prevalence and clinical significance of *TERT* promoter mutations in gynecological malignancies remains largely unclear because noncoding regions, including promoter sequences, were not routinely included in the previous analyses. In this study, we analyzed *TERT* promoter mutations in a total of 525 gynecological malignancies, and evaluated the biological and clinical significance of *TERT* promoter mutations in those tumors.

3.1 Methods

3.1.1 Screening *TERT* promoter mutations in gynecological

A total of 250 anonymous fresh-frozen tissues were obtained from the Johns Hopkins Hospital (Baltimore, MD, USA) and 275 anonymous formalin-fixed paraffin-embedded (FFPE) tissues were obtained from Asan Medical Centre (Seoul, Korea), National Taiwan University Hospital (Taipei, Taiwan), Seirei Mikatahara General Hospital (Hamamatsu, Japan), Toronto General Hospital (Toronto, Canada) and University of Tokyo Hospital (Tokyo, Japan). All samples were procured under appropriate approval of institutional review boards. Haematoxylin and eosin (H&E)-stained sections were re-reviewed by pathologists (RC, AA and IS) to confirm the diagnosis before experiments. Genomic DNA from frozen tissue was extracted by the DNeasy blood and tissue kit (Qiagen, Valencia, CA, USA). For FFPE tissues, tumor components were manually dissected from 10 μm sections to reduce normal tissue contamination. Genomic DNA of dissected tumor tissue was then extracted using the QIAmp DNA FFPE tissue kit (Qiagen). We obtained genomic DNA from a total of 525 gynecological malignancies, including 389 ovarian carcinomas, 58 uterine corpus malignancies and 78 uterine cervical carcinomas. More specifically, the ovarian carcinomas included 233 clear cell carcinomas (36 fresh-frozen and 197 FFPE), 43 endometrioid carcinomas (fresh-frozen), 80 high-grade serous carcinomas (fresh-frozen) and 33 low-grade serous carcinomas (fresh-frozen). The uterine corpus malignancies included 24 uterine endometrioid carcinomas (fresh-frozen), 12 uterine serous

carcinomas (fresh-frozen) and 22 leiomyosarcomas (fresh-frozen). The uterine cervical carcinomas included 53 squamous carcinomas (FFPE) and 25 endocervical adenocarcinomas (FFPE). The sources and types of each tissue specimen are specified in the supplementary material (Appendix 3).

The *TERT* promoter region containing the two mutation hot-spots (chr5: 1 295 228 and 1 295 250; hg19) were amplified by polymerase chain reaction (PCR), using the following primers: 5′-M13-CAGCGC TGCCTGAAACTC-3′ and 5′-GTCCTGCCCCTTCAC CTT-3′, where M13 is a universal sequencing primer with sequence 5′-GTAAAACGACGGCCAGT-3′. PCR was performed using the following conditions: 94°C for 2 min; three cycles at 94°C for 15 s, 64°C for 30 s and 70°C for 30 s; three cycles at 94°C for 15 s, 61°C for 30 s and 70°C for 30 s; three cycles at 94°C for 15 s, 58°C for 30 s and 70°C for 30 s; and 30 cycles at 94°C for 15 s, 57°C for 30 s and 70°C for 30 s, followed by 70°C for 5 min. Sanger DNA sequencing was performed by either Macrogen (Rockville, MD, USA) or Beckman Coulter Genomics (Danvers, MA, USA). Mutational analysis was performed using a software package (Mutation Surveyor 4.0; SoftGenetics LLC, PA, USA). All detected *TERT* promoter mutations were confirmed by resequencing.

3.1.2 *TERT* promoter mutation in precursor lesions of ovarian clear cell carcinoma

Nine ovarian clear cell carcinomas with *TERT* promoter mutations contained normal-appearing or atypical endometriotic cyst epithelium adjacent to the carcinoma. The cyst epithelium was carefully microdissected with 27-gauge needles and the genomic DNA of dissected tissue was then extracted using the QIAmp DNA FFPE tissue kit (Qiagen). TERT promoter sequences were analyzed separately for matched samples of clear cell carcinoma and adjacent normal/atypical cystic epithelium.

3.1.3 *TERT* promoter mutation and mRNA expression in ovarian clear cell carcinoma

Cell lines derived from ovarian clear cell carcinomas were cultured in RPMI 1640 medium (Life Technologies, Carlsbad, CA, USA) supplemented with 10% fetal bovine serum (FBS; Atlanta Biological, Lawrenceville, GA, USA) (JHOC5, KK, KOC-7C, OVCA429, OVISE, and OVTOKO) or Dulbecco's modified Eagle's medium (DMEM; Life Technologies) supplemented with 10% FBS (OV207, ES-2 and TOV21G). Genomic DNA was isolated from cell lines using the DNeasy blood and tissue kit (Qiagen) and RNA was extracted using the RNeasy blood and tissue kit (Qiagen). The TERT promoter region was amplified and sequenced and quantitative reverse-transcription PCR was performed, using the iScript cDNA synthesis kit (Bio-Rad, Hercules, CA, USA), Maxima

SYBR green qPCR master mix (Thermo Fisher Scientific, Waltham, MA, USA) and 500 nM primers. The TERT primers used were: 5′-CAGGATCTCCTCACGCAGAC-3′ and 5′GAGCTGACGTGGAAGATGAG-3′. APP was used as an internal expression control because of its stable expression among ovarian cancers. The APP primers used were: 5′-CTGAAGATGGATGCAGAATTCC-3′ and 5′-AAAGAACTTGTAGGTTGGATTT-3′.

3.1.4 Telomere length evaluation in ovarian clear cell carcinoma

Telomere length in ovarian clear cell carcinoma was assessed in our previous study (70) by telomere fluorescence in situ hybridization; 32 ovarian clear cell carcinomas from this previous cohort had quality DNA available for sequencing analysis and were included in the current study. The mean relative telomere length of carcinoma cells normalized to telomere length of stromal cells was calculated as the telomere index (70). Telomere indices were compared between ovarian clear cell carcinomas with *TERT* promoter mutation and those without.

3.1.5 Immunohistochemical staining for ARID1A in ovarian

Immunohistochemistry for ARID1A was performed on a total of 191 ovarian clear cell carcinoma samples. Among them, 99 cases had been previously stained and reported, including 84 from Tokyo (71) and 15 from Hamamatsu, Japan (72); 92

additional cases were analyzed in this report. Immunohistochemical staining for ARID1A was performed using the following protocol. Antigen retrieval was performed on rehydrated tissue sections in a pH 6.0 citrate buffer (Dako, Carpinteria, CA, USA) at 92°C for 30 min. The sections were incubated overnight at 4°C with a rabbit polyclonal antiARID1A antibody (HPA005456, Sigma-Aldrich) at a dilution of 1:1000, and visualized by the EnVision+ System (Dako). For each section, only nuclear staining was scored and positive nuclear staining in stromal cells was used as positive control. The tissues were examined in a blinded fashion without knowledge of clinical information or TERT mutation status.

3.1.6 Sequencing of *PIK3CA* in ovarian clear cell carcinoma

Of the ovarian clear cell carcinoma samples in this study, 45 have been previously sequenced for *PIK3CA* (73). An additional 35 ovarian clear cell carcinomas were sequenced for *PIK3CA* (coding exons 1, 9 and 20), following the afore-mentioned protocol. The amplification primers used for *PIK3CA* sequencing were as follows: proximal coding exon 1, 5′-TGCTTTGGGACAACCATACATC-3′ and 5′CTTGCTTCTTTAAATAGTTCATGCTTT-3′; distal coding exon 1, 5′-CCCCTCCATCAACTTCTTCAA-3′ and 5′-ATTGTATCATACCAATTTCTCGATTG-3′; coding exon 9, 5′-TTTTCTGTAAATCATCTGTGAAT CC-3′ and 5′-TCTCCATTTTAGCACTTACCTGTGA3′ ; proximal coding exon 20, 5′ -M13-TTTGCT

CCAAACTGACCAAAC-3′ and 5′-ACTCCAAAGC CTCTTGCTCA-3′; distal coding exon 20, 5′-ACATT CGAAAGACCCTAGCC-3′ and 5′-M13-GGTCTTTG CCTGCTGAGAGT-3′. The sequencing primers for *PIK3CA* were as follows: proximal coding exon 1, 5′-ACCATCATCAGGTGAACTGTGG-3′; distal coding exon 1, 5′-CTCAAGAAGCAGAAAGGGAAG-3′; coding exon 9, 5′-AAAATATGACAAAGAAAGCTATAT -3′ ; proximal and distal coding exon 20, 5′-GTAAAACGACGGCCAGT-3′ (M13).

3.1.7 Statistical analysis

Two-tailed Fisher's exact test and unpaired t-test were performed to determine the association between mutation status at the *TERT* promoter and clinicopathological features in ovarian clear cell carcinoma. Confidence intervals of mutation frequencies were determined using the Agresti–Coull method, and mutation frequencies of different cancer types were compared using two-tailed Fisher's exact test. Disease-specific overall survival of ovarian clear cell carcinoma, with and without *TERT* promoter mutations, was compared using the Kaplan–Meier method, followed by the log-rank test to determine significance. Comparison of TERT mRNA expression levels between mutant and wild-type ovarian clear cell carcinoma cell lines was performed using one-tailed Mann – Whitney U-test to determine whether *TERT* promoter mutation was associated with increased TERT mRNA expression. For comparison of telomere length between mutant

and wild-type ovarian clear cell carcinomas, one-tailed Mann – Whitney U-test was used when the telomere index was treated as a continuous variable, and Fisher's exact test was used when the telomere index was treated as a binary variable. Two-tailed Fisher's exact test was used to determine the association between *TERT* promoter mutation and loss of ARID1A immunoreactivity, as well as the association between *TERT* promoter mutation and *PIK3CA* mutation in ovarian clear cell carcinoma. $p < 0.05$ was considered significant for all tests. All statistical analyses were performed using R (version 2.14).

3.2 Results

3.2.1 *TERT* promoter mutations in gynecological malignancies

Sequencing analysis was performed in the *TERT* promoter region containing the two previously reported mutation hot-spots. The frequencies of *TERT* promoter mutations in various gynecological cancers are summarized in Table 3-1. *TERT* promoter mutations were detected in 40 of 525 tumor samples (7.6%; 95% CI 5.6–10.2%), the majority occurring in ovarian clear cell carcinomas. While present in only three of 292 other tumors (1.0%; 95% CI: 0.2–3.1%), 37 of 233 (15.9%; 95% CI 11.7–21.2%) ovarian clear cell carcinoma specimens harbored *TERT* promoter mutations. The difference in mutation frequency was significant between clear cell carcinoma and other gynecological neoplasms ($p < 0.0001$, two-tailed Fisher's exact test). Among the 40 mutations, 37 were located at –124 bp from the *TERT* translation start site, while only three were at –146 bp (Figure 3-1). Since ovarian clear cell carcinoma and endometrioid carcinoma are thought to arise from endometriotic cysts (endometriomas) (74), we compared the *TERT* promoter mutation frequency between these two cancer types, and found a significantly higher frequency of *TERT* promoter mutation in ovarian clear cell carcinoma than in ovarian endometrioid carcinoma ($p = 0.0024$, two-tailed Fisher's exact test). There was no significant difference in *TERT* promoter mutation frequency among the ovarian clear cell carcinoma samples collected from different institutions ($p = 0.3137$, Fisher's exact test) or from different countries ($p = 0.9278$, Fisher's exact test).

Table 3-1. Prevalence of *TERT* promoter mutation in gynecologic malignancies

	mutated/total	percentage	Specific mutations *
Ovarian Cancers			
clear cell carcinoma	40/243	16.5%	
clinical sample	37/233	15.9%	c.-124C>T (n=34); c.-146C>T (n=3)
cell line	3/10	30.0%	c.-124C>T(n=2); c.[-138C>T;-139C>T]**(n=1)
endometrioid carcinoma	0/43	0.0%	
high-grade serous carcinoma	0/80	0.0%	
low-grade serous carcinoma	1/33	3.3%	c.-124C>T (n=1)
Uterine Corpus Cancers			
endometrioid carcinoma	0/24	0.0%	
serous carcinoma	0/12	0.0%	
leiomyosarcoma	0/22	0.0%	
Uterine Cervix Cancer			
squamous cell carcinoma	2/53	3.7%	c.-124C>T (n=2)
endocervical adenocarcinoma	0/25	0.0%	

* TERT reference sequence: NM_001193376; **c.-139C>T is a rare reported polymorphism (rs35550267).

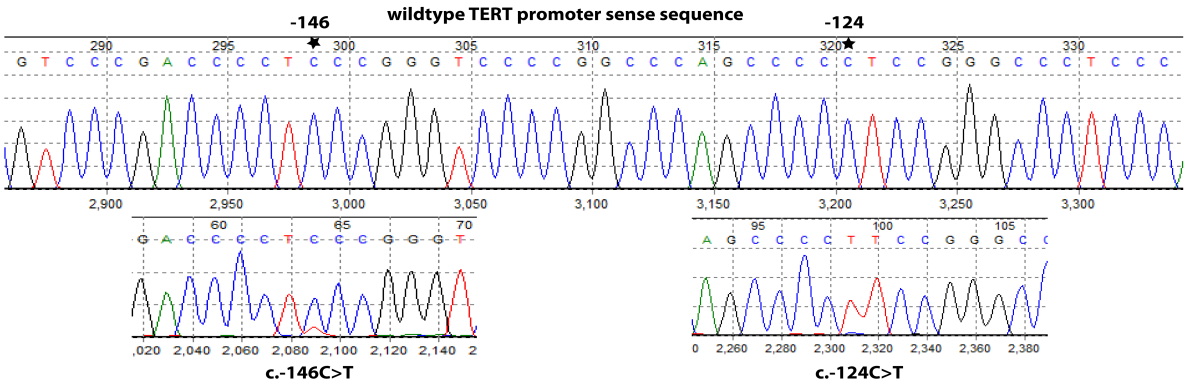

Figure 3-1. *TERT* promoter mutations in ovarian clear cell carcinoma. Shown are representative chromatograms of the wild-type *TERT* promoter and two mutated *TERT* promoters at two different hot spots. Both mutations create an identical 11bp sequence: CCCCTTCCGGG.

3.2.2 *TERT* promoter mutations are not present in endometriotic cyst epithelium adjacent to ovarian clear cell carcinoma

To determine whether *TERT* promoter mutation occurs early in the development of clear cell carcinoma, we analyzed nine ovarian clear cell carcinomas with *TERT* promoter mutations in which there was sufficient endometriotic cyst epithelium for mutational analysis. *TERT* promoter mutations were not identified in any of the nine specimens (Figure 3-2). This finding suggests that *TERT* promoter mutations do not occur early in the tumor progression from endometriotic cyst to clear cell carcinoma.

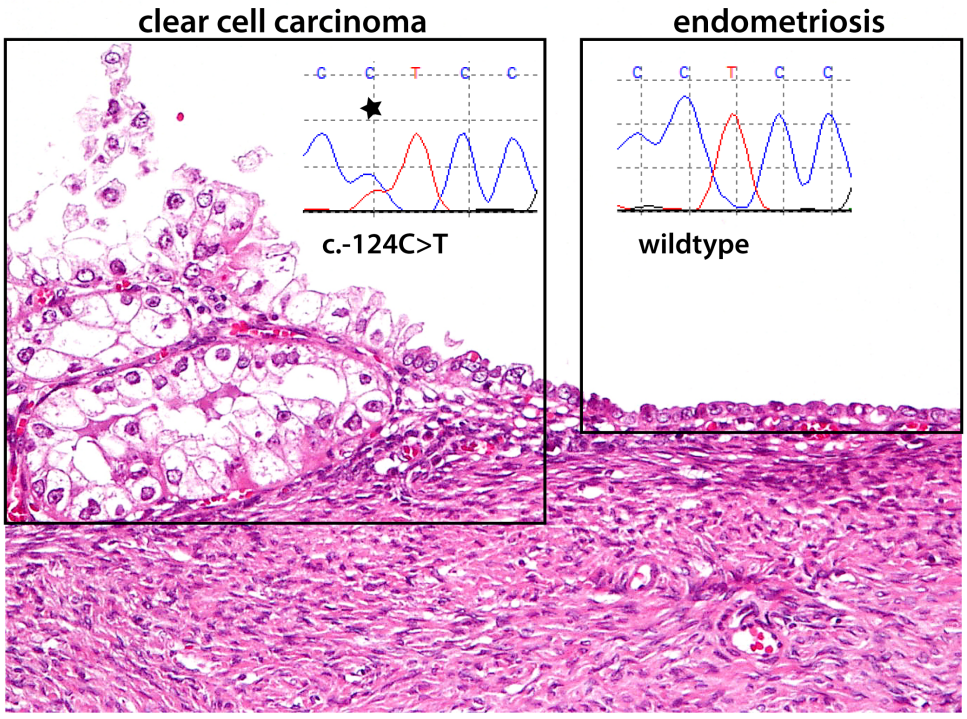

Figure 3-2. An example of ovarian clear cell carcinoma arising from an endometriotic cyst. *TERT* promoter mutation occurred in clear cell carcinoma but not in the adjacent endometriotic cyst epithelium.

3.2.3 *TERT* promoter mutation is associated with elevated mRNA expression in ovarian clear cell carcinoma cell lines

In a screen of nine ovarian clear cell carcinoma cell lines, we found that three (33.3%; 95% CI 11.7 – 64.9%) contained mutations at the *TERT* promoter. Cell lines JHOC5 and OV207 carried the hot-spot mutation c.–124C>T, whereas the ES-2 cell line harbored the less common tandem mutation c.[– 139C>T; – 138C>T], which has been reported in a few melanomas (16). Cell lines harboring the c.–124C>T mutation showed a five to eight-fold increase of TERT mRNA expression as compared to the cell lines without *TERT* promoter mutation (Figure 1c). Overall, clear cell carcinoma cell lines with *TERT* promoter mutations expressed higher levels of TERT mRNA than those with wild-type sequence (p = 0.0238, one-tailed Mann – Whitney U-test; Figure 3-3).

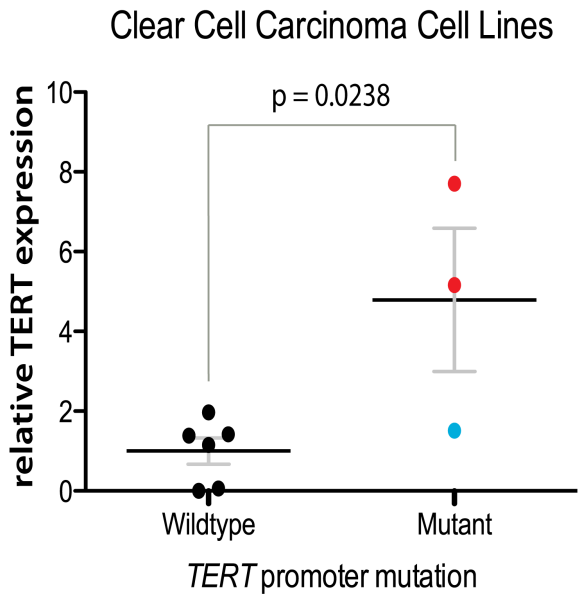

Figure 3-3. Ovarian clear cell carcinoma cell lines with mutated TERT promoter have increased expression of TERT mRNA. Red circles: OV207 and JHOC5 cells with c.-124C>T mutation; blue circle: ES-2 cell with c.[-139C>T;-138C>T] tandem mutation; black horizontal bar: mean; error bar: SEM.

3.2.4 Ovarian clear cell carcinomas with *TERT* promoter mutation tend to have longer telomere length

In a previous study (70), we assessed the telomere length in different types of ovarian carcinomas and found that clear cell carcinoma had the longest average telomere length compared to other histological types of ovarian carcinomas. To examine the relationship between *TERT* promoter mutation and telomere length, we compared *TERT* promoter mutation status and telomere length data in 32 ovarian clear cell carcinomas, including six with *TERT* promoter mutations and 26 without. There was a trend towards longer telomere length in ovarian clear cell carcinomas with *TERT* promoter mutation relative to those without, although statistical significance was not reached (median 1.1 versus 0.36; p = 0.2278, one-tailed Mann-Whitney U test; Figure 3-4). Similarly, when telomere length was coded as a binary variable (telomere index >1 versus ≤1), clear cell carcinomas with *TERT* promoter mutation showed higher, although not statistically significant, frequency of possessing long telomere length (index >1) than those without *TERT* promoter mutation (3/6 versus 3/26; p = 0.0629, Fisher's exact test; Figure 3-4).

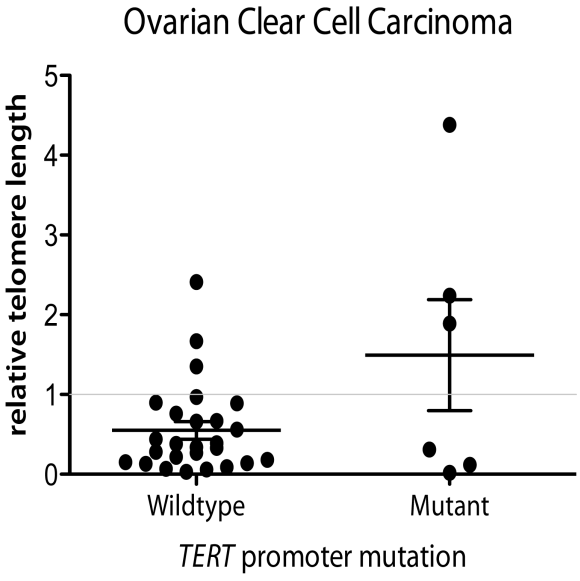

Figure 3-4. Comparison of telomere length between ovarian clear cell carcinomas with and without *TERT* promoter mutation. Black horizontal bar: mean; error bar: SEM; gray horizontal bar: cutoff for binary analysis.

3.2.5 *TERT* promoter mutation is inversely associated with loss of ARID1A protein expression in ovarian clear cell carcinomas

ARID1A, a tumor suppressor gene, is the most frequently mutated gene in ovarian clear cell carcinoma (23,75). It has been shown that loss of ARID1A expression is a surrogate marker for its mutation (71). To examine the correlation between *TERT* promoter mutation and ARID1A aberration, we compared the *TERT* promoter mutation status and ARID1A protein expression data in 191 of the analyzed ovarian clear cell carcinomas. Loss of ARID1A protein expression was detected by immunohistochemistry in 115/191 (60.4%) ovarian clear cell carcinoma samples: in four of 31 (12.9%) cases harboring the *TERT* promoter mutation compared to 111 of 160 (69.4%) cases without (Table 3-2). This result indicates a strong tendency towards mutual exclusivity between *TERT* promoter mutation and lack of ARID1A expression (odds ratio = 0.066, $p = 4.4 \times 10^{-9}$, two-tailed Fisher's exact test).

OR = 0.0664 $P = 4.4*10^{-9}$	***TERT*** **mutant**	***TERT*** **wild-type**	**Total**
ARID1A negative	**4**	**111**	**115**
ARID1A positive	**27**	**49**	**76**
Total	**31**	**160**	**191**

Table 3-2. Correlation between *TERT* promoter mutation and ARID1A immunoreactivity in ovarian clear cell carcinomas.

3.2.6 *TERT* promoter mutation and *PIK3CA* mutation tend to be mutually exclusive in ovarian clear cell carcinoma

PIK3CA is the second most commonly mutated gene in ovarian clear cell carcinoma (73). To determine the correlation between *TERT* promoter mutation and *PIK3CA* mutation, we sequenced *PIK3CA* hot-spot coding exons 1, 9 and 20 for 80 ovarian clear cell carcinomas, 45 of which, including nine ovarian clear cell carcinoma cell lines, had been reported previously (73). Interestingly, we observed a strong tendency towards mutual exclusivity between *TERT* promoter and *PIK3CA* mutations (odds ratio = 0.074; p = 0.0019, two-tailed Fisher's exact test), with only one of the 80 samples harboring both *TERT* promoter and *PIK3CA* mutations (Table 3-3). All clinical samples that had *PIK3CA* mutation, *TERT* promoter mutation and ARID1A immunostaining data (n = 71) are summarized in Figure 3-5.

OR = 0.0744 P = 0.0019	***TERT*** **mutant**	***TERT*** **wild-type**	**Total**
PIK3CA **mutant**	**1**	**27**	**28**
PIK3CA **wild-type**	**18**	**34**	**52**
Total	**19**	**61**	**80**

Table 3-3. Correlation between *TERT* promoter mutation and *PIK3CA* mutation in ovarian clear cell carcinomas.

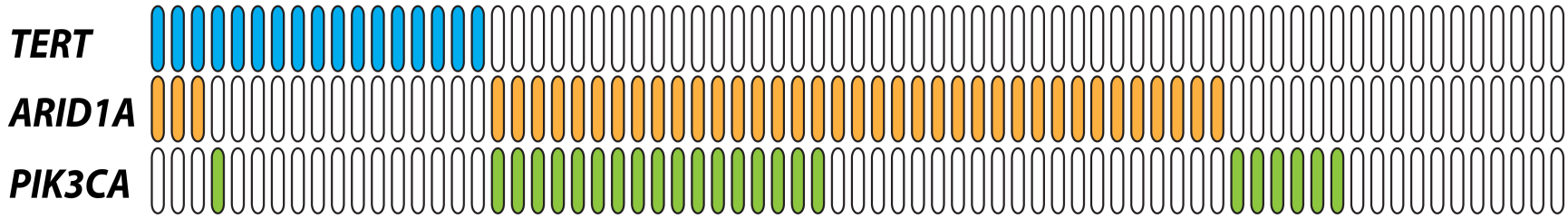

64**Figure 3-5.** Mutation status of *TERT* promoter and *PIK3CA,* and immunostaining result of ARID1A in 71 clear cell carcinoma tissues.

Blue: *TERT* promoter mutation; orange: loss of ARID1A expression; green: *PIK3CA* mutation.

3.2.7 *TERT* promoter mutation has no impact on prognosis in ovarian clear cell carcinoma

Next, we determined correlations between *TERT* promoter mutation status and clinicopathological features of ovarian clear cell carcinoma (Table 3-4). We found no association between *TERT* promoter mutation and patients' age, FIGO stage, lymph node metastasis, nuclear atypia and histological features. In 196 ovarian clear cell carcinomas with available survival data, there was no significant difference in disease-specific overall survival between patients with *TERT* promoter mutations and those without (hazard ratio 0.9790; 95% CI 0.4347–2.205; p = 0.9592, log-rank test; Figure 3-6).

Table 3-4. Clinicopathological features of ovarian clear cell carcinoma

	Mutant	Wild-type	*P* value
Age (n = 196)			
mean ± SD	51.6 ± 10.4	51.8 ± 9.3	0.9106
median	52	51	
range	33-73	25-76	
FIGO stage (n = 175)			
I / II	22	112	1.0000
III / IV	7	34	
Lymph node metastasis (n = 88)			
positive	0	15	0.1992
negative	11	62	
Nuclear atypia (n = 83)			
mild	3	25	0.8999
moderate	5	33	
severe	1	16	
Predominant histological pattern (n = 83)			
papillary	3	36	0.6623

tubulocystic	3	21
solid	3	17

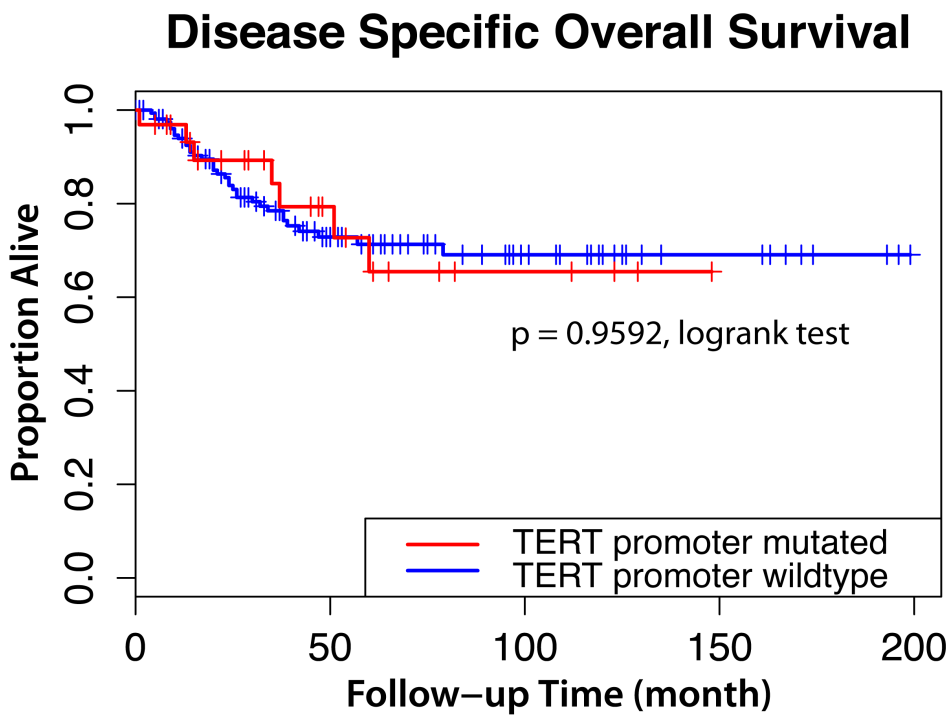

Figure 3-6. Kaplan-Meier survival curves of ovarian clear cell carcinoma patients. Overall survival time of patients with *TERT* promoter mutation is similar to patients with wild-type sequence.

3.3 Discussion

In this study, we found that among all types of gynecological cancers examined, ovarian clear cell carcinomas had the highest frequency of *TERT* mutations. Ovarian clear cell carcinoma is a unique type of ovarian cancer and advanced stage clear cell carcinoma is associated with a poorer prognosis because the tumor is resistant to platinum-based chemotherapy (76). Ovarian clear cell carcinoma has been thought to develop from endometriotic cyst (endometrioma) of the ovary, which has also been considered a precursor lesion of ovarian endometrioid carcinoma (74). Ovarian clear cell carcinoma and endometrioid carcinoma share several molecular genetic alterations, including activating mutations in *PIK3CA* and inactivating mutations and loss of expression in ARID1A and PTEN (73,75). Despite these similarities, ovarian clear cell carcinoma, as compared to ovarian endometrioid carcinoma, is characterized by distinct molecular features, including up-regulation of hepatocyte nuclear factor-1β and less frequent mutation in *CTNNB1* (68,73,77). The higher mutation frequency in *TERT* promoters, as reported here, underscores the difference in the pathogenesis of ovarian clear cell carcinoma and ovarian endometrioid carcinoma.

Analysis of the mutation types reveals the likely mechanism by which *TERT* promoter mutations contribute to tumor development. Both hot-spot mutations (c. – 124C>T and c. – 146C>T) at the *TERT* promoter create an 11 bp sequence that contains the binding motif (CCGGAA) of ETS-domain transcription factor family members, and both mutations have been shown to increase transcriptional activity of the *TERT* promoter (17). Likewise, in this study, we observed that *TERT* promoter mutation was associated

with higher TERT mRNA expression in the ovarian clear cell carcinoma cell lines examined. The less common tandem mutation c.[– 139C>T; – 138C>T] also generates an ETS binding motif. ETS-domain transcription factors act as activators or repressors of a compendium of genes that are involved in diverse biological processes, many of which are cancer-related, including cellular proliferation, inhibition of apoptosis, regulation of cellular senescence and angiogenesis (78). Abnormalities of ETS-domain family members have been implicated in a variety of human cancers through different mechanisms, including amplification, mutation, and translocation that generates fusion proteins (79). In addition, several ETS-domain transcription factors are activated by mitogen-activated protein kinase (MAPK), which is commonly up-regulated in cancer cells (78). Since all hot-spot mutations result in the creation of a new ETS-binding motif that is accessible to ETS factors, it is likely that these mutations turn the *TERT* promoter into a target of ETS-domain transcription factors.

Several molecular genetic abnormalities, including *ARID1A* mutation, *PIK3CA* mutation and *PTEN* deletion (loss of heterozygosity), have been thought to be early events in the development of ovarian clear cell carcinoma, as these alterations are frequently detected in both carcinoma and adjacent benign epithelium within the endometriotic cyst, the precursor lesion of ovarian clear cell carcinoma (72,80-82). In this study, we did not detect *TERT* promoter mutations in the contiguous endometriotic cyst epithelium associated with ovarian clear cell carcinomas that harbored *TERT* promoter mutations. This result indicates that *TERT* promoter mutation is unlikely to be an early event in tumorigenesis. This finding can be explained by the telomere crisis theory during tumor evolution (83,84), which proposes that incipient tumor clones slowly evolve, while

gradually acquiring somatic mutations, until they reach a sufficient number of cell divisions, when accumulated telomere erosion triggers senescence and/or deleterious genomic instability. Therefore, in order to survive, pre-cancer cells need to develop a strategy to escape from telomere crisis. *TERT* promoter mutation is dispensable during the very early stage of tumor initiation because it does not provide a survival advantage until telomere attrition becomes evident. During the telomere crisis stage, only the cells that acquire the ability to maintain telomere length through ways such as *TERT* promoter mutation will progress through this selection pressure.

Recent genome-wide analysis has revealed that *ARID1A*, a tumor suppressor gene, is the most frequently mutated gene in ovarian clear cell carcinoma; somatic mutation of *ARID1A* was found in approximately half of ovarian clear cell carcinomas (23,75). Because *ARID1A* mutations correlate with loss of expression, immunohistochemistry has been used to assess *ARID1A* mutation status on tissue sections (71). In this study, we found that *TERT* promoter mutation was inversely associated with loss of ARID1A protein expression (presumably through mutations) in ovarian clear cell carcinoma. This implies that intact ARID1A-containing BAF chromatin remodeling complexes may be required for TERT re-expression mediated by a mutated *TERT* promoter. Alternatively, loss of ARID1A may facilitate incipient tumor cells to achieve replicative immortality. Thus, it is not essential for those tumor cells to acquire *TERT* promoter mutation.

PIK3CA, an oncogene, was found to be mutated in about one-third of ovarian clear cell carcinomas (73). Interestingly, in this study, we demonstrated that *TERT* promoter mutation and *PIK3CA* mutation showed strong tendency towards mutual

exclusivity in 80 ovarian clear cell carcinoma samples examined. The PI3K/AKT signaling pathway plays a role in maintaining self-renewal in embryonic stem cells (85) and cancer stem cells (86-89). Moreover, the PI3K/AKT pathway is involved in transcriptional up-regulation of TERT and activation of telomerase through phosphorylation (90-93). Therefore, like *TERT* promoter mutation, activating *PIK3CA* mutation confers a growth advantage upon cancer cells by overcoming the hurdle of replicative senescence. Consequently, *TERT* promoter mutation is not selected in ovarian clear cell carcinomas with *PIK3CA* mutations.

Ovarian clear cell carcinoma patients with *TERT* promoter mutation have no difference in disease specific overall survival as compared to those without *TERT* promoter mutation. This finding contrasts with a previous study, in which primary gliobastoma with *TERT* promoter mutations had a worse prognosis than patients without *TERT* mutations (18). We note that most glioblastomas that do not have *TERT* promoter mutations exhibit the alternative lengthening of telomere (ALT) phenotype, which has been reported as an independent indicator of better prognosis (94), whereas only a small proportion of ovarian clear cell carcinomas exhibit the ATL phenotype (66). Therefore, the discrepancy is not surprising. To learn more about the effect of *TERT* promoter mutation on patients' outcome, it would be helpful to compare the prognosis between *TERT* promoter mutants and wild-types in other cancers in which ALT is uncommon, such as hepatocellular carcinomas, urothelial carcinomas or squamous cell carcinomas of the tongue (18,19,66).

In summary, we found that *TERT* promoter mutations were most common in ovarian clear cell carcinoma among gynecological malignancies. *TERT* promoter

mutation was associated with higher TERT mRNA levels in ovarian clear cell carcinoma cell lines. *TERT* promoter mutation showed strong tendency towards mutual exclusivity with loss of ARID1A expression and *PIK3CA* mutation in ovarian clear cell carcinoma. These results, in conjunction with our previous report showing longer telomeres in ovarian clear cell carcinomas compared to other types of ovarian cancer, suggest an important role of telomere biology in the development of ovarian clear cell carcinoma.

3.4 Acknowledgements

This study was supported by the National Institutes of Health (NIH; Grant Nos R21CA165807 and RO1CA129080) and the US Department of Defense (CDMRP Grant No. W81XWH-11-2-0230). We appreciated the tissue specimens previously contributed by Drs. Kuo and Mao from the Department of Pathology at the National Taiwan University Hospital.

4 Conclusions

To our knowledge, the integrative genomic analysis presented here is the first one trying to portray the genomic landscape of uterine serous carcinoma. We demonstrated that mutations in *TP53*, *PIK3CA*, *FBXW7*, and *PPP2R1A*, as well as amplification of *CCNE1*, are the most common genetic aberrations in this type of cancer. Both *FBXW7* mutation and *CCNE1* amplification, being mutually exclusive events and affecting more than half of uterine serous carcinomas, increase the expression of cyclin E protein, which facilitates cell cycle progression. On the other hand, activating mutation and/or amplification of *PIK3CA*, together affecting 48% of uterine serous carcinoma, enhance PI3K signaling pathway and subsequently, AKT activity, which promotes cellular proliferation and survival. Both PI3K and cyclin-E/FBXW7 pathways are likely work in concert to promote tumorigenesis in uterine serous carcinoma. These results suggest that inhibitors targeting PI3K or cyclin E pathways are potentially effective treatments against uterine serous carcinoma, especially at advanced-stage when the conventional chemotherapy is often not effective.

In this study, we also showed that the mutations in *FBXW7*, *PIK3CA*, *PPP2R1A*, and *TP53* are almost always concordant between uterine serous carcinoma and its precursor, serous endometrial intraepithelial carcinoma. This result indicates that mutations of these genes occurred before the in-situ carcinomas turn into invasive ones. This finding, if confirmed in a larger series of samples, may have clinical implications:

screening mutations in these genes can be used for early diagnosis of uterine serous carcinoma at a preinvasive stage in endometrial curettage or cervical lavage specimens using emerging molecular techniques that are highly sensitive.

In the second study, I discovered that ovarian clear cell carcinoma has a high frequency of *TERT* promoter mutations, a characteristic not shared by other major subtypes of gynecologic cancers, including ovarian endometrioid carcinoma. Ovarian endometrioid carcinoma bears a strong resemblance to ovarian clear cell carcinoma: they are both thought to develop from endometriotic cyst of the ovary (74); they share several molecular genetic features, with PI3K and ARID1A the two most commonly deregulated pathways in both carcinomas (73,75). Our discovery of higher mutation frequency in *TERT* promoter in clear cell carcinoma highlights the difference in the pathogenesis of these two carcinomas. Moreover, this molecular genetic attribute has the potential to serve as a useful biomarker for differential diagnosis between ovarian clear cell carcinoma and other subtypes of ovarian cancers, and may have an impact on personalized cancer management if small molecules targeting the *TERT* promoter function are developed in the future.

Almost all the *TERT* promoter mutations detected are confined to two hot-spots, both creating an 11-bp sequence that contains the binding motif of ETS-domain transcription factors. The promoter mutations are associated with higher TERT transcriptional activity. It is likely that the hot-spot mutations make the TERT promoter accessible to ETS-domain transcription factors, thereby inducing TERT mRNA transcription. A deeper investigation into the potential interaction between the mutated TERT promoter and ETS-domain is warranted, as this interaction may serve as a cancer-

specific therapeutic target.

ARID1A, encoding a subunit of the SWI/SNF chromatin remodeling complex, is mutated in about half of ovarian clear cell carcinomas (23,75). In this study, we found that *TERT* promoter mutations tend to be mutually exclusive with loss of ARID1A expression. This is a clue suggesting that ARID1A may play a role in telomere biology. One explanation is that ARID1A-containing SWI/SNF chromatin remodeling complexes may be required for TERT re-expression mediated by a mutated TERT promoter. Hence, the cancer cells without functioning ARID1A cannot employ *TERT* promoter mutation as a strategy to re-activate telomerase expression. Alternatively, loss of ARID1A may facilitate incipient tumor cells to overcome replicative senescence. Thus, it is not essential for tumor cells with *ARID1A* mutation to acquire *TERT* promoter mutation. Future work should focus on answering whether and how ARID1A actually works to regulate telomere homeostasis.

In summary, our study of the genome of uterine serous carcinoma identified the major genetic culprits in the development of this tumor: p53, cyclin E-FBXW7, and PI3K pathways. Our large scale screening of gynecologic cancers discovered frequent *TERT* promoter mutations in ovarian clear cell carcinoma. The findings generated from these works not only advance our understanding of the pathogenesis of uterine serous carcinoma and ovarian clear cell carcinoma, but also pave the way for future development of better classification and treatment for these two clinically aggressive cancers.

Appendix 1

Mutations identified in the discovery set†							
Sample	Gene	Transcript	Nucleotide (genomic)*	Nucleotide (cDNA)	Protein (amino acid)	Mutation Type	Validation
702TS	*ABCB4*	NM_000443.3	g.chr7:86894096C>A	c.1970G>T	p.(Gly657Val)	missense	somatic
555TS	*ABCC2*	NM_000392.2	g.chr10:101557822C>T	c.1669-8C>T	p.?	splice site	no data
702TS	*ABCD2*	NM_005164.2	g.chr12:38297194T>C	c.983A>G	p.(Asp328Gly)	missense	no data
993TCS	*ABCE1*	NM_002940.2	g.chr4:146260738T>C	c.1127T>C	p.(Val376Ala)	missense	no data
702TS	*ABHD12*	NM_001042472.2	g.chr20:25245700C>A	c.557G>T	p.(Arg186Leu)	missense	no data
DM851T	*ABHD3*	NM_138340.3	g.chr18:17538460C>T	c.162+3G>A	p.?	splice site	no data
863TCS	*ABI3BP*	NM_015429.3	g.chr3:102068424C>T	c.998G>A	p.(Arg333Gln)	missense	no data
900T	*ACAD8*	NM_014384.2	g.chr11:133634760C>T	c.616C>T	p.(Arg206*)	nonsense	no data
FM474T	*ACTA1*	NM_001100.3	g.chr1:227634516C>T	c.656G>A	p.(Cys219Tyr)	missense	somatic
FM403T	*ADAD2*	NM_139174.3	g.chr16:82787816C>T	c.1835C>T	p.(Ala612Val)	missense	somatic
900T	*ADAM29*	NM_001130703.1	g.chr4:176135307G>A	c.2056G>A	p.(Val686Ile)	missense	somatic
DM851T	*ADAMTS12*	NM_030955.2	g.chr5:33563151T>A	c.4684A>T	p.(Thr1562Ser)	missense	somatic
555TS	*ADNP*	NM_015339.2	g.chr20:48944374T>C	c.284A>G	p.(Asn95Ser)	missense	no data
702TS	*AGBL2*	NM_024783.3	g.chr11:47670288T>C	c.791A>G	p.(Asn264Ser)	missense	no data
702TS	*AIG1*	NM_016108.2	g.chr6:143696215A>T	c.619A>T	p.(Met207Leu)	missense	no data
863TCS	*AKAP9*	NM_005751.3	g.chr7:91562389G>A	c.9695G>A	p.(Gly3232Glu)	missense	somatic
DM851T	*ALDH9A1*	NM_000696.3	g.chr1:163898996_163898997del	c.1476_1477del	p.(Asn493Argfs*20)	frameshift	somatic
FM474T	*ALPK1*	NM_025144.3	g.chr4:113572735G>A	c.2583G>A	p.(Met861Ile)	missense	somatic
DM851T	*AMOTL2*	NM_016201.2	g.chr3:135569123G>A	c.947C>T	p.(Ala316Val)	missense	somatic
340TS	*AMPD2*	NM_004037.6	g.chr1:109973565G>T	c.1954G>T	p.(Asp652Tyr)	missense	somatic
FM474T	*ANAPC4*	NM_013367.2	g.chr4:25000869G>A	c.529G>A	p.(Val177Ile)	missense	somatic
900T	*ANK3*	NM_020987.2	g.chr10:61501932G>A	c.8713C>T	p.(Arg2905Cys)	missense	somatic
993TCS	*ANKFN1*	NM_153228.2	g.chr17:51875250G>A	c.1065G>A	p.(Trp355*)	nonsense	no data
FM403T	*ANLN*	NM_018685.2	g.chr7:36426850G>T	c.2135G>T	p.(Cys712Phe)	missense	no data
900T	*APBB1*	NM_001164.2	g.chr11:6380974G>A	c.1081C>T	p.(Arg361Trp)	missense	no data
900T	*ARAP2*	NM_015230.2	g.chr4:35825583T>A	c.3181A>T	p.(Arg1061*)	nonsense	no data
702TS	*ARFIP2*	NM_012402.2	g.chr11:6455522A>C	c.870+2T>G	p.?	splice site	somatic
FM403T	*ARPC1B*	NM_005720.2	g.chr7:98826661G>C	c.707+3G>C	p.?	splice site	somatic
DM851T	*ATAD5*	NM_024857.3	g.chr17:26186100C>T	c.875C>T	p.(Pro292Leu)	missense	somatic
FM403T	*ATN1*	NM_001007026.1	g.chr12:6920322C>T	c.3233C>T	p.(Pro1078Leu)	missense	somatic
900T	*ATP2A1*	NM_004320.3	g.chr16:28806487G>A	c.871G>A	p.(Gly291Arg)	missense	somatic
900T	*ATP6AP1L*	NM_001017971.1	g.chr5:81637056G>A	c.80G>A	p.(Trp27*)	nonsense	somatic
FM403T	*ATR*	NM_001184.3	g.chr3:143760841G>C	c.1674C>G	p.(Asp558Glu)	missense	somatic
900T	*ATXN2*	NM_002973.2	g.chr12:110443069G>A	c.1268C>T	p.(Thr423Ile)	missense	no data
340TS	*BAX*	NM_138761.2	g.chr19:54150778C>T	c.109C>T	p.(Arg37*)	nonsense	somatic

FM474T	*BCL9*	NM_004326.2	g.chr1:145558572C>T	c.1987C>T	p.(Pro663Ser)	missense	somatic
863TCS	*BCOR*	NM_001123385.1	g.chrX:39818331C>A	c.1212G>T	p.(Gln404His)	missense	no data
863TCS	*BRCA2*	NM_000059.3	g.chr13:31811617G>T	c.5125G>T	p.(Asp1709Tyr)	missense	somatic
993TCS	*BRPF1*	NM_004634.2	g.chr3:9756161G>T	c.1078G>T	p.(Val360Phe)	missense	somatic
366TS	*BSN*	NM_003458.3	g.chr3:49670367C>G	c.8374C>G	p.(Gln2792Glu)	missense	somatic
863TCS	*BSN*	NM_003458.3	g.chr3:49664680G>A	c.2687G>A	p.(Arg896His)	missense	somatic
993TCS	*C10orf131*	NM_001130446.2	g.chr10:97677018dup	c.250dup	p.(Ser84Lysfs*10)	frameshift	somatic
993TCS	*C12orf51*	NM_001109662.2	g.chr12:111141659dup	c.6473dup	p.(Glu2159Glyfs*5)	frameshift	somatic
900T	*C15orf2*	NM_018958.2	g.chr15:22475363G>A	c.3256G>A	p.(Ala1086Thr)	missense	no data
FM474T	*C18orf19*	NM_001098801.1	g.chr18:13672046G>A	c.31C>T	p.(Arg11*)	nonsense	no data
366TS	*C19orf45*	NM_198534.1	g.chr19:7476944T>C	c.1058T>C	p.(Phe353Ser)	missense	no data
FM403T	*C21orf66*	NM_016631.3	g.chr21:33045182C>G	c.1640G>C	p.(Gly547Ala)	missense	no data
702TS	*C22orf43*	NM_016449.3	g.chr22:22285482G>A	c.679C>T	p.(His227Tyr)	missense	no data
FM403T	*C4orf49*	NM_032623.3	g.chr4:140407397G>T	c.529C>A	p.(Pro177Thr)	missense	no data
900T	*C5orf38*	NM_178569.2	g.chr5:2806457C>A	c.392C>A	p.(Pro131Gln)	missense	no data
DM851T	*C6orf138*	NM_001013732.3	g.chr6:47954206G>A	c.2333C>T	p.(Ser778Leu)	missense	no data
702TS	*C8orf48*	NM_001007090.2	g.chr8:13469664C>G	c.793C>G	p.(Leu265Val)	missense	no data
366TS	*CACHD1*	NM_020925.2	g.chr1:64820479G>A	c.161G>A	p.(Arg54Gln)	missense	no data
FM474T	*CACNA1A*	NM_001127222.1	g.chr19:13183920G>T	c.6300C>A	p.(Asn2100Lys)	missense	somatic
702TS	*CACNA1B*	NM_000718.1	g.chr9:140087825G>A	c.4739G>A	p.(Arg1580His)	missense	somatic
FM474T	*CACNA1F*	NM_005183.2	g.chrX:48948687G>A	c.5788C>T	p.(Arg1930Cys)	missense	somatic
FM474T	*CAMSAP1*	NM_015447.3	g.chr9:137852716del	c.3612del	p.(Ser1204Argfs*2)	frameshift	somatic
366TS	*CAND1*	NM_018448.2	g.chr12:65985615C>G	c.1900C>G	p.(Leu634Val)	missense	somatic
555TS	*CAP1*	NM_006367.3	g.chr1:40309231G>A	c.1337G>A	p.(Gly446Asp)	missense	no data
555TS	*CASR*	NM_000388.3	g.chr3:123485980G>A	c.2489G>A	p.(Gly830Asp)	missense	no data
900T	*CATSPER3*	NM_178019.1	g.chr5:134360063C>T	c.454C>T	p.(Arg152Cys)	missense	no data
FM474T	*CCAR1*	NM_018237.2	g.chr10:70172262T>G	c.448T>G	p.(Phe150Val)	missense	somatic
900T	*CCBL1*	NM_004059.4	g.chr9:130644881G>T	c.74C>A	p.(Ala25Asp)	missense	no data
863TCS	*CCDC73*	NM_001008391.2	g.chr11:32591585T>C	c.2855A>G	p.(Lys952Arg)	missense	no data
FM474T	*CCDC88A*	NM_001135597.1	g.chr2:55414868C>T	c.2593G>A	p.(Glu865Lys)	missense	no data
FM474T	*CDK9*	NM_001261.3	g.chr9:129590061C>T	c.280C>T	p.(Arg94Cys)	missense	somatic
900T	*CEP290*	NM_025114.3	g.chr12:87001054G>T	c.4897C>A	p.(Gln1633Lys)	missense	somatic
863TCS	*CHADL*	NM_138481.1	g.chr22:39963347C>G	c.1675G>C	p.(Glu559Gln)	missense	somatic
900T	*CHD4*	NM_001273.2	g.chr12:6567357C>T	c.3485G>A	p.(Arg1162Gln)	missense	somatic
863TCS	*CHN2*	NM_004067.2	g.chr7:29360793G>A	c.77G>A	p.(Trp26*)	nonsense	no data
FM474T	*CHRNB4*	NM_000750.3	g.chr15:76708405A>C	c.1297T>G	p.(Phe433Val)	missense	no data
702TS	*CIT*	NM_007174.2	g.chr12:118745042_118745045del	c.1076_1079del	p.(Phe359Serfs*45)	frameshift	somatic
FM474T	*CLK1*	NM_001162407.1	g.chr2:201430948T>C	c.784A>G	p.(Ser262Gly)	missense	no data
FM474T	*CLUL1*	NM_014410.4	g.chr18:623407C>G	c.966C>G	p.(Cys322Trp)	missense	somatic
993TCS	*CNGB3*	NM_019098.4	g.chr8:87749503G>A	c.503C>T	p.(Thr168Met)	missense	somatic
900T	*CNTNAP2*	NM_014141.4	g.chr7:146448999C>T	c.755-5C>T	p.?	splice site	somatic
FM403T	*COG5*	NM_006348.2	g.chr7:106752162A>C	c.1160T>G	p.(Val387Gly)	missense	somatic
863TCS	*COG7*	NM_153603.3	g.chr16:23311237C>T	c.2111G>A	p.(Ser704Asn)	missense	somatic
DM851T	*COIL*	NM_004645.2	g.chr17:52382289T>G	c.1313A>C	p.(Gln438Pro)	missense	somatic

555TS	*COL19A1*	NM_001858.4	g.chr6:70951308C>T	c.2776-8C>T	p.?	splice site	no data
863TCS	*COL23A1*	NM_173465.2	g.chr5:177605855G>A	c.1413+6C>T	p.?	splice site	no data
DM851T	*CRISPLD1*	NM_031461.5	g.chr8:76100392G>T	c.1301G>T	p.(Gly434Val)	missense	no data
702TS	*CRNKL1*	NM_016652.4	g.chr20:19966059_19966061del	c.2290_2292del	p.(Glu764del)	in-frame indel	no data
555TS	*CSE1L*	NM_001316.2	g.chr20:47122567A>T	c.992A>T	p.(Lys331Met)	missense	no data
340TS	*CTNND2*	NM_001332.2	g.chr5:11071136C>T	c.3034G>A	p.(Val1012Ile)	missense	somatic
555TS	*CYBB*	NM_000397.3	g.chrX:37537884A>G	c.364A>G	p.(Asn122Asp)	missense	no data
FM474T	*CYBRD1*	NM_024843.3	g.chr2:172119387C>T	c.665C>T	p.(Pro222Leu)	missense	somatic
340TS	*CYP2D6*	NM_000106.4	g.chr22:40855113T>C	c.371A>G	p.(Tyr124Cys)	missense	no data
702TS	*DAZAP1*	NM_170711.1	g.chr19:1383662C>G	c.1210C>G	p.(Gln341Glu)	missense	somatic
993TCS	*DBC1*	NM_014618.2	g.chr9:120969598C>T	c.1871G>A	p.(Arg624Gln)	missense	somatic
900T	*DCST2*	NM_144622.2	g.chr1:153268325G>T	c.1342+8C>A	p.?	splice site	no data
366TS	*DECR2*	NM_020664.3	g.chr16:400983G>A	c.673G>A	p.(Ala225Thr)	missense	no data
FM403T	*DEF6*	NM_022047.3	g.chr6:35373661C>T	c.50C>T	p.(Ala17Val)	missense	no data
FM474T	*DEFA4*	NM_001925.1	g.chr8:6781741C>T	c.91G>A	p.(Gly31Ser)	missense	no data
702TS	*DEPDC5*	NM_014662.2	g.chr22:30596648G>C	c.3310G>C	p.(Asp1104His)	missense	no data
702TS	*DGKB*	NM_004080.1	g.chr7:14613621G>A	c.1399C>T	p.(Gln467*)	nonsense	no data
702TS	*DGKI*	NM_004717.2	g.chr7:136732696G>T	c.2948C>A	p.(Pro983His)	missense	somatic
FM403T	*DGKQ*	NM_001347.2	g.chr4:952591C>T	c.451+8G>A	p.?	splice site	somatic
900T	*DHRS11*	NM_024308.3	g.chr17:32028805G>A	c.452+6G>A	p.?	splice site	somatic
FM403T	*DHX37*	NM_032656.3	g.chr12:124016217G>A	c.1685C>T	p.(Ala562Val)	missense	somatic
702TS	*DHX9*	NM_001357.4	g.chr1:181079160G>C	c.220G>C	p.(Glu74Gln)	missense	no data
555TS	*DIO2*	NM_000793.4	g.chr14:79739389C>T	c.223-5G>A	p.?	splice site	no data
FM403T	*DKKL1*	NM_014419.3	g.chr19:54560885G>T	c.348G>T	p.(Glu116Asp)	missense	somatic
900T	*DNAH11*	NM_003777.3	g.chr7:21621329G>A	c.3925G>A	p.(Ala1309Thr)	missense	somatic
FM403T	*DNAH11*	NM_003777.3	g.chr7:21711649T>C	c.6537T>C	p.(Val2179Ala)	missense	no data
900T	*DOCK9*	NM_001130048.1	g.chr13:98281720C>G	c.4449G>C	p.(Lys1483Asn)	missense	no data
FM474T	*DSCR3*	NM_006052.1	g.chr21:37522393C>G	c.658+1G>C	p.?	splice site	no data
900T	*E2F8*	NM_024680.2	g.chr11:19212891G>T	c.742C>A	p.(Leu248Ile)	missense	no data
FM403T	*EML1*	NM_001008707.1	g.chr14:99456937G>C	c.1936G>C	p.(Glu646Gln)	missense	somatic
702TS	*EPHA5*	NM_004439.4	g.chr4:65899722C>A	c.2488G>T	p.(Glu830*)	nonsense	somatic
863TCS	*ERAP1*	NM_016442.3	g.chr5:96145526G>T	c.1958C>A	p.(Ser653Tyr)	missense	no data
900T	*ERCC5*	NM_000123.3	g.chr13:102316619T>G	c.2206T>G	p.(Leu736Val)	missense	somatic
FM474T	*F5*	NM_000130.4	g.chr1:167763840C>G	c.5536G>C	p.(Gly1846Arg)	missense	no data
702TS	*F9*	NM_000133.3	g.chrX:138471580G>A	c.1070G>A	p.(Gly357Glu)	missense	no data
DM851T	*FAIM2*	NM_012306.3	g.chr12:48569218A>T	c.686T>A	p.(Val229Glu)	missense	no data
366TS	*FAM134C*	NM_178126.3	g.chr17:37990698_37990701del	c.695_698del	p.(Gly232Alafs*2)	frameshift	no data
366TS	*FAM178A*	NM_018121.3	g.chr10:102666752A>T	c.620A>T	p.(Asp207Val)	missense	no data
863TCS	*FAM196A*	NM_001039762.2	g.chr10:128864117T>G	c.533A>C	p.(Asn178Thr)	missense	no data
702TS	*FAM38B*	NM_022068.2	g.chr18:10742821A>G	c.3905T>C	p.(Leu1302Pro)	missense	somatic
863TCS	*FAM55A*	NM_152315.2	g.chr11:113903801C>T	c.440G>A	p.(Arg147His)	missense	somatic
863TCS	*FAM65B*	NM_014722.2	g.chr6:24973582C>G	c.490G>C	p.(Ala164Pro)	missense	somatic
993TCS	*FAM71B*	NM_130899.2	g.chr5:156522665G>T	c.1189C>A	p.(Pro397Thr)	missense	somatic
366TS	*FBXW7*	NM_033632.2	g.chr4:153468834C>T	c.1394G>A	p.(Arg465His)	missense	somatic
900T	*FBXW7*	NM_033632.2	g.chr4:153468835G>A	c.1393C>T	p.(Arg465Cys)	missense	somatic

DM851T	*FBXW7*	NM_033632.2	g.chr4:153468834C>A	c.1394G>T	p.(Arg465Leu)	missense	somatic
340TS	*FBXW8*	NM_012174.1	g.chr12:115946462G>A	c.1297G>A	p.(Val433Met)	missense	somatic
863TCS	*FER1L5*	NM_001113382.1	g.chr2:96728258C>T	c.4561C>T	p.(Arg1521*)	nonsense	somatic
702TS	*FILIP1L*	NM_182909.2	g.chr3:101052199T>G	c.1011A>C	p.(Leu337Phe)	missense	somatic
340TS	*FMN2*	NM_020066.3	g.chr1:238438656G>A	c.4349+1G>A	p.?	splice site	no data
863TCS	*FNDC1*	NM_032532.2	g.chr6:159573602G>A	c.2068G>A	p.(Gly690Ser)	missense	no data
FM403T	*FRMD1*	NM_024919.2	g.chr6:168210321G>A	c.424C>T	p.(Arg142*)	nonsense	somatic
900T	*G6PD*	NM_000402.3	g.chrX:153413657G>C	c.1487C>G	p.(Thr496Ser)	missense	somatic
993TCS	*GABRA1*	NM_000806.4	g.chr5:161250560G>T	c.782G>T	p.(Cys261Phe)	missense	somatic
702TS	*GCH1*	NM_000161.2	g.chr14:54401881C>G	c.367G>C	p.(Asp123His)	missense	somatic
DM851T	*GDAP1*	NM_018972.2	g.chr8:75435064T>A	c.448T>A	p.(Ser150Thr)	missense	somatic
FM403T	*GGCT*	NM_024051.2	g.chr7:30504977G>C	c.390C>G	p.(Tyr130*)	nonsense	somatic
FM474T	*GIMAP1*	NM_130759.3	g.chr7:150048809G>T	c.784G>T	p.(Ala262Ser)	missense	no data
993TCS	*GPAA1*	NM_003801.3	g.chr8:145212595T>C	c.1583T>C	p.(Met528Thr)	missense	no data
DM851T	*GPC5*	NM_004466.4	g.chr13:90899124C>T	c.272C>T	p.(Thr91Met)	missense	no data
863TCS	*GPNMB*	NM_001005340.1	g.chr7:23266594T>A	c.701-6T>A	p.?	splice site	no data
863TCS	*GPR101*	NM_054021.1	g.chrX:135940171G>T	c.1329C>A	p.(Phe443Leu)	missense	no data
900T	*GPR115*	NM_153838.3	g.chr6:47790123T>G	c.1183T>G	p.(Ser395Ala)	missense	no data
FM474T	*GPR32*	NM_001506.1	g.chr19:55966712G>A	c.1043G>A	p.(Cys348Tyr)	missense	no data
FM474T	*GPRASP2*	NM_001004051.3	g.chrX:101858496A>C	c.2043A>C	p.(Gln681His)	missense	no data
FM403T	*GRB10*	NM_001001555.1	g.chr7:50704957G>A	c.286C>T	p.(Leu96Phe)	missense	no data
555TS	*GRIN3A*	NM_133445.2	g.chr9:103472603G>C	c.1912C>G	p.(Arg638Gly)	missense	no data
702TS	*GRLF1*	NM_004491.4	g.chr19:52184763G>T	c.4027G>T	p.(Glu1343*)	nonsense	no data
993TCS	*GRM5*	NM_000842.3	g.chr11:88420093G>T	c.596C>A	p.(Ala199Glu)	missense	no data
863TCS	*GTPBP3*	NM_133644.3	g.chr19:17311393G>A	c.1055G>A	p.(Arg352Gln)	missense	no data
FM403T	*HEBP2*	NM_014320.2	g.chr6:138768909A>G	c.347A>G	p.(Gln116Arg)	missense	somatic
863TCS	*HFM1*	NM_001017975.3	g.chr1:91591213C>T	c.1814G>A	p.(Gly605Glu)	missense	no data
993TCS	*HHLA1*	NM_001145095.1	g.chr8:133161359G>A	c.713C>T	p.(Pro238Leu)	missense	no data
900T	*HIST1H1D*	NM_005320.2	g.chr6:26342860_26342867del	c.277_284del	p.(Thr93Alafs*35)	frameshift	no data
FM474T	*HIST1H2BN*	NM_003520.3	g.chr6:27914794A>C	c.376A>C	p.(Lys126Gln)	missense	somatic
FM474T	*HNRNPL*	NM_001533.2	g.chr19:44019268G>A	c.1712-8C>T	p.?	splice site	no data
702TS	*HNRNPM*	NM_005968.3	g.chr19:8434397C>G	c.344+9C>G	p.?	splice site	no data
702TS	*HRG*	NM_000412.2	g.chr3:187870414C>G	c.301-7C>G	p.?	splice site	no data
555TS	*HS3ST4*	NM_006040.2	g.chr16:26054688C>A	c.989C>A	p.(Ala330Asp)	missense	no data
702TS	*HSF4*	NM_001040667.2	g.chr16:65761139G>A	c.1429G>A	p.(Glu477Lys)	missense	no data
702TS	*HSPG2*	NM_005529.5	g.chr1:22087146A>T	c.575T>A	p.(Val192Glu)	missense	no data
DM851T	*HUWE1*	NM_031407.4	g.chrX:53595086G>T	c.8962C>A	p.(Gln2988Lys)	missense	somatic
DM851T	*HUWE1*	NM_031407.4	g.chrX:53674666G>T	c.808C>A	p.(His270Asn)	missense	somatic
DM851T	*HYAL1*	NM_153281.1	g.chr3:50313509C>T	c.904G>A	p.(Glu302Lys)	missense	somatic
FM403T	*IBTK*	NM_015525.2	g.chr6:82977992C>T	c.2308G>A	p.(Val770Met)	missense	somatic
FM403T	*IGSF21*	NM_032880.4	g.chr1:18561222G>A	c.451G>A	p.(Ala151Thr)	missense	somatic
366TS	*IL1RAPL1*	NM_014271.3	g.chrX:29883626G>A	c.1859G>A	p.(Arg620His)	missense	somatic
FM403T	*IL1RL2*	NM_003854.2	g.chr2:102170745C>G	c.-12-3C>G	p.?	splice site	no data
555TS	*INTS2*	NM_020748.2	g.chr17:57357226C>T	c.334G>A	p.(Gly112Ser)	missense	no data
900T	*ISCA1*	NM_030940.3	g.chr9:88078982A>G	c.82-5T>C	p.?	splice site	no data
900T	*ITGAD*	NM_005353.2	g.chr16:31344928C>T	c.3464C>T	p.(Ala1155Val)	missense	no data

900T	*KALRN*	NM_001024660.2	g.chr3:125868613G>A	c.6593G>A	p.(Arg2198Lys)	missense	somatic
702TS	*KCNN2*	NM_021614.2	g.chr5:g.113726542_113726544dup	c.171_173dup	p.(Ala58dup)	in-frame indel	no data
FM403T	*KCNV2*	NM_133497.3	g.chr9:2708796G>A	c.1057G>A	p.(Glu353Lys)	missense	no data
FM403T	*KCTD1*	NM_001142730.1	g.chr18:22381781_22381784del	c.715_718del	p.(Leu239Metfs*22)	frameshift	no data
863TCS	*KCTD15*	NM_001129995.1	g.chr19:38989615C>T	c.250C>T	p.(Arg84Cys)	missense	somatic
863TCS	*KCTD8*	NM_198353.2	g.chr4:43871622dup	c.1368dup	p.(Pro457Serfs*10)	frameshift	somatic
702TS	*KIAA0564*	NM_015058.1	g.chr13:41047887C>T	c.5359G>A	p.(Glu1787Lys)	missense	no data
FM403T	*KIAA0802*	NM_015210.3	g.chr18:8783089A>G	c.1981A>G	p.(Thr661Ala)	missense	somatic
FM403T	*KIAA1009*	NM_014895.2	g.chr6:84919053T>C	c.3559A>G	p.(Ile1187Val)	missense	no data
FM474T	*KIAA1370*	NM_019600.2	g.chr15:50666718A>G	c.2809-10T>C	p.?	splice site	no data
FM403T	*KIAA1731*	NM_033395.1	g.chr11:93095966G>A	c.6059G>A	p.(Arg2020Gln)	missense	no data
993TCS	*KIAA2022*	NM_001008537.2	g.chrX:73877839C>G	c.3278G>C	p.(Gly1093Ala)	missense	somatic
FM403T	*KIF20B*	NM_016195.2	g.chr10:91504408A>T	c.4381A>T	p.(Met1461Leu)	missense	somatic
FM403T	*KLHDC8A*	NM_018203.1	g.chr1:203579235C>G	c.121G>C	p.(Asp41His)	missense	no data
FM474T	*KLHL15*	NM_030624.2	g.chrX:23916963T>A	c.811A>T	p.(Lys271*)	nonsense	no data
FM474T	*KLK8*	NM_007196.2	g.chr19:56192946A>T	c.500T>A	p.(Phe167Tyr)	missense	no data
863TCS	*KRAS*	NM_033360.2	g.chr12:25289548C>T	c.38G>A	p.(Gly13Asp)	missense	somatic
702TS	*KRT76*	NM_015848.4	g.chr12:51452839C>T	c.967G>A	p.(Glu323Lys)	missense	no data
863TCS	*LAG3*	NM_002286.5	g.chr12:6756904_6756906dup	c.1271_1273dup	p.(Ala424dup)	in-frame indel	somatic
DM851T	*LAMA5*	NM_005560.3	g.chr20:60361618del	c.536del	p.(Gly179Alafs*57)	frameshift	somatic
FM474T	*LDB3*	NM_007078.2	g.chr10:88431381C>T	c.530C>T	p.(Ala177Val)	missense	somatic
702TS	*LEO1*	NM_138792.2	g.chr15:50038281C>T	c.1195G>A	p.(Glu399Lys)	missense	no data
FM474T	*LEPREL1*	NM_018192.3	g.chr3:191187313T>C	c.1146A>G	p.(Ile382Met)	missense	somatic
FM474T	*LGALS12*	NM_001142535.1	g.chr11:63032987G>T	c.389G>T	p.(Arg130Leu)	missense	somatic
555TS	*LHFP*	NM_005780.2	g.chr13:38850603C>T	c.446G>A	p.(Arg149Gln)	missense	no data
993TCS	*LOC643677*	NM_001146197.1	g.chr13:102183533G>A	c.17515C>T	p.(Arg5839Trp)	missense	no data
900T	*LOC645961*	NM_001166137.1	g.chr9:89937258C>T	c.514G>A	p.(Ala172Thr)	missense	no data
FM474T	*LRCH3*	NM_032773.2	g.chr3:199043592A>G	c.1102+7A>G	p.?	splice site	somatic
702TS	*LRIT2*	NM_001017924.2	g.chr10:85972257T>G	c.1052A>C	p.(His351Pro)	missense	no data
555TS	*LSM14A*	NM_015578.2	g.chr19:39398414C>A	c.781+8C>A	p.?	splice site	no data
FM474T	*MADD*	NM_003682.2	g.chr11:47263100G>T	c.2190G>T	p.(Lys730Asn)	missense	somatic
702TS	*MAGEE2*	NM_138703.4	g.chrX:74921009G>T	c.603C>A	p.(Asp201Glu)	missense	somatic
900T	*MAGEL2*	NM_019066.3	g.chr15:21440792C>T	c.1382G>A	p.(Arg461His)	missense	somatic
555TS	*MAPK10*	NM_138982.1	g.chr4:87171559A>G	c.1160T>C	p.(Ile387Thr)	missense	no data
FM403T	*MAPRE3*	NM_012326.2	g.chr2:27100631A>C	c.431A>C	p.(Gln144Pro)	missense	somatic
863TCS	*MATN2*	NM_002380.3	g.chr8:99023288C>G	c.820C>G	p.(Gln274Glu)	missense	somatic
FM403T	*MBOAT4*	NM_001100916.1	g.chr8:30109022C>A	c.1287G>T	p.(Lys429Asn)	missense	somatic
993TCS	*MCAT*	NM_173467.4	g.chr22:41859424G>C	c.742C>G	p.(Leu248Val)	missense	somatic
DM851T	*MESDC1*	NM_022566.2	g.chr15:79082484C>T	c.817C>T	p.(Arg273Cys)	missense	no data
702TS	*MGAM*	NM_004668.1	g.chr7:141373951T>A	c.1168T>A	p.(Leu390Ile)	missense	no data
702TS	*MKS1*	NM_017777.3	g.chr17:53645404C>T	c.796G>A	p.(Asp266Asn)	missense	no data
702TS	*MLL3*	NM_170606.2	g.chr7:151466914T>C	c.14543A>G	p.(Asn4848Ser)	missense	somatic
DM851T	*MRGPRX4*	NM_054032.3	g.chr11:18151635C>T	c.256C>T	p.(Arg86Cys)	missense	no data
702TS	*MRPS23*	NM_016070.2	g.chr17:53273342C>T	c.364G>A	p.(Gly122Arg)	missense	no data

863TCS	*MTHFSD*	NM_001159378.1	g.chr16:85145861G>T	c.17-3C>A	p.?	splice site	no data
FM474T	*MTUS2*	NM_001033602.2	g.chr13:28498054G>T	c.1249G>T	p.(Asp417Tyr)	missense	somatic
702TS	*MYCBPAP*	NM_032133.3	g.chr17:45955426C>T	c.1403C>T	p.(Pro468Leu)	missense	somatic
702TS	*MYH1*	NM_005963.3	g.chr17:10340126C>T	c.5035G>A	p.(Glu1679Lys)	missense	somatic
340TS	*MYH11*	NM_001040113.1	g.chr16:15722276G>A	c.4733C>T	p.(Ala1578Val)	missense	somatic
FM474T	*MYH7*	NM_000257.2	g.chr14:22954093A>G	c.5510T>C	p.(Val1837Ala)	missense	somatic
FM474T	*MYH7*	NM_000257.2	g.chr14:22954094C>A	c.5509G>T	p.(Val1837Leu)	missense	somatic
FM474T	*MYO16*	NM_015011.1	g.chr13:108177882C>G	c.391C>G	p.(His131Asp)	missense	no data
FM474T	*MYO18B*	NM_032608.5	g.chr22:24554897C>T	c.2941C>T	p.(Gln981*)	nonsense	somatic
DM851T	*NADK*	NM_023018.4	g.chr1:1674334G>A	c.1210C>T	p.(Pro404Ser)	missense	somatic
FM403T	*NBEAL1*	NM_001114132.1	g.chr2:203705036_203705038del	c.3574_3576del	p.(Leu1192del)	in-frame indel	no data
863TCS	*NBPF3*	NM_032264.2	g.chr1:21678443C>G	c.1171C>G	p.(Gln391Glu)	missense	no data
FM403T	*NCOA2*	NM_006540.2	g.chr8:71231846C>T	c.1308G>A	p.(Met436Ile)	missense	somatic
863TCS	*NCOA3*	NM_006534.3	g.chr20:45696353A>T	c.1112+7A>T	p.?	splice site	somatic
555TS	*NDOR1*	NM_001144026.1	g.chr9:139229707G>A	c.1201G>A	p.(Val401Met)	missense	no data
863TCS	*NEB*	NM_001164508.1	g.chr2:152112226A>G	c.20330T>C	p.(Val6777Ala)	missense	somatic
FM403T	*NEB*	NM_001164508.1	g.chr2:152071734T>A	c.23491A>T	p.(Ile7831Phe)	missense	somatic
702TS	*NEDD4*	NM_198400.2	g.chr15:53995781A>G	c.541T>C	p.(Tyr181His)	missense	somatic
900T	*NFATC1*	NM_006162.3	g.chr18:75272172C>A	c.909C>A	p.(Asn303Lys)	missense	no data
702TS	*NFXL1*	NM_152995.4	g.chr4:47571924G>C	c.2223C>G	p.(Ile741Met)	missense	somatic
FM474T	*NGEF*	NM_019850.2	g.chr2:233452546C>T	c.2030G>A	p.(Arg677Gln)	missense	somatic
900T	*NHS*	NM_198270.2	g.chrX:17654355_17654356del	c.2145_2146del	p.(Asp716Phefs*2)	frameshift	somatic
FM474T	*NKAIN4*	NM_152864.3	g.chr20:61351745C>T	c.179G>A	p.(Arg60His)	missense	somatic
FM474T	*NKAIN4*	NM_152864.3	g.chr20:61351746_61351747del	c.179_180del	p.(Arg60Leufs*49)	frameshift	somatic
DM851T	*NLRP13*	NM_176810.2	g.chr19:61101967G>A	c.2963C>T	p.(Ala988Val)	missense	no data
FM403T	*NMD3*	NM_015938.3	g.chr3:162449969dup	c.1236dup	p.(Arg413Thrfs*5)	frameshift	somatic
702TS	*NOLC1*	NM_004741.3	g.chr10:103907043_103907045del	c.285_287del	p.(Glu96del)	in-frame indel	no data
FM474T	*NOTCH3*	NM_000435.2	g.chr19:15152049A>C	c.3161T>G	p.(Leu1054Arg)	missense	no data
863TCS	*NSD1*	NM_022455.3	g.chr5:176653628T>C	c.6653T>C	p.(Ile2218Thr)	missense	no data
900T	*NSUN2*	NM_017755.4	g.chr5:6675214C>T	c.538-1G>A	p.?	splice site	no data
863TCS	*NTSR1*	NM_002531.2	g.chr20:60811420C>T	c.416C>T	p.(Ala139Val)	missense	no data
863TCS	*NUAK1*	NM_014840.2	g.chr12:104984900C>T	c.1796G>A	p.(Arg599His)	missense	no data
863TCS	*NUP205*	NM_015135.2	g.chr7:134926735C>T	c.1474-3C>T	p.?	splice site	no data
FM474T	*NUP54*	NM_017426.2	g.chr4:77276523G>A	c.362C>T	p.(Ala121Val)	missense	no data
FM474T	*NXT2*	NM_018698.4	g.chrX:108666846G>C	c.120G>C	p.(Glu40Asp)	missense	no data
555TS	*OBSCN*	NM_001098623.1	g.chr1:226631126A>T	c.22967A>T	p.(Glu7656Val)	missense	no data
863TCS	*OBSCN*	NM_001098623.1	g.chr1:226548617_226548618del	c.11274_11275del	p.(His3758Glnfs*10)	frameshift	somatic
FM403T	*ODZ2*	NM_001122679.1	g.chr5:167457629C>T	c.1732C>T	p.(Arg578Cys)	missense	somatic
702TS	*OR1E1*	NM_003553.2	g.chr17:3248271A>T	c.184T>A	p.(Phe62Ile)	missense	somatic
993TCS	*OR2L13*	NM_175911.2	g.chr1:246329935G>A	c.635G>A	p.(Gly212Asp)	missense	somatic
DM851T	*OR4L1*	NM_001004717.1	g.chr14:19598968G>T	c.925G>T	p.(Ala309Ser)	missense	somatic
FM403T	*OR5H14*	NM_001005514.1	g.chr3:99351050G>A	c.131G>A	p.(Gly44Asp)	missense	no data
555TS	*OR5P2*	NM_153444.1	g.chr11:7774393G>A	c.673C>T	p.(Arg225Cys)	missense	no data
702TS	*OR5W2*	NM_001001960.1	g.chr11:55437741T>A	c.894A>T	p.(Lys298Asn)	missense	no data

FM474T	*OR7D2*	NM_175883.1	g.chr19:9158328A>G	c.871A>G	p.(Ser291Gly)	missense	no data
DM851T	*ORAI2*	NM_001126340.1	g.chr7:101866622G>A	c.214G>A	p.(Gly72Ser)	missense	somatic
FM474T	*ORAI2*	NM_001126340.1	g.chr7:101874136T>G	c.397T>G	p.(Ser133Ala)	missense	somatic
702TS	*ORC1L*	NM_004153.3	g.chr1:52611557A>T	c.2470T>A	p.(Ser824Thr)	missense	somatic
863TCS	*OSBPL5*	NM_020896.2	g.chr11:3082059T>C	c.1184A>G	p.(Glu395Gly)	missense	somatic
863TCS	*PA2G4*	NM_006191.2	g.chr12:54791061G>A	c.889G>A	p.(Ala297Thr)	missense	somatic
702TS	*PAH*	NM_000277.1	g.chr12:101770846A>C	c.719T>G	p.(Phe240Cys)	missense	somatic
FM474T	*PAPPA*	NM_002581.3	g.chr9:118073475G>T	c.2912G>T	p.(Cys971Phe)	missense	somatic
900T	*PAPPA2*	NM_020318.2	g.chr1:174831226G>A	c.1863G>A	p.(Trp621*)	nonsense	somatic
900T	*PARP15*	NM_001113523.1	g.chr3:123812025G>A	c.307-6G>A	p.?	splice site	no data
366TS	*PCDH15*	NM_001142772.1	g.chr10:55452828C>G	c.2356G>C	p.(Glu786Gln)	missense	somatic
FM474T	*PCDHA12*	NM_018903.2	g.chr5:140237277C>T	c.2036C>T	p.(Ser679Leu)	missense	somatic
702TS	*PCDHA6*	NM_018909.2	g.chr5:140189776A>G	c.1916A>G	p.(Glu639Gly)	missense	no data
702TS	*PCDHB12*	NM_018932.3	g.chr5:140570717C>T	c.2054C>T	p.(Ser685Leu)	missense	somatic
702TS	*PCDHGA7*	NM_018920.2	g.chr5:140745036G>T	c.2386G>T	p.(Asp796Tyr)	missense	no data
FM403T	*PCNXL2*	NM_014801.3	g.chr1:231227628C>G	c.4492G>C	p.(Glu1498Gln)	missense	no data
FM403T	*PCSK2*	NM_002594.3	g.chr20:17410611C>G	c.1813C>G	p.(Arg605Gly)	missense	somatic
FM474T	*PDCD6IP*	NM_013374.4	g.chr3:33861996A>T	c.1553A>T	p.(Asp518Val)	missense	somatic
702TS	*PDE1A*	NM_005019.3	g.chr2:182761989C>A	c.1217G>T	p.(Cys406Phe)	missense	somatic
993TCS	*PDGFRA*	NM_006206.4	g.chr4:54849968C>T	c.2810C>T	p.(Pro937Leu)	missense	somatic
702TS	*PDS5A*	NM_015200.2	g.chr4:39586517T>G	c.1006A>C	p.(Ile336Leu)	missense	somatic
702TS	*PDS5A*	NM_015200.2	g.chr4:39595064T>C	c.755A>G	p.(Lys252Arg)	missense	no data
DM851T	*PHF16*	NM_001077445.1	g.chrX:46730049C>G	c.47-9C>G	p.?	splice site	no data
FM474T	*PHF3*	NM_015153.2	g.chr6:64479500C>T	c.4057C>T	p.(Arg1353*)	nonsense	no data
FM474T	*PHF3*	NM_015153.2	g.chr6:64479503C>T	c.4060C>T	p.(Gln1354*)	nonsense	no data
FM474T	*PI16*	NM_153370.2	g.chr6:37039604_37039606del	c.1299_1301del	p.(Val434del)	in-frame indel	no data
900T	*PIK3C2B*	NM_002646.2	g.chr1:202661477C>T	c.4603G>A	p.(Gly1535Arg)	missense	somatic
702TS	*PIK3CA*	NM_006218.2	g.chr3:180410668G>A	c.1252G>A	p.(Glu418Lys)	missense	somatic
863TCS	*PIK3CA*	NM_006218.2	g.chr3:180400172G>A	c.353G>A	p.(Gly118Asp)	missense	somatic
FM403T	*PIK3CA*	NM_006218.2	g.chr3:180405018G>A	c.1093G>A	p.(Glu365Lys)	missense	somatic
FM474T	*PIK3CA*	NM_006218.2	g.chr3:180404243T>G	c.1031T>G	p.(Val344Gly)	missense	somatic
702TS	*PIK3R4*	NM_014602.2	g.chr3:131883108C>T	c.3625G>A	p.(Glu1209Lys)	missense	somatic
366TS	*PKD2L2*	NM_014386.2	g.chr5:137269945G>C	c.898G>C	p.(Glu300Gln)	missense	somatic
702TS	*PKHD1*	NM_138694.3	g.chr6:51591933A>C	c.12130T>G	p.(Leu4044Val)	missense	somatic
FM403T	*PLCH1*	NM_014996.1	g.chr3:156682064C>G	c.4355G>C	p.(Cys1452Ser)	missense	no data
FM403T	*PLD5*	NM_152666.1	g.chr1:240337705C>G	c.854G>C	p.(Arg285Thr)	missense	no data
FM474T	*PLEKHG7*	NM_001004330.2	g.chr12:91672033G>T	c.352G>T	p.(Val118Leu)	missense	no data
366TS	*PLG*	NM_000301.1	g.chr6:161072146G>A	c.1330G>A	p.(Val444Ile)	missense	no data
702TS	*PLK4*	NM_014264.4	g.chr4:129030572G>A	c.1561G>A	p.(Asp521Asn)	missense	no data
863TCS	*PLLP*	NM_015993.2	g.chr16:55853490G>T	c.136-7C>A	p.?	splice site	no data
FM474T	*POLR2E*	NM_002695.3	g.chr19:1045037A>G	c.98T>C	p.(Leu33Pro)	missense	somatic
993TCS	*POP1*	NM_015029.1	g.chr8:99237447T>C	c.2058-7T>C	p.?	splice site	no data
555TS	*PPP2R1A*	NM_014225.3	g.chr19:57407783C>G	c.536C>G	p.(Pro179Arg)	missense	somatic
702TS	*PPP2R1A*	NM_014225.3	g.chr19:57408135C>A	c.767C>A	p.(Ser256Tyr)	missense	no data
900T	*PRKACB*	NM_002731.2	g.chr1:84417471A>G	c.70A>G	p.(Lys24Glu)	missense	somatic
FM474T	*PRPH2*	NM_000322.4	g.chr6:42797938C>T	c.113G>A	p.(Gly38Glu)	missense	somatic

FM403T	*PRR14*	NM_024031.2	g.chr16:30573107C>A	c.604C>A	p.(Pro202Thr)	missense	no data
DM851T	*PTCHD2*	NM_020780.1	g.chr1:11484387C>T	c.751C>T	p.(Arg251*)	nonsense	somatic
FM403T	*PTGIR*	NM_000960.3	g.chr19:51818632C>T	c.691G>A	p.(Gly231Arg)	missense	no data
366TS	*PTGS1*	NM_000962.2	g.chr9:124194279C>T	c.1445-10C>T	p.?	splice site	no data
900T	*PTPLA*	NM_014241.3	g.chr10:17685566G>T	c.482C>A	p.(Pro161Gln)	missense	somatic
FM403T	*PTPN7*	NM_080588.1	g.chr1:200395159G>A	c.112C>T	p.(Leu38Phe)	missense	somatic
FM403T	*PUS7*	NM_019042.3	g.chr7:104919230C>G	c.913G>C	p.(Val305Leu)	missense	no data
FM403T	*PWP1*	NM_007062.1	g.chr12:106626872C>T	c.1117C>T	p.(Arg373Cys)	missense	no data
863TCS	*RALGAPA2*	NM_020343.3	g.chr20:20533849C>A	c.2008G>T	p.(Glu670*)	nonsense	no data
900T	*RALGPS2*	NM_152663.2	g.chr1:177127980T>C	c.1248-8T>C	p.?	splice site	no data
FM474T	*RASA1*	NM_002890.2	g.chr5:86709990G>A	c.2366G>A	p.(Arg789Gln)	missense	no data
FM403T	*RASGEF1B*	NM_152545.1	g.chr4:82585758C>A	c.874G>T	p.(Val292Leu)	missense	no data
900T	*RELN*	NM_005045.2	g.chr7:103109828C>T	c.1260G>A	p.(Trp420*)	nonsense	somatic
FM403T	*RHBDL3*	NM_138328.2	g.chr17:27672162G>T	c.1016G>T	p.(Ser339Ile)	missense	no data
702TS	*RNF19B*	NM_153341.2	g.chr1:33186559G>C	c.842-5C>G	p.?	splice site	somatic
FM403T	*RNF19B*	NM_153341.2	g.chr1:33183702C>A	c.1264G>T	p.(Gly422Cys)	missense	somatic
863TCS	*RNF220*	NM_018150.2	g.chr1:44650448C>T	c.92C>T	p.(Thr31Met)	missense	no data
555TS	*RNF40*	NM_014771.2	g.chr16:30685588del	c.1319del	p.(Lys440Serfs*47)	frameshift	no data
FM474T	*ROBO1*	NM_133631.3	g.chr3:78767696T>G	c.3155A>C	p.(Lys1052Thr)	missense	somatic
FM403T	*RPRD1A*	NM_018170.3	g.chr18:31867688C>T	c.262G>A	p.(Ala88Thr)	missense	somatic
DM851T	*RYR2*	NM_001035.2	g.chr1:235726459G>A	c.1987G>A	p.(Val663Ile)	missense	no data
863TCS	*RYR3*	NM_001036.3	g.chr15:31937393G>A	c.14128G>A	p.(Asp4710Asn)	missense	somatic
366TS	*SCAMP3*	NM_052837.2	g.chr1:153495231C>T	c.439+10G>A	p.?	splice site	no data
993TCS	*SCN7A*	NM_002976.2	g.chr2:167037086C>T	c.559G>A	p.(Val187Ile)	missense	no data
DM851T	*SDK2*	NM_001144952.1	g.chr17:68873039dup	c.5260dup	p.(Leu1754Profs*144)	frameshift	somatic
DM851T	*SDR16C6*	NM_001145251.1	g.chr8:57470436G>T	c.43C>A	p.(Pro15Thr)	missense	somatic
900T	*SEC23B*	NM_006363.4	g.chr20:18444339G>A	c.325G>A	p.(Glu109Lys)	missense	somatic
555TS	*SEC24D*	NM_014822.2	g.chr4:119869258G>A	c.2869-5C>T	p.?	splice site	no data
366TS	*SEMA3E*	NM_012431.2	g.chr7:82957527C>A	c.116-1G>T	p.?	splice site	no data
863TCS	*SENP7*	NM_001077203.1	g.chr3:102702663C>A	c.41-10G>T	p.?	splice site	no data
555TS	*SEPW1*	NM_003009.2	g.chr19:52976167C>G	c.109-10C>G	p.?	splice site	no data
702TS	*SERPINB10*	NM_005024.1	g.chr18:59751313T>C	c.685T>C	p.(Phe229Leu)	missense	no data
863TCS	*SF1*	NM_004630.2	g.chr11:64293596C>T	c.541G>A	p.(Gly181Arg)	missense	no data
863TCS	*SF3A1*	NM_005877.4	g.chr22:29070958dup	c.617dup	p.(Asn206Lysfs*29)	frameshift	no data
DM851T	*SFMBT2*	NM_001029880.1	g.chr10:7270679G>A	c.1721C>T	p.(Ala574Val)	missense	no data
863TCS	*SGSM3*	NM_015705.4	g.chr22:39131149G>A	c.533G>A	p.(Ser178Asn)	missense	no data
340TS	*SH2B1*	NM_015503.2	g.chr16:28787895_28787898del	c.1109_1112del	p.(Asp370Alafs*5)	frameshift	somatic
900T	*SHC1*	NM_001130040.1	g.chr1:153205295G>A	c.1219C>T	p.(Arg407Cys)	missense	somatic
DM851T	*SIGLEC7*	NM_014385.2	g.chr19:56337865G>T	c.427G>T	p.(Val143Leu)	missense	no data
702TS	*SLC26A9*	NM_052934.2	g.chr1:204157406C>T	c.1966G>A	p.(Val656Ile)	missense	somatic
FM403T	*SLC28A1*	NM_004213.3	g.chr15:83288891G>A	c.1754G>A	p.(Cys585Tyr)	missense	somatic
863TCS	*SLC2A3*	NM_006931.1	g.chr12:7969742C>T	c.931G>A	p.(Ala311Thr)	missense	somatic
900T	*SLC34A2*	NM_006424.2	g.chr4:25287260_25287262del	c.1864_1866del	p.(Cys622del)	in-frame indel	no data
366TS	*SLC35B3*	NM_001142541.1	g.chr6:8373250C>A	c.338G>T	p.(Trp113Leu)	missense	no data

FM474T	*SLC37A3*	NM_032295.2	g.chr7:139698328C>A	c.703+3G>T	p.?	splice site	no data
FM474T	*SLC37A3*	NM_207113.1	g.chr7:139698329A>C	c.703+2T>G	p.?	splice site	no data
FM474T	*SLC38A4*	NM_018018.3	g.chr12:45459918A>C	c.576-6T>G	p.?	splice site	no data
DM851T	*SLC39A7*	NM_006979.2	g.chr6:33277608A>G	c.520A>G	p.(Ser174Gly)	missense	no data
863TCS	*SLC47A2*	NM_152908.3	g.chr17:19556619G>T	c.475C>A	p.(Pro159Thr)	missense	no data
555TS	*SLC4A1AP*	NM_018158.2	g.chr2:27758720G>T	c.1865G>T	p.(Gly622Val)	missense	no data
FM474T	*SLC4A4*	NM_001098484.1	g.chr4:72648475G>A	c.3196+5G>A	p.?	splice site	no data
DM851T	*SLC8A3*	NM_183002.1	g.chr14:69704096C>T	c.797G>A	p.(Arg266His)	missense	no data
702TS	*SLC9A9*	NM_173653.1	g.chr3:145049708C>A	c.147G>T	p.(Leu49Phe)	missense	no data
900T	*SLITRK2*	NM_001144003.2	g.chrX:144713965G>T	c.2330G>T	p.(Cys777Phe)	missense	no data
863TCS	*SLITRK3*	NM_014926.2	g.chr3:166389136G>C	c.2177C>G	p.(Thr726Ser)	missense	no data
555TS	*SMAD9*	NM_001127217.2	g.chr13:36320869C>G	c.1348G>C	p.(Asp450His)	missense	no data
DM851T	*SMPD4*	NM_017951.4	g.chr2:130627966C>A	c.1789G>T	p.(Ala597Ser)	missense	somatic
FM474T	*SNAP25*	NM_130811.2	g.chr20:10221821G>A	c.176G>A	p.(Arg59His)	missense	no data
702TS	*SNIP*	NM_025248.2	g.chr17:33970089C>T	c.1793+6G>A	p.?	splice site	no data
900T	*SNRK*	NM_017719.4	g.chr3:43364425A>G	c.1670A>G	p.(Asp557Gly)	missense	no data
366TS	*SPAG5*	NM_006461.3	g.chr17:23936552C>T	c.1865G>A	p.(Gly622Glu)	missense	no data
FM403T	*SPOP*	NM_003563.3	g.chr17:45051724C>T	c.223G>A	p.(Gly75Arg)	missense	somatic
DM851T	*SPRYD3*	NM_032840.2	g.chr12:51746648G>A	c.997C>T	p.(Arg333Trp)	missense	somatic
900T	*SPTA1*	NM_003126.2	g.chr1:156917066del	c.610del	p.(Gln204Lysfs*5)	frameshift	somatic
DM851T	*SPTA1*	NM_003126.2	g.chr1:156884940C>T	c.3697G>A	p.(Val1233Ile)	missense	somatic
993TCS	*SPTBN5*	NM_016642.2	g.chr15:39950013G>A	c.5485C>T	p.(Arg1794*)	nonsense	somatic
DM851T	*SSB*	NM_003142.3	g.chr2:170375043C>T	c.674C>T	p.(Ser225Phe)	missense	no data
900T	*SSX2IP*	NM_001166417.1	g.chr1:84900639C>T	c.757G>A	p.(Asp253Asn)	missense	no data
702TS	*ST8SIA3*	NM_015879.2	g.chr18:53172714C>G	c.263C>G	p.(Ser88Cys)	missense	no data
DM851T	*STAG3L4*	NM_022906.2	g.chr7:66411555del	c.286del	p.(Leu96Trpfs*4)	frameshift	no data
863TCS	*STRN4*	NM_013403.2	g.chr19:51922563C>T	c.1234G>A	p.(Asp412Asn)	missense	somatic
340TS	*SUPT5H*	NM_001130824.1	g.chr19:44655971G>A	c.2462G>A	p.(Trp821*)	nonsense	somatic
993TCS	*SVIL*	NM_021738.2	g.chr10:29879649G>A	c.710C>T	p.(Ser237Phe)	missense	somatic
863TCS	*SYNE1*	NM_182961.3	g.chr6:152594314C>T	c.20944G>A	p.(Val6982Met)	missense	somatic
DM851T	*SYNE2*	NM_182914.2	g.chr14:63546528G>A	c.4669G>A	p.(Val1557Ile)	missense	somatic
FM474T	*TACR3*	NM_001059.2	g.chr4:104798867T>A	c.691A>T	p.(Thr231Ser)	missense	somatic
993TCS	*TAF1L*	NM_153809.2	g.chr9:32621851G>A	c.3727C>T	p.(Arg1243Trp)	missense	somatic
FM403T	*TARBP1*	NM_005646.3	g.chr1:232669901C>G	c.1218G>C	p.(Lys406Asn)	missense	no data
FM403T	*TAS2R16*	NM_016945.2	g.chr7:122422234C>T	c.691G>A	p.(Val231Ile)	missense	no data
FM403T	*TBX6*	NM_004608.2	g.chr16:30007814G>A	c.572C>T	p.(Ser191Phe)	missense	somatic
340TS	*TIMM44*	NM_006351.3	g.chr19:7909083C>A	c.142-1G>T	p.?	splice site	no data
FM474T	*TKTL1*	NM_012253.3	g.chrX:153190927G>A	c.289G>A	p.(Gly97Arg)	missense	somatic
FM403T	*TKTL2*	NM_032136.4	g.chr4:164613159A>G	c.1178T>C	p.(Phe393Ser)	missense	somatic
702TS	*TLE4*	NM_007005.3	g.chr9:81527185G>C	c.1987-1G>C	p.?	splice site	somatic
900T	*TLR8*	NM_138636.3	g.chrX:12847265G>A	c.185G>A	p.(Gly62Asp)	missense	somatic
DM851T	*TMEM2*	NM_013390.2	g.chr9:73535525G>C	c.1689C>G	p.(Tyr563*)	nonsense	no data
702TS	*TMEM22*	NM_025246.2	g.chr3:138056122G>C	c.130G>C	p.(Gly44Arg)	missense	no data
FM403T	*TMPO*	NM_003276.2	g.chr12:97452066G>C	c.1900G>C	p.(Asp634His)	missense	no data
366TS	*TNPO3*	NM_012470.3	g.chr7:128399832C>T	c.2314G>A	p.(Val772Met)	missense	somatic

340TS	*TP53*	NM_000546.4	g.chr17:7519174C>T	c.481G>A	p.(Ala161Thr)	missense	somatic
555TS	*TP53*	NM_000546.4	g.chr17:7518276C>G	c.730G>C	p.(Gly244Arg)	missense	no data
702TS	*TP53*	NM_000546.4	g.chr17:7518264G>A	c.742C>T	p.(Arg248Trp)	missense	somatic
863TCS	*TP53*	NM_000546.4	g.chr17:7518284G>A	c.722C>T	p.(Ser241Phe)	missense	no data
900T	*TP53*	NM_000546.4	g.chr17:7518330del	c.677del	p.(Gly226Alafs*21)	frameshift	somatic
993TCS	*TP53*	NM_000546.4	g.chr17:7517831G>T	c.832C>A	p.(Pro278Thr)	missense	somatic
DM851T	*TP53*	NM_000546.4	g.chr17:7518293C>T	c.713G>A	p.(Cys238Tyr)	missense	somatic
FM403T	*TP53*	NM_000546.4	g.chr17:7518899_7518927del	c.647_672+3del	p.(Val216Glyfs)	frameshift	no data
FM474T	*TP53*	NM_000546.4	g.chr17:7518264G>A	c.742C>T	p.(Arg248Trp)	missense	no data
993TCS	*TP53BP1*	NM_005657.1	g.chr15:41571538G>T	c.225C>A	p.(Asp75Glu)	missense	somatic
900T	*TRAF7*	NM_032271.2	g.chr16:2166310G>A	c.1922G>A	p.(Arg641His)	missense	somatic
702TS	*TRAM1L1*	NM_152402.2	g.chr4:118225657G>T	c.341C>A	p.(Ala114Glu)	missense	no data
FM474T	*TRERF1*	NM_033502.2	g.chr6:42312013C>T	c.2974G>A	p.(Val992Ile)	missense	no data
993TCS	*TRIM59*	NM_173084.2	g.chr3:161639163T>G	c.503A>C	p.(Lys168Thr)	missense	no data
FM474T	*TRIO*	NM_007118.2	g.chr5:14350224G>A	c.1220G>A	p.(Arg407His)	missense	no data
702TS	*TRMT6*	NM_015939.3	g.chr20:5872263C>T	c.609G>A	p.(Met203Ile)	missense	no data
863TCS	*TRPS1*	NM_014112.2	g.chr8:116668393A>G	c.2700+10T>C	p.?	splice site	no data
702TS	*TTC28*	NM_001145418.1	g.chr22:26719314G>A	c.5437C>T	p.(Arg1813Trp)	missense	no data
FM474T	*TTN*	NM_133378.4	g.chr2:179136688_179136689insGAGGG	c.74711_74712insCCCTC	p.(Ser24906Leufs*16)	frameshift	somatic
DM851T	*TUBB1*	NM_030773.3	g.chr20:57028027A>C	c.55A>C	p.(Lys19Gln)	missense	somatic
702TS	*UBA2*	NM_005499.2	g.chr19:39616146T>C	c.347T>C	p.(Leu116Ser)	missense	somatic
FM474T	*UBA2*	NM_005499.2	g.chr19:39614604A>T	c.223-2A>T	p.?	splice site	somatic
FM403T	*UBAP1*	NM_016525.3	g.chr9:34239816A>T	c.1123A>T	p.(Met375Leu)	missense	no data
FM474T	*UBQLNL*	NM_145053.4	g.chr11:5493415T>C	c.833A>G	p.(Asn278Ser)	missense	somatic
702TS	*UGT1A8*	NM_019075.2	g.chr2:234345771G>T	c.1420G>T	p.(Ala474Ser)	missense	somatic
900T	*UGT2B4*	NM_021139.2	g.chr4:70381153G>A	c.1375C>T	p.(Arg459*)	nonsense	somatic
555TS	*UPP2*	NM_001135098.1	g.chr2:158682678G>A	c.607G>A	p.(Gly203Ser)	missense	no data
FM474T	*UQCRC2*	NM_003366.2	g.chr16:21887515T>C	c.670+8T>C	p.?	splice site	somatic
900T	*URB2*	NM_014777.2	g.chr1:227839624G>T	c.2641G>T	p.(Asp881Tyr)	missense	somatic
FM403T	*URG4*	NM_001077664.1	g.chr7:43885364C>A	c.94G>T	p.(Glu32*)	nonsense	somatic
863TCS	*USP36*	NM_025090.3	g.chr17:74314718G>A	c.2003C>T	p.(Pro668Leu)	missense	somatic
FM403T	*USP53*	NM_019050.2	g.chr4:120400479C>T	c.626C>T	p.(Ala209Val)	missense	somatic
863TCS	*USP6*	NM_004505.2	g.chr17:5015596T>C	c.3955-10T>C	p.?	splice site	no data
863TCS	*UTRN*	NM_007124.2	g.chr6:145144900G>A	c.8782G>A	p.(Val2928Ile)	missense	no data
FM474T	*UTRN*	NM_007124.2	g.chr6:144877478G>A	c.5074-1G>A	p.?	splice site	no data
FM474T	*WBP5*	NM_016303.2	g.chrX:102499522A>G	c.254A>G	p.(Asn85Ser)	missense	somatic
FM403T	*WDR7*	NM_015285.2	g.chr18:52509508A>C	c.781A>C	p.(Thr261Pro)	missense	somatic
FM474T	*WDR90*	NM_145294.4	g.chr16:641035C>A	c.599C>A	p.(Pro200His)	missense	somatic
863TCS	*XKR7*	NM_001011718.1	g.chr20:30048458C>T	c.1277C>T	p.(Ala426Val)	missense	no data
FM474T	*ZBTB7B*	NM_015872.2	g.chr1:153253875C>T	c.115C>T	p.(Arg39Trp)	missense	no data
555TS	*ZCCHC6*	NM_024617.3	g.chr9:88147844G>A	c.1052C>T	p.(Ser351Leu)	missense	no data
FM474T	*ZFP1*	NM_153688.2	g.chr16:73761273T>C	c.764T>C	p.(Leu255Pro)	missense	somatic
FM474T	*ZMYND10*	NM_015896.2	g.chr3:50354521A>C	c.928T>G	p.(Leu310Val)	missense	somatic
993TCS	*ZNF280C*	NM_017666.4	g.chrX:129177612T>C	c.1672A>G	p.(Ser558Gly)	missense	no data
993TCS	*ZNF445*	NM_181489.5	g.chr3:44467908C>A	c.500G>T	p.(Trp167Leu)	missense	no data

FM403T	*ZNF513*	NM_144631.5	g.chr2:27454236G>A	c.1306C>T	p.(Arg436Cys)	missense	somatic
FM403T	*ZNF518A*	NM_014803.3	g.chr10:97907690C>A	c.1621C>A	p.(Leu541Ile)	missense	no data
340TS	*ZNF770*	NM_014106.3	g.chr15:33061556G>A	c.1372C>T	p.(Gln458*)	nonsense	somatic
993TCS	*ZPBP*	NM_001159878.1	g.chr7:49993649T>G	c.793A>C	p.(Ile265Leu)	missense	somatic
702TS	*ZYG11A*	NM_001004339.2	g.chr1:53116026C>T	c.1627C>T	p.(Leu543Phe)	missense	somatic
*Coordinates refer to human reference genome hg18 release (NCBI 36.1, March 2006)							

Appendix 2

Profiles of somatic mutations in *TP53, PIK3CA, FBXW7* and *PPP2R1A* genes

Sample	Gene	Transcript	Nucleotide (genomic)*	Nucleotide (cDNA)	Amino Acid (protein)	Mutation type	Sample Group
900T	*TP53*	NM_000546.4	g.chr17:7518330del	c.677del	p.(Gly226Alafs*21)	frameshift	discovery
702TS	*TP53*	NM_000546.4	g.chr17:7518264G>A	c.742C>T	p.(Arg248Trp)	missense	discovery
863TCS	*TP53*	NM_000546.4	g.chr17:7518284G>A	c.722C>T	p.(Ser241Phe)	missense	discovery
340TS	*TP53*	NM_000546.4	g.chr17:7519174C>T	c.481G>A	p.(Ala161Thr)	missense	discovery
993TCS	*TP53*	NM_000546.4	g.chr17:7517831G>T	c.832C>A	p.(Pro278Thr)	missense	discovery
FM403T	*TP53*	NM_000546.4	g.chr17:7518899_7518927del	c.647_672+3del	p.(Val216Glyfs)	frameshift	discovery
DM851T	*TP53*	NM_000546.4	g.chr17:7518293C>T	c.713G>A	p.(Cys238Tyr)	missense	discovery
FM474T	*TP53*	NM_000546.4	g.chr17:7518264G>A	c.742C>T	p.(Arg248Trp)	missense	discovery
555TS	*TP53*	NM_000546.4	g.chr17:7518276C>G	c.730G>C	p.(Gly244Arg)	missense	discovery
1FFPE	*TP53*	NM_000546.4	g.chr17:7517831G>C	c.832C>G	p.(Pro278Ala)	missense	validation
2FFPE	*TP53*	NM_000546.4	g.chr17:7520121_7520130del	c.282_291del	p.(Ser95Leufs*25)	frameshift	validation
2FFPE	*TP53*	NM_000546.4	g.chr17:7518982C>A	c.592G>T	p.(Glu198*)	nonsense	validation
3FFPE	*TP53*	NM_000546.4	g.chr17:7519120G>T	c.535C>A	p.(His179Asn)	missense	validation
3FFPE	*TP53*	NM_000546.4	g.chr17:7517864G>A	c.799C>T	p.(Arg267Trp)	missense	validation
4FFPE	*TP53*	NM_000546.4	g.chr17:7518281C>G	c.725G>C	p.(Cys242Ser)	missense	validation
5FFPE	*TP53*	NM_000546.4	g.chr17:7519168A>G	c.487T>C	p.(Tyr163His)	missense	validation
5FFPE	*TP53*	NM_000546.4	g.chr17:7519119T>G	c.536A>C	p.(His179Pro)	missense	validation
6FFPE	*TP53*	NM_000546.4	g.chr17:7518982C>A	c.592G>T	p.(Glu198*)	nonsense	validation
7FFPE	*TP53*	NM_000546.4	g.chr17:7518264G>A	c.742C>T	p.(Arg248Trp)	missense	validation
8FFPE	*TP53*	NM_000546.4	g.chr17:7518284G>C	c.722C>G	p.(Ser241Cys)	missense	validation
9FFPE	*TP53*	NM_000546.4	g.chr17:7519131C>T	c.524G>A	p.(Arg175His)	missense	validation
14FFPE	*TP53*	NM_000546.4	g.chr17:7517845C>T	c.818G>A	p.(Arg273His)	missense	validation
15FFPE	*TP53*	NM_000546.4	g.chr17:7518915T>C	c.659A>G	p.(Tyr220Cys)	missense	validation
16FFPE	*TP53*	NM_000546.4	g.chr17:7519263T>C	c.392A>G	p.(Asn131Ser)	missense	validation
19FFPE	*TP53*	NM_000546.4	g.chr17:7518264G>A	c.742C>T	p.(Arg248Trp)	missense	validation
20FFPE	*TP53*	NM_000546.4	g.chr17:7517839C>A	c.824G>T	p.(Cys275Phe)	missense	validation
21FFPE	*TP53*	NM_000546.4	g.chr17:7517846G>A	c.817C>T	p.(Arg273Cys)	missense	validation
22FFPE	*TP53*	NM_000546.4	g.chr17:7518263C>T	c.743G>A	p.(Arg248Gln)	missense	validation
22FFPE	*TP53*	NM_000546.4	g.chr17:7517580G>A	c.991C>T	p.(Gln331*)	nonsense	validation
23FFPE	*TP53*	NM_000546.4	g.chr17:7519131C>T	c.524G>A	p.(Arg175His)	missense	validation
24FFPE	*TP53*	NM_000546.4	g.chr17:7519131C>T	c.524G>A	p.(Arg175His)	missense	validation
25FFPE	*TP53*	NM_000546.4	g.chr17:7517833C>T	c.830G>A	p.(Cys277Tyr)	missense	validation
25FFPE	*TP53*	NM_000546.4	g.chr17:7517748_7517757del	c.906_915del	p.(Ser303Glufs*39)	frameshift	validation
28FFPE	*TP53*	NM_000546.4	g.chr17:7518263C>T	c.743G>A	p.(Arg248Gln)	missense	validation
29FFPE	*TP53*	NM_000546.4	g.chr17:7518306A>G	c.700T>C	p.(Tyr234His)	missense	validation
30FFPE	*TP53*	NM_000546.4	g.chr17:7519131C>T	c.524G>A	p.(Arg175His)	missense	validation
31FFPE	*TP53*	NM_000546.4	g.chr17:7517846G>A	c.817C>T	p.(Arg273Cys)	missense	validation
32FFPE	*TP53*	NM_000546.4	g.chr17:7519006G>A	c.568C>T	p.(Pro190Ser)	missense	validation

32FFPE	*TP53*	NM_000546.4	g.chr17:7518993A>G	c.581T>C	p.(Leu194Pro)	missense	validation
2360T	*TP53*	NM_000546.4	g.chr17:7518243T>A	c.763A>T	p.(Ile255Phe)	missense	validation
2748T	*TP53*	NM_000546.4	g.chr17:7517580del	c.991del	p.(Gln331Argfs*14)	frameshift	validation
2771T	*TP53*	NM_000546.4	g.chr17:7518933T>C	c.641A>G	p.(His214Arg)	missense	validation
2910T	*TP53*	NM_000546.4	g.chr17:7518996T>A	c.578A>T	p.(His193Leu)	missense	validation
30020T	*TP53*	NM_000546.4	g.chr17:7518273C>T	c.733G>A	p.(Gly245Ser)	missense	validation
34347T	*TP53*	NM_000546.4	g.chr17:7520093A>C	c.319T>G	p.(Tyr107Asp)	missense	validation
34451T	*TP53*	NM_000546.4	g.chr17:7518291T>C	c.715A>G	p.(Asn239Asp)	missense	validation
3572T	*TP53*	NM_000546.4	g.chr17:7517813T>G	c.850A>C	p.(Thr284Pro)	missense	validation
3746T	*TP53*	NM_000546.4	g.chr17:7514727C>G	c.1025G>C	p.(Arg342Pro)	missense	validation
4040TCS	*TP53*	NM_000546.4	g.chr17:7518990_7518992del	c.582_584del	p.(Ile195del)	in-frame indel	validation
4059T	*TP53*	NM_000546.4	g.chr17:7519131C>T	c.659A>G	p.(Tyr220Cys)	missense	validation
4059T	*TP53*	NM_000546.4	g.chr17:7517846G>A	c.817C>T	p.(Arg273Cys)	missense	validation
4285T	*TP53*	NM_000546.4	g.chr17:7518960T>C	c.614A>G	p.(Tyr205Cys)	missense	validation
4435T	*TP53*	NM_000546.4	g.chr17:7520269_7520288dup	c.124_143dup	p.(Asp48Glufs*3)	frameshift	validation
460TS	*TP53*	NM_000546.4	g.chr17:7520119_7520120del	c.292_293del	p.(Pro98Phefs*50)	frameshift	validation
62073T	*TP53*	NM_000546.4	g.chr17:7517846G>A	c.817C>T	p.(Arg273Cys)	missense	validation
62958	*TP53*	NM_000546.4	g.chr17:7517846G>A	c.817C>T	p.(Arg273Cys)	missense	validation
64646	*TP53*	NM_000546.4	g.chr17:7519131C>T	c.524G>A	p.(Arg175His)	missense	validation
64646	*TP53*	NM_000546.4	g.chr17:7517747G>A	c.916C>T	p.(Arg306*)	nonsense	validation
EM66	*TP53*	NM_000546.4	g.chr17:7518263C>T	c.743G>A	p.(Arg248Gln)	missense	validation
JB1428T	*TP53*	NM_000546.4	g.chr17:7518272C>A	c.734G>T	p.(Gly245Val)	missense	validation
JB2285	*TP53*	NM_000546.4	g.chr17:7518943del	c.631del	p.(Thr211Leufs*36)	frameshift	validation
JB2411T	*TP53*	NM_000546.4	g.chr17:7518289G>T	c.717C>A	p.(Asn239Lys)	missense	validation
JB2582T	*TP53*	NM_000546.4	g.chr17:7518249del	c.757del	p.(Thr253Profs*92)	frameshift	validation
JB2653T	*TP53*	NM_000546.4	g.chr17:7517846G>A	c.817C>T	p.(Arg273Cys)	missense	validation
JB2985T	*TP53*	NM_000546.4	g.chr17:7519260T>C	c.395A>G	p.(Lys132Arg)	missense	validation
JB3014T	*TP53*	NM_000546.4	g.chr17:7517840A>G	c.823T>C	p.(Cys275Arg)	missense	validation
JB3953T	*TP53*	NM_000546.4	g.chr17:7518290T>C	c.716A>G	p.(Asn239Ser)	missense	validation
JB938T	*TP53*	NM_000546.4	g.chr17:7518263C>T	c.743G>A	p.(Arg248Gln)	missense	validation
JH108T	*TP53*	NM_000546.4	g.chr17:7519129A>G	c.526T>C	p.(Cys176Arg)	missense	validation
JH666T	*TP53*	NM_000546.4	g.chr17:7518937G>A	c.637C>T	p.(Arg213*)	nonsense	validation
702TS	*PIK3CA*	NM_006218.2	g.chr3:180410668G>A	c.1252G>A	p.(Glu418Lys)	missense	discovery
863TCS	*PIK3CA*	NM_006218.2	g.chr3:180400172G>A	c.353G>A	p.(Gly118Asp)	missense	discovery
FM403T	*PIK3CA*	NM_006218.2	g.chr3:180405018G>A	c.1093G>A	p.(Glu365Lys)	missense	discovery
FM474T	*PIK3CA*	NM_006218.2	g.chr3:180404243T>G	c.1031T>G	p.(Val344Gly)	missense	discovery
3FFPE	*PIK3CA*	NM_006218.2	g.chr3:180434779A>G	c.3140A>G	p.(His1047Arg)	missense	validation
5FFPE	*PIK3CA*	NM_006218.2	g.chr3:180418786A>C	c.1634A>C	p.(Glu545Ala)	missense	validation
5FFPE	*PIK3CA*	NM_006218.2	g.chr3:180418810del	c.1658del	p.(Ser553Ilefs*7)	frameshift	validation
5FFPE	*PIK3CA*	NM_006218.2	g.chr3:180434779A>G	c.3140A>G	p.(His1047Arg)	missense	validation
7FFPE	*PIK3CA*	NM_006218.2	g.chr3:180434766A>G	c.3127A>G	p.(Met1043Val)	missense	validation
10FFPE	*PIK3CA*	NM_006218.2	g.chr3:180399618C>T	c.311C>T	p.(Pro104Leu)	missense	validation
10FFPE	*PIK3CA*	NM_006218.2	g.chr3:180434658G>C	c.3019G>C	p.(Gly1007Arg)	missense	validation
19FFPE	*PIK3CA*	NM_006218.2	g.chr3:180434779A>G	c.3140A>G	p.(His1047Arg)	missense	validation
2771T	*PIK3CA*	NM_006218.2	g.chr3:180434768G>A	c.3129G>A	p.(Met1043Ile)	missense	validation

2910T	*PIK3CA*	NM_006218.2	g.chr3:180418785G>A	c.1633G>A	p.(Glu545Lys)	missense	validation
34347T	*PIK3CA*	NM_006218.2	g.chr3:180399624G>T	c.317G>T	p.(Gly106Val)	missense	validation
34451T	*PIK3CA*	NM_006218.2	g.chr3:180399638A>G	c.331A>G	p.(Lys111Glu)	missense	validation
4435T	*PIK3CA*	NM_006218.2	g.chr3:180418770C>G	c.1618C>G	p.(Leu540Val)	missense	validation
62958	*PIK3CA*	NM_006218.2	g.chr3:180418785G>A	c.1633G>A	p.(Glu545Lys)	missense	validation
EM66	*PIK3CA*	NM_006218.2	g.chr3:180399635_180399637 del	c.328_330del	p.(Glu110del)	in-frame indel	validation
JB2411T	*PIK3CA*	NM_006218.2	g.chr3:180410674T>C	c.1258T>C	p.(Cys420Arg)	missense	validation
JB2985T	*PIK3CA*	NM_006218.2	g.chr3:180434779A>G	c.3140A>G	p.(His1047Arg)	missense	validation
366TS	*FBXW7*	NM_033632.2	g.chr4:153468834C>T	c.1394G>A	p.(Arg465His)	missense	discovery
900T	*FBXW7*	NM_033632.2	g.chr4:153468835G>A	c.1393C>T	p.(Arg465Cys)	missense	discovery
DM851T	*FBXW7*	NM_033632.2	g.chr4:153468834C>A	c.1394G>T	p.(Arg465Leu)	missense	discovery
1FFPE	*FBXW7*	NM_033632.2	g.chr4:153468910C>T	c.1318G>A	p.(Asp440Asn)	missense	validation
1FFPE	*FBXW7*	NM_033632.2	g.chr4:153471333del	c.1122+1del	p.?	splice site	validation
6FFPE	*FBXW7*	NM_033632.2	g.chr4:153466745C>T	c.1507G>A	p.(Ala503Thr)	missense	validation
7FFPE	*FBXW7*	NM_033632.2	g.chr4:153468834C>T	c.1394G>A	p.(Arg465His)	missense	validation
16FFPE	*FBXW7*	NM_033632.2	g.chr4:153468835G>A	c.1393C>T	p.(Arg465Cys)	missense	validation
19FFPE	*FBXW7*	NM_033632.2	g.chr4:153468835G>A	c.1393C>T	p.(Arg465Cys)	missense	validation
23FFPE	*FBXW7*	NM_033632.2	g.chr4:153468811del	c.1417del	p.(Arg473Glufs*25)	frameshift	validation
31FFPE	*FBXW7*	NM_033632.2	g.chr4:153466739G>A	c.1513C>T	p.(Arg505Cys)	missense	validation
32FFPE	*FBXW7*	NM_033632.2	g.chr4:153468834C>T	c.1394G>A	p.(Arg465His)	missense	validation
2360T	*FBXW7*	NM_033632.2	g.chr4:153466739G>T	c.1513C>A	p.(Arg505Ser)	missense	validation
2748T	*FBXW7*	NM_033632.2	g.chr4:153468835G>A	c.1393C>T	p.(Arg465Cys)	missense	validation
64646	*FBXW7*	NM_033632.2	g.chr4:153468907G>A	c.1321C>T	p.(Arg441Trp)	missense	validation
JB2985T	*FBXW7*	NM_033632.2	g.chr4:153468835G>A	c.1393C>T	p.(Arg465Cys)	missense	validation
555TS	*PPP2R1A*	NM_014225.5	g.chr19:57407783C>G	c.536C>G	p.(Pro179Arg)	missense	discovery
702TS	*PPP2R1A*	NM_014225.5	g.chr19:57408135C>A	c.767C>A	p.(Ser256Tyr)	missense	discovery
1FFPE	*PPP2R1A*	NM_014225.5	g.chr19:57408137T>G	c.769T>G	p.(Trp257Gly)	missense	validation
3FFPE	*PPP2R1A*	NM_014225.5	g.chr19:57408135C>T	c.767C>T	p.(Ser256Phe)	missense	validation
15FFPE	*PPP2R1A*	NM_014225.5	g.chr19:57407783C>G	c.536C>G	p.(Pro179Arg)	missense	validation
26FFPE	*PPP2R1A*	NM_014225.5	g.chr19:57407783C>G	c.536C>G	p.(Pro179Arg)	missense	validation
2910T	*PPP2R1A*	NM_014225.5	g.chr19:57407794C>T	c.547C>T	p.(Arg183Trp)	missense	validation
30020T	*PPP2R1A*	NM_014225.5	g.chr19:57407783C>G	c.536C>G	p.(Pro179Arg)	missense	validation
34451T	*PPP2R1A*	NM_014225.5	g.chr19:57407783C>G	c.536C>G	p.(Pro179Arg)	missense	validation
4435T	*PPP2R1A*	NM_014225.5	g.chr19:57407794C>T	c.547C>T	p.(Arg183Trp)	missense	validation
62958	*PPP2R1A*	NM_014225.5	g.chr19:57408139G>C	c.771G>C	p.(Trp257Cys)	missense	validation
JB2411T	*PPP2R1A*	NM_014225.5	g.chr19:57407794C>T	c.547C>T	p.(Arg183Trp)	missense	validation
JB3953T	*PPP2R1A*	NM_014225.5	g.chr19:57407783C>G	c.536C>G	p.(Pro179Arg)	missense	validation
JB938T	*PPP2R1A*	NM_014225.5	g.chr19:57407783C>G	c.536C>G	p.(Pro179Arg)	missense	validation
*Coordinates refer to human reference genome hg18 release (NCBI 36.1, March 2006)							

Appendix 3

Samples evaluated for *TERT* promoter mutations							
ID	**Primary site**	**Tumor type**	***TERT* promoter mutation**	**ARID1A protein**	***PIK3CA* mutation**	**Specimen source**	**Specimen type**
TOK1	ovary	clear cell carcinoma	none	positive	n/a	Japan	FFPE
TOK2	ovary	clear cell carcinoma	none	negative	n/a	Japan	FFPE
TOK3	ovary	clear cell carcinoma	c.-124C>T	positive	n/a	Japan	FFPE
TOK4	ovary	clear cell carcinoma	none	negative	n/a	Japan	FFPE
TOK5	ovary	clear cell carcinoma	none	positive	n/a	Japan	FFPE
TOK6	ovary	clear cell carcinoma	none	positive	n/a	Japan	FFPE
TOK7	ovary	clear cell carcinoma	none	negative	n/a	Japan	FFPE
TOK8	ovary	clear cell carcinoma	none	negative	n/a	Japan	FFPE
TOK9	ovary	clear cell carcinoma	c.-124C>T	positive	n/a	Japan	FFPE
TOK10	ovary	clear cell carcinoma	none	negative	n/a	Japan	FFPE
TOK11	ovary	clear cell carcinoma	none	positive	n/a	Japan	FFPE
TOK12	ovary	clear cell carcinoma	none	negative	n/a	Japan	FFPE
TOK13	ovary	clear cell carcinoma	none	negative	n/a	Japan	FFPE
TOK14	ovary	clear cell carcinoma	none	negative	n/a	Japan	FFPE
TOK15	ovary	clear cell carcinoma	none	negative	n/a	Japan	FFPE
TOK16	ovary	clear cell carcinoma	none	positive	n/a	Japan	FFPE
TOK17	ovary	clear cell carcinoma	none	negative	n/a	Japan	FFPE
TOK18	ovary	clear cell carcinoma	none	negative	n/a	Japan	FFPE
TOK19	ovary	clear cell carcinoma	c.-124C>T	negative	n/a	Japan	FFPE
TOK21	ovary	clear cell carcinoma	none	negative	n/a	Japan	FFPE
TOK22	ovary	clear cell carcinoma	none	positive	n/a	Japan	FFPE
TOK23	ovary	clear cell carcinoma	none	negative	n/a	Japan	FFPE
TOK24	ovary	clear cell carcinoma	none	negative	n/a	Japan	FFPE
TOK25	ovary	clear cell carcinoma	none	positive	n/a	Japan	FFPE
TOK26	ovary	clear cell carcinoma	none	negative	n/a	Japan	FFPE
TOK27	ovary	clear cell carcinoma	none	negative	n/a	Japan	FFPE
TOK28	ovary	clear cell carcinoma	none	negative	n/a	Japan	FFPE
TOK29	ovary	clear cell carcinoma	none	negative	n/a	Japan	FFPE
TOK30	ovary	clear cell carcinoma	none	negative	n/a	Japan	FFPE
TOK31	ovary	clear cell carcinoma	none	negative	n/a	Japan	FFPE
TOK32	ovary	clear cell carcinoma	c.-124C>T	positive	n/a	Japan	FFPE
TOK33	ovary	clear cell carcinoma	none	negative	n/a	Japan	FFPE
TOK34	ovary	clear cell carcinoma	none	positive	n/a	Japan	FFPE
TOK35	ovary	clear cell carcinoma	none	negative	n/a	Japan	FFPE
TOK36	ovary	clear cell carcinoma	none	negative	n/a	Japan	FFPE
TOK37	ovary	clear cell carcinoma	none	negative	n/a	Japan	FFPE
TOK38	ovary	clear cell carcinoma	none	positive	n/a	Japan	FFPE
TOK39	ovary	clear cell carcinoma	none	positive	n/a	Japan	FFPE
TOK40	ovary	clear cell carcinoma	none	positive	n/a	Japan	FFPE

TOK41	ovary	clear cell carcinoma	c.-124C>T	positive	n/a	Japan	FFPE
TOK42	ovary	clear cell carcinoma	none	negative	n/a	Japan	FFPE
TOK43	ovary	clear cell carcinoma	none	positive	n/a	Japan	FFPE
TOK44	ovary	clear cell carcinoma	none	positive	n/a	Japan	FFPE
TOK45	ovary	clear cell carcinoma	none	negative	n/a	Japan	FFPE
TOK46	ovary	clear cell carcinoma	none	negative	n/a	Japan	FFPE
TOK47	ovary	clear cell carcinoma	none	positive	n/a	Japan	FFPE
TOK48	ovary	clear cell carcinoma	none	negative	n/a	Japan	FFPE
TOK49	ovary	clear cell carcinoma	none	negative	n/a	Japan	FFPE
TOK52	ovary	clear cell carcinoma	none	negative	n/a	Japan	FFPE
TOK53	ovary	clear cell carcinoma	none	negative	n/a	Japan	FFPE
TOK54	ovary	clear cell carcinoma	c.-124C>T	positive	n/a	Japan	FFPE
TOK55	ovary	clear cell carcinoma	none	negative	n/a	Japan	FFPE
TOK56	ovary	clear cell carcinoma	none	positive	n/a	Japan	FFPE
TOK57	ovary	clear cell carcinoma	none	positive	n/a	Japan	FFPE
TOK58	ovary	clear cell carcinoma	none	negative	n/a	Japan	FFPE
TOK59	ovary	clear cell carcinoma	none	negative	n/a	Japan	FFPE
TOK60	ovary	clear cell carcinoma	none	negative	n/a	Japan	FFPE
TOK61	ovary	clear cell carcinoma	none	negative	n/a	Japan	FFPE
TOK62	ovary	clear cell carcinoma	none	negative	n/a	Japan	FFPE
TOK63	ovary	clear cell carcinoma	none	negative	n/a	Japan	FFPE
TOK64	ovary	clear cell carcinoma	none	negative	n/a	Japan	FFPE
TOK65	ovary	clear cell carcinoma	none	negative	n/a	Japan	FFPE
TOK66	ovary	clear cell carcinoma	none	negative	n/a	Japan	FFPE
TOK67	ovary	clear cell carcinoma	none	negative	n/a	Japan	FFPE
TOK68	ovary	clear cell carcinoma	none	negative	n/a	Japan	FFPE
TOK69	ovary	clear cell carcinoma	c.-124C>T	positive	none	Japan	FFPE
TOK70	ovary	clear cell carcinoma	none	positive	n/a	Japan	FFPE
TOK71	ovary	clear cell carcinoma	none	negative	n/a	Japan	FFPE
TOK72	ovary	clear cell carcinoma	none	negative	n/a	Japan	FFPE
TOK73	ovary	clear cell carcinoma	none	negative	n/a	Japan	FFPE
TOK74	ovary	clear cell carcinoma	none	negative	n/a	Japan	FFPE
TOK75	ovary	clear cell carcinoma	c.-146C>T	positive	n/a	Japan	FFPE
TOK76	ovary	clear cell carcinoma	none	negative	n/a	Japan	FFPE
TOK77	ovary	clear cell carcinoma	c.-124C>T	positive	none	Japan	FFPE
TOK78	ovary	clear cell carcinoma	none	positive	n/a	Japan	FFPE
TOK79	ovary	clear cell carcinoma	none	negative	n/a	Japan	FFPE
TOK80	ovary	clear cell carcinoma	none	negative	n/a	Japan	FFPE
TOK82	ovary	clear cell carcinoma	none	negative	n/a	Japan	FFPE
TOK83	ovary	clear cell carcinoma	none	negative	n/a	Japan	FFPE
TOK85	ovary	clear cell carcinoma	none	negative	n/a	Japan	FFPE
TOK86	ovary	clear cell carcinoma	none	positive	n/a	Japan	FFPE
TOK87	ovary	clear cell carcinoma	none	positive	n/a	Japan	FFPE
TOK88	ovary	clear cell carcinoma	none	positive	n/a	Japan	FFPE
TOK89	ovary	clear cell carcinoma	none	negative	n/a	Japan	FFPE
TPE1	ovary	clear cell carcinoma	none	negative	none	Taiwan	FFPE
TPE2	ovary	clear cell carcinoma	none	positive	none	Taiwan	FFPE

TPE3	ovary	clear cell carcinoma	c.-124C>T	negative	none	Taiwan	FFPE
TPE5	ovary	clear cell carcinoma	none	positive	none	Taiwan	FFPE
TPE8	ovary	clear cell carcinoma	none	positive	none	Taiwan	FFPE
TPE9	ovary	clear cell carcinoma	none	negative	none	Taiwan	FFPE
TPE10	ovary	clear cell carcinoma	none	positive	none	Taiwan	FFPE
TPE12	ovary	clear cell carcinoma	none	negative	none	Taiwan	FFPE
TPE13	ovary	clear cell carcinoma	none	negative	none	Taiwan	FFPE
TPE14	ovary	clear cell carcinoma	none	positive	p.1047H>R (c.3140A>G)	Taiwan	FFPE
TPE17	ovary	clear cell carcinoma	none	negative	p.545E>A (c.1634A>C)	Taiwan	FFPE
TPE18	ovary	clear cell carcinoma	none	negative	none	Taiwan	FFPE
TPE19	ovary	clear cell carcinoma	c.-124C>T	positive	none	Taiwan	FFPE
TPE20	ovary	clear cell carcinoma	none	positive	none	Taiwan	FFPE
TPE21	ovary	clear cell carcinoma	none	negative	none	Taiwan	FFPE
TPE22	ovary	clear cell carcinoma	none	positive	none	Taiwan	FFPE
TPE23	ovary	clear cell carcinoma	none	negative	none	Taiwan	FFPE
TPE24	ovary	clear cell carcinoma	none	positive	none	Taiwan	FFPE
TPE25	ovary	clear cell carcinoma	none	negative	none	Taiwan	FFPE
TPE26	ovary	clear cell carcinoma	none	negative	p.1021Y>C (c.3062A>G)	Taiwan	FFPE
TPE27	ovary	clear cell carcinoma	c.-124C>T	positive	none	Taiwan	FFPE
TPE28	ovary	clear cell carcinoma	none	negative	none	Taiwan	FFPE
TPE29	ovary	clear cell carcinoma	none	positive	p.1049G>R (c.3145G>C)	Taiwan	FFPE
TPE30	ovary	clear cell carcinoma	none	negative	none	Taiwan	FFPE
TPE31	ovary	clear cell carcinoma	c.-124C>T	positive	none	Taiwan	FFPE
TPE32	ovary	clear cell carcinoma	c.-124C>T	positive	none	Taiwan	FFPE
TPE33	ovary	clear cell carcinoma	none	negative	p.1047H>R (c.3140A>G)	Taiwan	FFPE
TPE35	ovary	clear cell carcinoma	c.-124C>T	negative	none	Taiwan	FFPE
TPE36	ovary	clear cell carcinoma	none	positive	none	Taiwan	FFPE
TPE37	ovary	clear cell carcinoma	none	positive	p.39E>K (c.115G>A); p.545E>A(c.1634A>C)	Taiwan	FFPE
TPE38	ovary	clear cell carcinoma	none	negative	none	Taiwan	FFPE
TPE39	ovary	clear cell carcinoma	none	positive	none	Taiwan	FFPE
TPE40	ovary	clear cell carcinoma	none	negative	none	Taiwan	FFPE
TPE41	ovary	clear cell carcinoma	none	negative	p.542E>K (c.1624G>A)	Taiwan	FFPE
TPE43	ovary	clear cell carcinoma	none	negative	p.1043M>I (c.3129G>A)	Taiwan	FFPE
TPE44	ovary	clear cell carcinoma	none	negative	p.111K>E (c.331A>G)	Taiwan	FFPE
TOR1	ovary	clear cell carcinoma	none	positive	n/a	Canada	FFPE
TOR2	ovary	clear cell carcinoma	none	negative	n/a	Canada	FFPE
TOR3	ovary	clear cell carcinoma	none	negative	n/a	Canada	FFPE
TOR4	ovary	clear cell carcinoma	none	negative	n/a	Canada	FFPE
TOR5	ovary	clear cell carcinoma	c.-124C>T	n/a	n/a	Canada	FFPE
TOR6	ovary	clear cell carcinoma	none	negative	n/a	Canada	FFPE
TOR7	ovary	clear cell carcinoma	none	negative	n/a	Canada	FFPE
TOR8	ovary	clear cell carcinoma	none	positive	n/a	Canada	FFPE

TOR9	ovary	clear cell carcinoma	none	negative	n/a	Canada	FFPE
TOR10	ovary	clear cell carcinoma	none	negative	n/a	Canada	FFPE
TOR11	ovary	clear cell carcinoma	none	negative	n/a	Canada	FFPE
TOR12	ovary	clear cell carcinoma	none	negative	n/a	Canada	FFPE
TOR13	ovary	clear cell carcinoma	c.-124C>T	positive	n/a	Canada	FFPE
TOR14	ovary	clear cell carcinoma	none	n/a	n/a	Canada	FFPE
TOR15	ovary	clear cell carcinoma	none	n/a	n/a	Canada	FFPE
TOR17	ovary	clear cell carcinoma	c.-124C>T	positive	n/a	Canada	FFPE
TOR18	ovary	clear cell carcinoma	c.-146C>T	positive	n/a	Canada	FFPE
TOR19	ovary	clear cell carcinoma	none	negative	n/a	Canada	FFPE
TOR20	ovary	clear cell carcinoma	none	positive	n/a	Canada	FFPE
TOR21	ovary	clear cell carcinoma	none	negative	n/a	Canada	FFPE
TOR22	ovary	clear cell carcinoma	none	negative	n/a	Canada	FFPE
TOR23	ovary	clear cell carcinoma	none	negative	n/a	Canada	FFPE
TOR24	ovary	clear cell carcinoma	none	positive	n/a	Canada	FFPE
TOR25	ovary	clear cell carcinoma	c.-146C>T	positive	n/a	Canada	FFPE
TOR26	ovary	clear cell carcinoma	none	n/a	n/a	Canada	FFPE
TOR27	ovary	clear cell carcinoma	none	negative	n/a	Canada	FFPE
TOR28	ovary	clear cell carcinoma	none	negative	n/a	Canada	FFPE
TOR29	ovary	clear cell carcinoma	none	positive	n/a	Canada	FFPE
TOR30	ovary	clear cell carcinoma	none	negative	n/a	Canada	FFPE
TOR31	ovary	clear cell carcinoma	none	negative	n/a	Canada	FFPE
TOR32	ovary	clear cell carcinoma	none	negative	n/a	Canada	FFPE
TOR33	ovary	clear cell carcinoma	none	negative	n/a	Canada	FFPE
TOR34	ovary	clear cell carcinoma	c.-124C>T	positive	n/a	Canada	FFPE
TOR35	ovary	clear cell carcinoma	none	positive	n/a	Canada	FFPE
TOR36	ovary	clear cell carcinoma	none	positive	n/a	Canada	FFPE
TOR37	ovary	clear cell carcinoma	none	positive	n/a	Canada	FFPE
TOR38	ovary	clear cell carcinoma	c.-124C>T	positive	n/a	Canada	FFPE
TOR40	ovary	clear cell carcinoma	none	positive	n/a	Canada	FFPE
TOR41	ovary	clear cell carcinoma	none	positive	n/a	Canada	FFPE
TOR42	ovary	clear cell carcinoma	none	negative	n/a	Canada	FFPE
TOR43	ovary	clear cell carcinoma	c.-124C>T	positive	n/a	Canada	FFPE
TOR44	ovary	clear cell carcinoma	none	positive	n/a	Canada	FFPE
HAM1	ovary	clear cell carcinoma	none	n/a	n/a	Japan	FFPE
HAM2	ovary	clear cell carcinoma	c.-124C>T	positive	none	Japan	FFPE
HAM3	ovary	clear cell carcinoma	none	negative	p.545E>K (c.1633G>A)	Japan	FFPE
HAM4	ovary	clear cell carcinoma	c.-124C>T	negative	none	Japan	FFPE
HAM5	ovary	clear cell carcinoma	none	n/a	n/a	Japan	FFPE
HAM6	ovary	clear cell carcinoma	c.-124C>T	positive	none	Japan	FFPE
HAM7	ovary	clear cell carcinoma	c.-124C>T	positive	none	Japan	FFPE
HAM8	ovary	clear cell carcinoma	none	negative	none	Japan	FFPE
HAM9	ovary	clear cell carcinoma	none	positive	p.1047H>R (c.3140A>G)	Japan	FFPE
HAM10	ovary	clear cell carcinoma	none	negative	p.545E>K (c.1633G>A)	Japan	FFPE
HAM11	ovary	clear cell carcinoma	none	positive	p.1021Y>C (c.3062A>G)	Japan	FFPE

HAM12	ovary	clear cell carcinoma	none	negative	p.545E>K (c.1633G>A)	Japan	FFPE
HAM13	ovary	clear cell carcinoma	none	negative	p.1047H>R (c.3140A>G)	Japan	FFPE
HAM14	ovary	clear cell carcinoma	c.-124C>T	positive	p.546Q>R (c.1637A>G)	Japan	FFPE
HAM15	ovary	clear cell carcinoma	none	negative	p.546Q>K (c.1636C>A)	Japan	FFPE
HAM16	ovary	clear cell carcinoma	c.-124C>T	positive	none	Japan	FFPE
HAM17	ovary	clear cell carcinoma	c.-124C>T	positive	none	Japan	FFPE
HAM18	ovary	clear cell carcinoma	none	negative	none	Japan	FFPE
HAM19	ovary	clear cell carcinoma	none	negative	p.1047H>L (c.3140A>T)	Japan	FFPE
HAM20	ovary	clear cell carcinoma	none	negative	none	Japan	FFPE
HAM21	ovary	clear cell carcinoma	none	positive	none	Japan	FFPE
HAM22	ovary	clear cell carcinoma	none	negative	p.545E>K (c.1633G>A)	Japan	FFPE
HAM23	ovary	clear cell carcinoma	none	negative	none	Japan	FFPE
HAM24	ovary	clear cell carcinoma	c.-124C>T	positive	none	Japan	FFPE
HAM25	ovary	clear cell carcinoma	none	negative	none	Japan	FFPE
HAM26	ovary	clear cell carcinoma	none	negative	p.545E>K (c.1633G>A)	Japan	FFPE
HAM27	ovary	clear cell carcinoma	none	negative	none	Japan	FFPE
HAM28	ovary	clear cell carcinoma	none	positive	none	Japan	FFPE
HAM29	ovary	clear cell carcinoma	none	negative	p.545E>K (c.1633G>A)	Japan	FFPE
HAM30	ovary	clear cell carcinoma	none	positive	p.546Q>R (c.1637A>G)	Japan	FFPE
HAM31	ovary	clear cell carcinoma	none	negative	none	Japan	FFPE
HAM32	ovary	clear cell carcinoma	none	negative	p.1047H>R (c.3140A>G)	Japan	FFPE
HAM33	ovary	clear cell carcinoma	none	negative	none	Japan	FFPE
HAM34	ovary	clear cell carcinoma	c.-124C>T	positive	none	Japan	FFPE
HAM35	ovary	clear cell carcinoma	none	negative	p.1049G>R (c.3145G>C)	Japan	FFPE
JOC1	ovary	clear cell carcinoma	none	n/a	n/a	USA	frozen
JOC2	ovary	clear cell carcinoma	none	n/a	n/a	USA	frozen
JOC3	ovary	clear cell carcinoma	none	n/a	n/a	USA	frozen
JOC4	ovary	clear cell carcinoma	none	n/a	n/a	USA	frozen
JOC5	ovary	clear cell carcinoma	c.-124C>T	n/a	n/a	USA	frozen
JOC6	ovary	clear cell carcinoma	c.-124C>T	n/a	n/a	USA	frozen
JOC7	ovary	clear cell carcinoma	none	n/a	n/a	USA	frozen
JOC8	ovary	clear cell carcinoma	none	n/a	n/a	USA	frozen
JOC9	ovary	clear cell carcinoma	none	n/a	n/a	USA	frozen
JOC10	ovary	clear cell carcinoma	none	n/a	n/a	USA	frozen
JOC11	ovary	clear cell carcinoma	none	n/a	n/a	USA	frozen
JOC12	ovary	clear cell carcinoma	none	n/a	n/a	USA	frozen
JOC13	ovary	clear cell carcinoma	none	n/a	n/a	USA	frozen
JOC14	ovary	clear cell carcinoma	none	n/a	n/a	USA	frozen
JOC15	ovary	clear cell carcinoma	none	n/a	n/a	USA	frozen
JOC16	ovary	clear cell carcinoma	c.-124C>T	n/a	n/a	USA	frozen
JOC17	ovary	clear cell carcinoma	none	n/a	n/a	USA	frozen
JOC18	ovary	clear cell carcinoma	c.-124C>T	n/a	n/a	USA	frozen

JOC19	ovary	clear cell carcinoma	none	n/a	n/a	USA	frozen
JOC20	ovary	clear cell carcinoma	none	n/a	n/a	USA	frozen
JOC21	ovary	clear cell carcinoma	none	n/a	n/a	USA	frozen
JOC22	ovary	clear cell carcinoma	none	n/a	n/a	USA	frozen
JOC23	ovary	clear cell carcinoma	none	n/a	n/a	USA	frozen
JOC24	ovary	clear cell carcinoma	none	n/a	n/a	USA	frozen
JOC25	ovary	clear cell carcinoma	none	n/a	n/a	USA	frozen
JOC26	ovary	clear cell carcinoma	none	n/a	n/a	USA	frozen
JOC27	ovary	clear cell carcinoma	c.-124C>T	n/a	n/a	USA	frozen
JOC28	ovary	clear cell carcinoma	none	n/a	n/a	USA	frozen
JOC29	ovary	clear cell carcinoma	none	n/a	n/a	USA	frozen
JOC30	ovary	clear cell carcinoma	none	n/a	n/a	USA	frozen
JOC31	ovary	clear cell carcinoma	none	n/a	n/a	USA	frozen
JOC32	ovary	clear cell carcinoma	none	n/a	n/a	USA	frozen
JOC33	ovary	clear cell carcinoma	none	n/a	n/a	USA	frozen
JOC34	ovary	clear cell carcinoma	none	n/a	n/a	USA	frozen
JOC35	ovary	clear cell carcinoma	none	n/a	n/a	USA	frozen
JOC36	ovary	clear cell carcinoma	none	n/a	n/a	USA	frozen
ES-2	ovary	clear cell carcinoma	c.[-138C>T ;-139C>T]	n/a	none	n/a	cell line
JHOC5	ovary	clear cell carcinoma	c.-124C>T	n/a	none	n/a	cell line
KK	ovary	clear cell carcinoma	none	n/a	p.545E>A (c.1634A>C)	n/a	cell line
KOC-7C	ovary	clear cell carcinoma	none	n/a	n/a	n/a	cell line
OV207	ovary	clear cell carcinoma	c.-124C>T	n/a	none	n/a	cell line
OVCA429	ovary	clear cell carcinoma	none	n/a	p.545E>K (c.1633G>A)	n/a	cell line
OVISE	ovary	clear cell carcinoma	none	n/a	none	n/a	cell line
OVMANA	ovary	clear cell carcinoma	none	n/a	p.545E>V (1634A>T)	n/a	cell line
OVTOKO	ovary	clear cell carcinoma	none	n/a	none	n/a	cell line
TOV21G	ovary	clear cell carcinoma	none	n/a	p.1047H>Y (c.3139C>T)	n/a	cell line
OEM1	ovary	endometrioid carcinoma	none	n/a	n/a	USA	frozen
OEM2	ovary	endometrioid carcinoma	none	n/a	n/a	USA	frozen
OEM3	ovary	endometrioid carcinoma	none	n/a	n/a	USA	frozen
OEM4	ovary	endometrioid carcinoma	none	n/a	n/a	USA	frozen
OEM5	ovary	endometrioid carcinoma	none	n/a	n/a	USA	frozen
OEM6	ovary	endometrioid carcinoma	none	n/a	n/a	USA	frozen
OEM7	ovary	endometrioid carcinoma	none	n/a	n/a	USA	frozen
OEM8	ovary	endometrioid carcinoma	none	n/a	n/a	USA	frozen
OEM9	ovary	endometrioid carcinoma	none	n/a	n/a	USA	frozen
OEM10	ovary	endometrioid carcinoma	none	n/a	n/a	USA	frozen
OEM11	ovary	endometrioid carcinoma	none	n/a	n/a	USA	frozen
OEM12	ovary	endometrioid carcinoma	none	n/a	n/a	USA	frozen
OEM13	ovary	endometrioid carcinoma	none	n/a	n/a	USA	frozen
OEM14	ovary	endometrioid carcinoma	none	n/a	n/a	USA	frozen
OEM15	ovary	endometrioid carcinoma	none	n/a	n/a	USA	frozen
OEM16	ovary	endometrioid carcinoma	none	n/a	n/a	USA	frozen
OEM17	ovary	endometrioid carcinoma	none	n/a	n/a	USA	frozen

OEM18	ovary	endometrioid carcinoma	none	n/a	n/a	USA	frozen
OEM19	ovary	endometrioid carcinoma	none	n/a	n/a	USA	frozen
OEM20	ovary	endometrioid carcinoma	none	n/a	n/a	USA	frozen
OEM21	ovary	endometrioid carcinoma	none	n/a	n/a	USA	frozen
OEM22	ovary	endometrioid carcinoma	none	n/a	n/a	USA	frozen
OEM23	ovary	endometrioid carcinoma	none	n/a	n/a	USA	frozen
OEM24	ovary	endometrioid carcinoma	none	n/a	n/a	USA	frozen
OEM25	ovary	endometrioid carcinoma	none	n/a	n/a	USA	frozen
OEM26	ovary	endometrioid carcinoma	none	n/a	n/a	USA	frozen
OEM27	ovary	endometrioid carcinoma	none	n/a	n/a	USA	frozen
OEM28	ovary	endometrioid carcinoma	none	n/a	n/a	USA	frozen
OEM29	ovary	endometrioid carcinoma	none	n/a	n/a	USA	frozen
OEM30	ovary	endometrioid carcinoma	none	n/a	n/a	USA	frozen
OEM31	ovary	endometrioid carcinoma	none	n/a	n/a	USA	frozen
OEM32	ovary	endometrioid carcinoma	none	n/a	n/a	USA	frozen
OEM33	ovary	endometrioid carcinoma	none	n/a	n/a	USA	frozen
OEM34	ovary	endometrioid carcinoma	none	n/a	n/a	USA	frozen
OEM35	ovary	endometrioid carcinoma	none	n/a	n/a	USA	frozen
OEM36	ovary	endometrioid carcinoma	none	n/a	n/a	USA	frozen
OEM37	ovary	endometrioid carcinoma	none	n/a	n/a	USA	frozen
OEM38	ovary	endometrioid carcinoma	none	n/a	n/a	USA	frozen
OEM39	ovary	endometrioid carcinoma	none	n/a	n/a	USA	frozen
OEM40	ovary	endometrioid carcinoma	none	n/a	n/a	USA	frozen
OEM41	ovary	endometrioid carcinoma	none	n/a	n/a	USA	frozen
OEM42	ovary	endometrioid carcinoma	none	n/a	n/a	USA	frozen
OEM43	ovary	endometrioid carcinoma	none	n/a	n/a	USA	frozen
JHS1	ovary	high grade serous carcinoma	none	n/a	n/a	USA	frozen
JHS2	ovary	high grade serous carcinoma	none	n/a	n/a	USA	frozen
JHS3	ovary	high grade serous carcinoma	none	n/a	n/a	USA	frozen
JHS4	ovary	high grade serous carcinoma	none	n/a	n/a	USA	frozen
JHS5	ovary	high grade serous carcinoma	none	n/a	n/a	USA	frozen
JHS6	ovary	high grade serous carcinoma	none	n/a	n/a	USA	frozen
JHS7	ovary	high grade serous carcinoma	none	n/a	n/a	USA	frozen
JHS8	ovary	high grade serous carcinoma	none	n/a	n/a	USA	frozen
JHS9	ovary	high grade serous carcinoma	none	n/a	n/a	USA	frozen
JHS10	ovary	high grade serous carcinoma	none	n/a	n/a	USA	frozen
JHS11	ovary	high grade serous carcinoma	none	n/a	n/a	USA	frozen
JHS12	ovary	high grade serous carcinoma	none	n/a	n/a	USA	frozen
JHS13	ovary	high grade serous carcinoma	none	n/a	n/a	USA	frozen
JHS14	ovary	high grade serous carcinoma	none	n/a	n/a	USA	frozen
JHS15	ovary	high grade serous carcinoma	none	n/a	n/a	USA	frozen
JHS16	ovary	high grade serous carcinoma	none	n/a	n/a	USA	frozen
JHS17	ovary	high grade serous carcinoma	none	n/a	n/a	USA	frozen
JHS18	ovary	high grade serous carcinoma	none	n/a	n/a	USA	frozen
JHS19	ovary	high grade serous carcinoma	none	n/a	n/a	USA	frozen
JHS20	ovary	high grade serous carcinoma	none	n/a	n/a	USA	frozen
JHS21	ovary	high grade serous carcinoma	none	n/a	n/a	USA	frozen

JHS22	ovary	high grade serous carcinoma	none	n/a	n/a	USA	frozen
JHS23	ovary	high grade serous carcinoma	none	n/a	n/a	USA	frozen
JHS24	ovary	high grade serous carcinoma	none	n/a	n/a	USA	frozen
JHS25	ovary	high grade serous carcinoma	none	n/a	n/a	USA	frozen
JHS26	ovary	high grade serous carcinoma	none	n/a	n/a	USA	frozen
JHS27	ovary	high grade serous carcinoma	none	n/a	n/a	USA	frozen
JHS28	ovary	high grade serous carcinoma	none	n/a	n/a	USA	frozen
JHS29	ovary	high grade serous carcinoma	none	n/a	n/a	USA	frozen
JHS30	ovary	high grade serous carcinoma	none	n/a	n/a	USA	frozen
JHS31	ovary	high grade serous carcinoma	none	n/a	n/a	USA	frozen
JHS32	ovary	high grade serous carcinoma	none	n/a	n/a	USA	frozen
JHS33	ovary	high grade serous carcinoma	none	n/a	n/a	USA	frozen
JHS34	ovary	high grade serous carcinoma	none	n/a	n/a	USA	frozen
JHS35	ovary	high grade serous carcinoma	none	n/a	n/a	USA	frozen
JHS36	ovary	high grade serous carcinoma	none	n/a	n/a	USA	frozen
JHS37	ovary	high grade serous carcinoma	none	n/a	n/a	USA	frozen
JHS38	ovary	high grade serous carcinoma	none	n/a	n/a	USA	frozen
JHS39	ovary	high grade serous carcinoma	none	n/a	n/a	USA	frozen
JHS40	ovary	high grade serous carcinoma	none	n/a	n/a	USA	frozen
JHS41	ovary	high grade serous carcinoma	none	n/a	n/a	USA	frozen
JHS42	ovary	high grade serous carcinoma	none	n/a	n/a	USA	frozen
JHS43	ovary	high grade serous carcinoma	none	n/a	n/a	USA	frozen
JHS44	ovary	high grade serous carcinoma	none	n/a	n/a	USA	frozen
JHS45	ovary	high grade serous carcinoma	none	n/a	n/a	USA	frozen
JHS46	ovary	high grade serous carcinoma	none	n/a	n/a	USA	frozen
JHS47	ovary	high grade serous carcinoma	none	n/a	n/a	USA	frozen
JHS48	ovary	high grade serous carcinoma	none	n/a	n/a	USA	frozen
JHS49	ovary	high grade serous carcinoma	none	n/a	n/a	USA	frozen
JHS50	ovary	high grade serous carcinoma	none	n/a	n/a	USA	frozen
JHS51	ovary	high grade serous carcinoma	none	n/a	n/a	USA	frozen
JHS52	ovary	high grade serous carcinoma	none	n/a	n/a	USA	frozen
JHS53	ovary	high grade serous carcinoma	none	n/a	n/a	USA	frozen
JHS54	ovary	high grade serous carcinoma	none	n/a	n/a	USA	frozen
JHS55	ovary	high grade serous carcinoma	none	n/a	n/a	USA	frozen
JHS56	ovary	high grade serous carcinoma	none	n/a	n/a	USA	frozen
JHS57	ovary	high grade serous carcinoma	none	n/a	n/a	USA	frozen
JHS58	ovary	high grade serous carcinoma	none	n/a	n/a	USA	frozen
JHS59	ovary	high grade serous carcinoma	none	n/a	n/a	USA	frozen
JHS60	ovary	high grade serous carcinoma	none	n/a	n/a	USA	frozen
JHS61	ovary	high grade serous carcinoma	none	n/a	n/a	USA	frozen
JHS62	ovary	high grade serous carcinoma	none	n/a	n/a	USA	frozen
JHS63	ovary	high grade serous carcinoma	none	n/a	n/a	USA	frozen
JHS64	ovary	high grade serous carcinoma	none	n/a	n/a	USA	frozen
JHS65	ovary	high grade serous carcinoma	none	n/a	n/a	USA	frozen
JHS66	ovary	high grade serous carcinoma	none	n/a	n/a	USA	frozen
JHS67	ovary	high grade serous carcinoma	none	n/a	n/a	USA	frozen
JHS68	ovary	high grade serous carcinoma	none	n/a	n/a	USA	frozen

JHS69	ovary	high grade serous carcinoma	none	n/a	n/a	USA	frozen
JHS70	ovary	high grade serous carcinoma	none	n/a	n/a	USA	frozen
JHS71	ovary	high grade serous carcinoma	none	n/a	n/a	USA	frozen
JHS72	ovary	high grade serous carcinoma	none	n/a	n/a	USA	frozen
JHS73	ovary	high grade serous carcinoma	none	n/a	n/a	USA	frozen
JHS74	ovary	high grade serous carcinoma	none	n/a	n/a	USA	frozen
JHS75	ovary	high grade serous carcinoma	none	n/a	n/a	USA	frozen
JHS76	ovary	high grade serous carcinoma	none	n/a	n/a	USA	frozen
JHS77	ovary	high grade serous carcinoma	none	n/a	n/a	USA	frozen
JHS78	ovary	high grade serous carcinoma	none	n/a	n/a	USA	frozen
JHS79	ovary	high grade serous carcinoma	none	n/a	n/a	USA	frozen
JHS80	ovary	high grade serous carcinoma	none	n/a	n/a	USA	frozen
LGS1	ovary	low grade serous carcinoma	none	n/a	n/a	USA	frozen
LGS2	ovary	low grade serous carcinoma	none	n/a	n/a	USA	frozen
LGS3	ovary	low grade serous carcinoma	none	n/a	n/a	USA	frozen
LGS4	ovary	low grade serous carcinoma	none	n/a	n/a	USA	frozen
LGS5	ovary	low grade serous carcinoma	none	n/a	n/a	USA	frozen
LGS6	ovary	low grade serous carcinoma	none	n/a	n/a	USA	frozen
LGS7	ovary	low grade serous carcinoma	c.-124C>T	n/a	n/a	USA	frozen
LGS8	ovary	low grade serous carcinoma	none	n/a	n/a	USA	frozen
LGS9	ovary	low grade serous carcinoma	none	n/a	n/a	USA	frozen
LGS10	ovary	low grade serous carcinoma	none	n/a	n/a	USA	frozen
LGS11	ovary	low grade serous carcinoma	none	n/a	n/a	USA	frozen
LGS12	ovary	low grade serous carcinoma	none	n/a	n/a	USA	frozen
LGS13	ovary	low grade serous carcinoma	none	n/a	n/a	USA	frozen
LGS14	ovary	low grade serous carcinoma	none	n/a	n/a	USA	frozen
LGS15	ovary	low grade serous carcinoma	none	n/a	n/a	USA	frozen
LGS16	ovary	low grade serous carcinoma	none	n/a	n/a	USA	frozen
LGS17	ovary	low grade serous carcinoma	none	n/a	n/a	USA	frozen
LGS18	ovary	low grade serous carcinoma	none	n/a	n/a	USA	frozen
LGS19	ovary	low grade serous carcinoma	none	n/a	n/a	USA	frozen
LGS20	ovary	low grade serous carcinoma	none	n/a	n/a	USA	frozen
LGS21	ovary	low grade serous carcinoma	none	n/a	n/a	USA	frozen
LGS22	ovary	low grade serous carcinoma	none	n/a	n/a	USA	frozen
LGS23	ovary	low grade serous carcinoma	none	n/a	n/a	USA	frozen
LGS24	ovary	low grade serous carcinoma	none	n/a	n/a	USA	frozen
LGS25	ovary	low grade serous carcinoma	none	n/a	n/a	USA	frozen
LGS26	ovary	low grade serous carcinoma	none	n/a	n/a	USA	frozen
LGS27	ovary	low grade serous carcinoma	none	n/a	n/a	USA	frozen
LGS28	ovary	low grade serous carcinoma	none	n/a	n/a	USA	frozen
LGS29	ovary	low grade serous carcinoma	none	n/a	n/a	USA	frozen
LGS30	ovary	low grade serous carcinoma	none	n/a	n/a	USA	frozen
LGS31	ovary	low grade serous carcinoma	none	n/a	n/a	USA	frozen
LGS32	ovary	low grade serous carcinoma	none	n/a	n/a	USA	frozen
LGS33	ovary	low grade serous carcinoma	none	n/a	n/a	USA	frozen
UEM1	uterine corpus	endometrioid carcinoma	none	n/a	n/a	USA	frozen
UEM2	uterine corpus	endometrioid carcinoma	none	n/a	n/a	USA	frozen

UEM3	uterine corpus	endometrioid carcinoma	none	n/a	n/a	USA	frozen
UEM4	uterine corpus	endometrioid carcinoma	none	n/a	n/a	USA	frozen
UEM5	uterine corpus	endometrioid carcinoma	none	n/a	n/a	USA	frozen
UEM6	uterine corpus	endometrioid carcinoma	none	n/a	n/a	USA	frozen
UEM7	uterine corpus	endometrioid carcinoma	none	n/a	n/a	USA	frozen
UEM8	uterine corpus	endometrioid carcinoma	none	n/a	n/a	USA	frozen
UEM9	uterine corpus	endometrioid carcinoma	none	n/a	n/a	USA	frozen
UEM10	uterine corpus	endometrioid carcinoma	none	n/a	n/a	USA	frozen
UEM11	uterine corpus	endometrioid carcinoma	none	n/a	n/a	USA	frozen
UEM12	uterine corpus	endometrioid carcinoma	none	n/a	n/a	USA	frozen
UEM13	uterine corpus	endometrioid carcinoma	none	n/a	n/a	USA	frozen
UEM14	uterine corpus	endometrioid carcinoma	none	n/a	n/a	USA	frozen
UEM15	uterine corpus	endometrioid carcinoma	none	n/a	n/a	USA	frozen
UEM16	uterine corpus	endometrioid carcinoma	none	n/a	n/a	USA	frozen
UEM17	uterine corpus	endometrioid carcinoma	none	n/a	n/a	USA	frozen
UEM18	uterine corpus	endometrioid carcinoma	none	n/a	n/a	USA	frozen
UEM19	uterine corpus	endometrioid carcinoma	none	n/a	n/a	USA	frozen
UEM20	uterine corpus	endometrioid carcinoma	none	n/a	n/a	USA	frozen
UEM21	uterine corpus	endometrioid carcinoma	none	n/a	n/a	USA	frozen
UEM22	uterine corpus	endometrioid carcinoma	none	n/a	n/a	USA	frozen
UEM23	uterine corpus	endometrioid carcinoma	none	n/a	n/a	USA	frozen
UEM24	uterine corpus	endometrioid carcinoma	none	n/a	n/a	USA	frozen
USC1	uterine corpus	serous carcinoma	none	n/a	n/a	USA	frozen
USC2	uterine corpus	serous carcinoma	none	n/a	n/a	USA	frozen
USC3	uterine corpus	serous carcinoma	none	n/a	n/a	USA	frozen
USC4	uterine corpus	serous carcinoma	none	n/a	n/a	USA	frozen
USC5	uterine corpus	serous carcinoma	none	n/a	n/a	USA	frozen
USC6	uterine corpus	serous carcinoma	none	n/a	n/a	USA	frozen
USC7	uterine corpus	serous carcinoma	none	n/a	n/a	USA	frozen
USC8	uterine corpus	serous carcinoma	none	n/a	n/a	USA	frozen
USC9	uterine corpus	serous carcinoma	none	n/a	n/a	USA	frozen
USC10	uterine corpus	serous carcinoma	none	n/a	n/a	USA	frozen
USC11	uterine corpus	serous carcinoma	none	n/a	n/a	USA	frozen
USC12	uterine corpus	serous carcinoma	none	n/a	n/a	USA	frozen
LMS1	uterine corpus	leiomyosarcoma	none	n/a	n/a	USA	frozen
LMS2	uterine corpus	leiomyosarcoma	none	n/a	n/a	USA	frozen
LMS3	uterine corpus	leiomyosarcoma	none	n/a	n/a	USA	frozen
LMS4	uterine corpus	leiomyosarcoma	none	n/a	n/a	USA	frozen
LMS5	uterine corpus	leiomyosarcoma	none	n/a	n/a	USA	frozen
LMS6	uterine corpus	leiomyosarcoma	none	n/a	n/a	USA	frozen
LMS7	uterine corpus	leiomyosarcoma	none	n/a	n/a	USA	frozen
LMS8	uterine corpus	leiomyosarcoma	none	n/a	n/a	USA	frozen
LMS9	uterine corpus	leiomyosarcoma	none	n/a	n/a	USA	frozen
LMS10	uterine corpus	leiomyosarcoma	none	n/a	n/a	USA	frozen
LMS11	uterine corpus	leiomyosarcoma	none	n/a	n/a	USA	frozen
LMS12	uterine corpus	leiomyosarcoma	none	n/a	n/a	USA	frozen
LMS13	uterine corpus	leiomyosarcoma	none	n/a	n/a	USA	frozen

LMS14	uterine corpus	leiomyosarcoma	none	n/a	n/a	USA	frozen
LMS15	uterine corpus	leiomyosarcoma	none	n/a	n/a	USA	frozen
LMS16	uterine corpus	leiomyosarcoma	none	n/a	n/a	USA	frozen
LMS17	uterine corpus	leiomyosarcoma	none	n/a	n/a	USA	frozen
LMS18	uterine corpus	leiomyosarcoma	none	n/a	n/a	USA	frozen
LMS19	uterine corpus	leiomyosarcoma	none	n/a	n/a	USA	frozen
LMS20	uterine corpus	leiomyosarcoma	none	n/a	n/a	USA	frozen
LMS21	uterine corpus	leiomyosarcoma	none	n/a	n/a	USA	frozen
LMS22	uterine corpus	leiomyosarcoma	none	n/a	n/a	USA	frozen
SCC1	uterine cervix	squamous cell carcinoma	none	n/a	n/a	USA	FFPE
SCC2	uterine cervix	squamous cell carcinoma	none	n/a	n/a	USA	FFPE
SCC3	uterine cervix	squamous cell carcinoma	none	n/a	n/a	USA	FFPE
SCC4	uterine cervix	squamous cell carcinoma	none	n/a	n/a	USA	FFPE
SCC5	uterine cervix	squamous cell carcinoma	none	n/a	n/a	USA	FFPE
SCC6	uterine cervix	squamous cell carcinoma	none	n/a	n/a	USA	FFPE
SCC7	uterine cervix	squamous cell carcinoma	none	n/a	n/a	USA	FFPE
SCC8	uterine cervix	squamous cell carcinoma	none	n/a	n/a	USA	FFPE
SCC9	uterine cervix	squamous cell carcinoma	none	n/a	n/a	USA	FFPE
SCC10	uterine cervix	squamous cell carcinoma	none	n/a	n/a	USA	FFPE
SCC11	uterine cervix	squamous cell carcinoma	none	n/a	n/a	USA	FFPE
SCC12	uterine cervix	squamous cell carcinoma	none	n/a	n/a	USA	FFPE
SCC13	uterine cervix	squamous cell carcinoma	none	n/a	n/a	USA	FFPE
SCC14	uterine cervix	squamous cell carcinoma	none	n/a	n/a	USA	FFPE
SCC15	uterine cervix	squamous cell carcinoma	none	n/a	n/a	USA	FFPE
SCC16	uterine cervix	squamous cell carcinoma	none	n/a	n/a	USA	FFPE
SCC17	uterine cervix	squamous cell carcinoma	none	n/a	n/a	USA	FFPE
SCC18	uterine cervix	squamous cell carcinoma	none	n/a	n/a	USA	FFPE
SCC19	uterine cervix	squamous cell carcinoma	none	n/a	n/a	USA	FFPE
SCC20	uterine cervix	squamous cell carcinoma	none	n/a	n/a	USA	FFPE
SCC21	uterine cervix	squamous cell carcinoma	c.-124C>T	n/a	n/a	USA	FFPE
SCC22	uterine cervix	squamous cell carcinoma	none	n/a	n/a	USA	FFPE
SCC23	uterine cervix	squamous cell carcinoma	none	n/a	n/a	USA	FFPE
SCC24	uterine cervix	squamous cell carcinoma	none	n/a	n/a	USA	FFPE
SCC25	uterine cervix	squamous cell carcinoma	none	n/a	n/a	USA	FFPE
SCC26	uterine cervix	squamous cell carcinoma	none	n/a	n/a	USA	FFPE
SCC27	uterine cervix	squamous cell carcinoma	none	n/a	n/a	USA	FFPE
SCC28	uterine cervix	squamous cell carcinoma	none	n/a	n/a	USA	FFPE
SCC29	uterine cervix	squamous cell carcinoma	none	n/a	n/a	USA	FFPE
SCC30	uterine cervix	squamous cell carcinoma	none	n/a	n/a	USA	FFPE
SCC31	uterine cervix	squamous cell carcinoma	none	n/a	n/a	USA	FFPE
SCC32	uterine cervix	squamous cell carcinoma	none	n/a	n/a	USA	FFPE
SCC33	uterine cervix	squamous cell carcinoma	none	n/a	n/a	USA	FFPE
SCC34	uterine cervix	squamous cell carcinoma	none	n/a	n/a	USA	FFPE
SCC35	uterine cervix	squamous cell carcinoma	none	n/a	n/a	USA	FFPE
SCC36	uterine cervix	squamous cell carcinoma	none	n/a	n/a	USA	FFPE
SCC37	uterine cervix	squamous cell carcinoma	none	n/a	n/a	USA	FFPE
SCC38	uterine cervix	squamous cell carcinoma	none	n/a	n/a	USA	FFPE

SCC39	uterine cervix	squamous cell carcinoma	none	n/a	n/a	USA	FFPE
SCC40	uterine cervix	squamous cell carcinoma	none	n/a	n/a	USA	FFPE
SCC41	uterine cervix	squamous cell carcinoma	none	n/a	n/a	USA	FFPE
SCC42	uterine cervix	squamous cell carcinoma	none	n/a	n/a	USA	FFPE
SCC43	uterine cervix	squamous cell carcinoma	c.-124C>T	n/a	n/a	USA	FFPE
SCC44	uterine cervix	squamous cell carcinoma	none	n/a	n/a	USA	FFPE
SCC45	uterine cervix	squamous cell carcinoma	none	n/a	n/a	USA	FFPE
SCC46	uterine cervix	squamous cell carcinoma	none	n/a	n/a	USA	FFPE
SCC47	uterine cervix	squamous cell carcinoma	none	n/a	n/a	USA	FFPE
SCC48	uterine cervix	squamous cell carcinoma	none	n/a	n/a	USA	FFPE
SCC49	uterine cervix	squamous cell carcinoma	none	n/a	n/a	USA	FFPE
SCC50	uterine cervix	squamous cell carcinoma	none	n/a	n/a	USA	FFPE
SCC51	uterine cervix	squamous cell carcinoma	none	n/a	n/a	USA	FFPE
SCC52	uterine cervix	squamous cell carcinoma	none	n/a	n/a	USA	FFPE
SCC53	uterine cervix	squamous cell carcinoma	none	n/a	n/a	USA	FFPE
KEN1	uterine cervix	endocervical adenocarcinoma	none	n/a	n/a	Korea	FFPE
KEN2	uterine cervix	endocervical adenocarcinoma	none	n/a	n/a	Korea	FFPE
KEN3	uterine cervix	endocervical adenocarcinoma	none	n/a	n/a	Korea	FFPE
KEN4	uterine cervix	endocervical adenocarcinoma	none	n/a	n/a	Korea	FFPE
KEN5	uterine cervix	endocervical adenocarcinoma	none	n/a	n/a	Korea	FFPE
KEN6	uterine cervix	endocervical adenocarcinoma	none	n/a	n/a	Korea	FFPE
KEN7	uterine cervix	endocervical adenocarcinoma	none	n/a	n/a	Korea	FFPE
KEN8	uterine cervix	endocervical adenocarcinoma	none	n/a	n/a	Korea	FFPE
KEN9	uterine cervix	endocervical adenocarcinoma	none	n/a	n/a	Korea	FFPE
KEN10	uterine cervix	endocervical adenocarcinoma	none	n/a	n/a	Korea	FFPE
KEN11	uterine cervix	endocervical adenocarcinoma	none	n/a	n/a	Korea	FFPE
KEN12	uterine cervix	endocervical adenocarcinoma	none	n/a	n/a	Korea	FFPE
KEN13	uterine cervix	endocervical adenocarcinoma	none	n/a	n/a	Korea	FFPE
KEN14	uterine cervix	endocervical adenocarcinoma	none	n/a	n/a	Korea	FFPE
KEN15	uterine cervix	endocervical adenocarcinoma	none	n/a	n/a	Korea	FFPE
KEN16	uterine cervix	endocervical adenocarcinoma	none	n/a	n/a	Korea	FFPE
KEN17	uterine cervix	endocervical adenocarcinoma	none	n/a	n/a	Korea	FFPE
KEN18	uterine cervix	endocervical adenocarcinoma	none	n/a	n/a	Korea	FFPE
KEN19	uterine cervix	endocervical adenocarcinoma	none	n/a	n/a	Korea	FFPE
KEN20	uterine cervix	endocervical adenocarcinoma	none	n/a	n/a	Korea	FFPE
KEN21	uterine cervix	endocervical adenocarcinoma	none	n/a	n/a	Korea	FFPE
KEN22	uterine cervix	endocervical adenocarcinoma	none	n/a	n/a	Korea	FFPE
KEN23	uterine cervix	endocervical adenocarcinoma	none	n/a	n/a	Korea	FFPE
KEN24	uterine cervix	endocervical adenocarcinoma	none	n/a	n/a	Korea	FFPE
KEN25	uterine cervix	endocervical adenocarcinoma	none	n/a	n/a	Korea	FFPE

Bibliography

1. Tavassoli FA, Devilee P, editors. Pathology and genetics of tumours of the breast and female genital organs. IARCPress Lyon; 2003.

2. Kurman RJ, Ellenson LH, Ronnett BM, editors. Blaustein's Pathology of the Female Genital Tract. Springer; 2011.

3. American Cancer Society. Cancer Facts and Figures 2014. Atlanta; 2014.

4. Wartko P, Sherman ME, Yang HP, Felix AS, Brinton LA, Trabert B. Recent changes in endometrial cancer trends among menopausal-age U.S. women. 2013 Aug;37(4):374–7.

5. Siegel R, Ma J, Zou Z, Jemal A. Cancer statistics, 2014. CA Cancer J Clin. 2014 Jan;64(1):9–29.

6. Bokhman JV. Two pathogenetic types of endometrial carcinoma. Gynecol Oncol. 1983 Feb;15(1):10–7.

7. Hamilton CA, Cheung MK, Osann K, Chen L, Teng NN, Longacre TA, et al. Uterine papillary serous and clear cell carcinomas predict for poorer survival compared to grade 3 endometrioid corpus cancers. Br J Cancer. 2006 Mar 13;94(5):642–6.

8. de Lange T. Shelterin: the protein complex that shapes and safeguards human telomeres. Genes & Development. 2005 Sep 15;19(18):2100–10.

9. Deng Y, Chan SS, Chang S. Telomere dysfunction and tumour suppression: the senescence connection. Nat Rev Cancer. 2008 Jun;8(6):450–8.

10. Bailey SM. Telomeres, chromosome instability and cancer. Nucleic Acids Res. 2006 Apr 28;34(8):2408–17.

11. Artandi SE, DePinho RA. Telomeres and telomerase in cancer. Carcinogenesis. 2010 Jan 6;31(1):9–18.

12. Harley CB. Telomerase and cancer therapeutics. Nat Rev Cancer. 2008 Mar;8(3):167–79.

13. Pirker C, Holzmann K, Spiegl-Kreinecker S, Elbling L, Thallinger C, Pehamberger H, et al. Chromosomal imbalances in primary and metastatic melanomas: over-representation of essential telomerase genes. Melanoma Res. 2003 Oct;13(5):483–92.

14. Dalla-Favera R, Wu K-J, Grandori C, Amacker M, Simon-Vermot N, Polack A, et al. Direct activation of TERT transcription by c-MYC. Nat Genet. 1999 Feb

1;21(2):220–4.

15. Castelo-Branco P, Choufani S, Mack S, Gallagher D, Zhang C, Lipman T, et al. Methylation of the TERT promoter and risk stratification of childhood brain tumours: an integrative genomic and molecular study. Lancet Oncol. 2013 May;14(6):534–42.

16. Horn S, Figl A, Rachakonda PS, Fischer C, Sucker A, Gast A, et al. TERT Promoter Mutations in Familial and Sporadic Melanoma. Science. 2013;339(6122):959–61.

17. Huang FW, Hodis E, Xu MJ, Kryukov GV, Chin L, Garraway LA. Highly recurrent TERT promoter mutations in human melanoma. Science. 2013 Feb 22;339(6122):957–9.

18. Killela PJ, Reitman ZJ, Jiao Y, Bettegowda C, Agrawal N, Diaz LA, et al. TERT promoter mutations occur frequently in gliomas and a subset of tumors derived from cells with low rates of self-renewal. Proc Natl Acad Sci U S A. 2013 Apr 9;110(15):6021–6.

19. Liu X, Wu G, Shan Y, Hartmann C, Deimling von A, Xing M. Highly prevalent TERT promoter mutations in bladder cancer and glioblastoma. Cell Cycle. 2013 May 15;12(10):1637–8.

20. Vinagre J, Almeida A, Pópulo H, Batista R, Lyra J, Pinto V, et al. Frequency of TERT promoter mutations in human cancers. Nat Commun. 2013 Jul 26;4:2185.

21. Di Cristofano A, Ellenson LH. Endometrial Carcinoma. Annu Rev Pathol Mech Dis. Annual Reviews; 2007 Feb;2(1):57–85.

22. Guan B, Mao T-L, Panuganti PK, Kuhn E, Kurman RJ, Maeda D, et al. Mutation and loss of expression of ARID1A in uterine low-grade endometrioid carcinoma. Am J Surg Pathol. 2011 May;35(5):625–32.

23. Jones S, Wang T-L, Shih I-M, Mao T-L, Nakayama K, Roden R, et al. Frequent mutations of chromatin remodeling gene ARID1A in ovarian clear cell carcinoma. Science. 2010 Oct 8;330(6001):228–31.

24. Jones S, Wang T-L, Kurman RJ, Nakayama K, Velculescu VE, Vogelstein B, et al. Low-grade serous carcinomas of the ovary contain very few point mutations. J Pathol. 2011 Nov 21.

25. Li H, Durbin R. Fast and accurate short read alignment with Burrows-Wheeler transform. Bioinformatics. 2009 Jul 15;25(14):1754–60.

26. Edmonson MN, Zhang J, Yan C, Finney RP, Meerzaman DM, Buetow KH. Bambino: a variant detector and alignment viewer for next-generation sequencing

data in the SAM/BAM format. Bioinformatics. 2011 Mar 15;27(6):865–6.

27. Pruitt KD, Tatusova T, Klimke W, Maglott DR. NCBI Reference Sequences: current status, policy and new initiatives. Nucleic Acids Res. 2009 Jan;37(Database issue):D32–6.

28. Zhang J, Benavente CA, McEvoy J, Flores-Otero J, Ding L, Chen X, et al. A novel retinoblastoma therapy from genomic and epigenetic analyses. Nature. 2012 Jan 19;481(7381):329–34.

29. Zhang J, Ding L, Holmfeldt L, Wu G, Heatley SL, Payne-Turner D, et al. The genetic basis of early T-cell precursor acute lymphoblastic leukaemia. Nature. 2012 Jan 12;481(7380):157–63.

30. McLendon R, Friedman A, Bigner D, Van Meir EG, Brat DJ, M Mastrogianakis G, et al. Comprehensive genomic characterization defines human glioblastoma genes and core pathways. Nature. 2008 Sep 4;455(7216):1061–8.

31. Kuo KT, Mao TL, Chen X, Feng Y, Nakayama K, Wang Y, et al. DNA Copy Numbers Profiles in Affinity-Purified Ovarian Clear Cell Carcinoma. Clin Cancer Res. 2010 Mar 31;16(7):1997–2008.

32. Kuo KT, Guan B, Feng Y, Mao TL, Chen X, Jinawath N, et al. Analysis of DNA Copy Number Alterations in Ovarian Serous Tumors Identifies New Molecular Genetic Changes in Low-Grade and High-Grade Carcinomas. Cancer Res. 2009 Apr 30;69(9):4036–42.

33. Olshen AB, Venkatraman ES, Lucito R, Wigler M. Circular binary segmentation for the analysis of array-based DNA copy number data. Biostatistics. 2004 Oct;5(4):557–72.

34. Venkatraman ES, Olshen AB. A faster circular binary segmentation algorithm for the analysis of array CGH data. Bioinformatics. 2007 Mar 15;23(6):657–63.

35. Beroukhim R, Getz G, Nghiemphu L, Barretina J, Hsueh T, Linhart D, et al. Assessing the significance of chromosomal aberrations in cancer: methodology and application to glioma. Proc Natl Acad Sci U S A. 2007 Dec 11;104(50):20007–12.

36. Kuhn E, Kurman RJ, Vang R, Sehdev AS, Han G, Soslow R, et al. TP53 mutations in serous tubal intraepithelial carcinoma and concurrent pelvic high-grade serous carcinoma-evidence supporting the clonal relationship of the two lesions. J Pathol. 2011 Dec 23;226(3):421–6.

37. Cancer Genome Atlas Research Network. Integrated genomic analyses of ovarian carcinoma. Nature. 2011 Jun 30;474(7353):609–15.

38. Calhoun ES, Jones JB, Ashfaq R, Adsay V, Baker SJ, Valentine V, et al. BRAF and FBXW7 (CDC4, FBW7, AGO, SEL10) mutations in distinct subsets of pancreatic cancer: potential therapeutic targets. Am J Pathol. 2003 Oct;163(4):1255–60.

39. Samuels Y, Wang Z, Bardelli A, Silliman N, Ptak J, Szabo S, et al. High frequency of mutations of the PIK3CA gene in human cancers. Science. 2004 Apr 23;304(5670):554–4.

40. Fortier JM, Kornbluth J. NK lytic-associated molecule, involved in NK cytotoxic function, is an E3 ligase. J Immunol. 2006 Jun 1;176(11):6454–63.

41. Ambrose EC, Kornbluth J. Downregulation of uridine-cytidine kinase like-1 decreases proliferation and enhances tumor susceptibility to lysis by apoptotic agents and natural killer cells. Apoptosis. 2009 Oct;14(10):1227–36.

42. Kashuba E, Kashuba V, Sandalova T, Klein G, Szekely L. Epstein-Barr virus encoded nuclear protein EBNA-3 binds a novel human uridine kinase/uracil phosphoribosyltransferase. BMC Cell Biol. 2002 Aug 29;3:23.

43. Okabe H, Lee S-H, Phuchareon J, Albertson DG, McCormick F, Tetsu O. A critical role for FBXW8 and MAPK in cyclin D1 degradation and cancer cell proliferation. Jin D-Y, editor. PLoS ONE. 2006;1(1):e128.

44. Foster FM, Traer CJ, Abraham SM, Fry MJ. The phosphoinositide (PI) 3-kinase family. J Cell Sci. 2003 Aug 1;116(Pt 15):3037–40.

45. Pickart CM. Mechanisms underlying ubiquitination. Annu Rev Biochem. 2001;70(1):503–33.

46. Rajagopalan H, Nowak MA, Vogelstein B, Lengauer C. The significance of unstable chromosomes in colorectal cancer. Nat Rev Cancer. 2003 Sep;3(9):695–701.

47. Ambros RA, Sherman ME, Zahn CM, Bitterman P, Kurman RJ. Endometrial intraepithelial carcinoma: a distinctive lesion specifically associated with tumors displaying serous differentiation. Hum Pathol. 1995 Nov;26(11):1260–7.

48. Sherman ME, Bur ME, Kurman RJ. p53 in endometrial cancer and its putative precursors: evidence for diverse pathways of tumorigenesis. Hum Pathol. 1995 Nov;26(11):1268–74.

49. Tashiro H, Isacson C, Levine R, Kurman RJ, Cho KR, Hedrick L. p53 gene mutations are common in uterine serous carcinoma and occur early in their pathogenesis. Am J Pathol. 1997 Jan;150(1):177–85.

50. Baergen RN, Warren CD, Isacson C, Ellenson LH. Early uterine serous carcinoma:

clonal origin of extrauterine disease. Int J Gynecol Pathol. 2001 Jul;20(3):214–9.

51. Lax SF, Kendall B, Tashiro H, Slebos RJ, Hedrick L. The frequency of p53, K-ras mutations, and microsatellite instability differs in uterine endometrioid and serous carcinoma: evidence of distinct molecular genetic pathways. Cancer. 2000 Feb 15;88(4):814–24.

52. Kovalev S, Marchenko ND, Gugliotta BG, Chalas E, Chumas J, Moll UM. Loss of p53 function in uterine papillary serous carcinoma. Hum Pathol. 1998 Jun;29(6):613–9.

53. Hayes MP, Douglas W, Ellenson LH. Molecular alterations of EGFR and PIK3CA in uterine serous carcinoma. Gynecol Oncol. 2009 Jun;113(3):370–3.

54. Shih I-M, Wang T-L. Mutation of PPP2R1A: a new clue in unveiling the pathogenesis of uterine serous carcinoma. J Pathol. 2011 May;224(1):1–4.

55. Welcker M, Clurman BE. FBW7 ubiquitin ligase: a tumor suppressor at the crossroads of cell division, growth and differentiation. Nat Rev Cancer. 2008 Feb;8(2):83–93.

56. Onoyama I, Nakayama KI. Fbxw7 in cell cycle exit and stem cell maintenance: insight from gene-targeted mice. Cell Cycle. 2008 Nov 1;7(21):3307–13.

57. Sancho R, Jandke A, Davis H, Diefenbacher ME, Tomlinson I, Behrens A. F-box and WD repeat domain-containing 7 regulates intestinal cell lineage commitment and is a haploinsufficient tumor suppressor. Gastroenterology. 2010 Sep;139(3):929–41.

58. Onoyama I, Tsunematsu R, Matsumoto A, Kimura T, de Alborán IM, Nakayama K, et al. Conditional inactivation of Fbxw7 impairs cell-cycle exit during T cell differentiation and results in lymphomatogenesis. J Exp Med. 2007 Nov 26;204(12):2875–88.

59. Tan Y, Sangfelt O, Spruck C. The Fbxw7/hCdc4 tumor suppressor in human cancer. Cancer Lett. 2008 Nov 18;271(1):1–12.

60. Akhoondi S, Sun D, Lehr von der N, Apostolidou S, Klotz K, Maljukova A, et al. FBXW7/hCDC4 is a general tumor suppressor in human cancer. Cancer Res. 2007 Oct 1;67(19):9006–12.

61. Wertz IE, Kusam S, Lam C, Okamoto T, Sandoval W, Anderson DJ, et al. Sensitivity to antitubulin chemotherapeutics is regulated by MCL1 and FBW7. Nature. 2011 Mar 3;471(7336):110–4.

62. Tetzlaff MT, Yu W, Li M, Zhang P, Finegold M, Mahon K, et al. Defective cardiovascular development and elevated cyclin E and Notch proteins in mice

lacking the Fbw7 F-box protein. Proc Natl Acad Sci U S A. 2004 Mar 9;101(10):3338–45.

63. Tavassoli FA, Devilee P, editors. Tumors of the ovary and peritoneum- surface epithelial-stromal tumors. Pathology and genetics of tumours of the breast and female genital organs. IARCPress Lyon; 2003.

64. de Lange T. How telomeres solve the end-protection problem. Science. 2009 Nov 13;326(5955):948–52.

65. Prieur A, Peeper DS. Cellular senescence in vivo: a barrier to tumorigenesis. Curr Opin Cell Biol. 2008 Apr;20(2):150–5.

66. Heaphy CM, Subhawong AP, Hong S-M, Goggins MG, Montgomery EA, Gabrielson E, et al. Prevalence of the alternative lengthening of telomeres telomere maintenance mechanism in human cancer subtypes. Am J Pathol. 2011 Oct;179(4):1608–15.

67. Henson J, Neumann A, Yeager T. Alternative lengthening of telomeres in mammalian cells. Oncogene. 2002.

68. Cancer Genome Atlas Research Network, Kandoth C, Schultz N, Cherniack AD, Akbani R, Liu Y, et al. Integrated genomic characterization of endometrial carcinoma. Nature. 2013 May 2;497(7447):67–73.

69. Kuhn E, Wu R-C, Guan B, Wu G, Zhang J, Wang Y, et al. Identification of molecular pathway aberrations in uterine serous carcinoma by genome-wide analyses. J Natl Cancer Inst. 2012 Oct 3;104(19):1503–13.

70. Kuhn E, Meeker AK, Visvanathan K, Gross AL, Wang T-L, Kurman RJ, et al. Telomere length in different histologic types of ovarian carcinoma with emphasis on clear cell carcinoma. Mod Pathol. 2011 Aug;24(8):1139–45.

71. Maeda D, Mao T-L, Fukayama M, Nakagawa S, Yano T, Taketani Y, et al. Clinicopathological Significance of Loss of ARID1A Immunoreactivity in Ovarian Clear Cell Carcinoma. Int J Mol Sci. 2010;11(12):5120–8.

72. Ayhan A, Mao T-L, Seckin T, Wu C-H, Guan B, Ogawa H, et al. Loss of ARID1A expression is an early molecular event in tumor progression from ovarian endometriotic cyst to clear cell and endometrioid carcinoma. Int J Gynecol Cancer. 2012 Oct;22(8):1310–5.

73. Kuo K-T, Mao T-L, Jones S, Veras E, Ayhan A, Wang T-L, et al. Frequent activating mutations of PIK3CA in ovarian clear cell carcinoma. Am J Pathol. 2009 May;174(5):1597–601.

74. Viganó P, Somigliana E, Chiodo I, Abbiati A, Vercellini P. Molecular mechanisms

and biological plausibility underlying the malignant transformation of endometriosis: a critical analysis. Hum Reprod Update. 2006 Jan;12(1):77–89.

75. Wiegand KC, Shah SP, Al-Agha OM, Zhao Y, Tse K, Zeng T, et al. ARID1AMutations in Endometriosis-Associated Ovarian Carcinomas. N Engl J Med. 2010 Oct 14;363(16):1532–43.

76. Tan DSP, Kaye S. Ovarian clear cell adenocarcinoma: a continuing enigma. J Clin Pathol. 2007 Apr;60(4):355–60.

77. Tsuchiya A, Sakamoto M, Yasuda J, Chuma M, Ohta T, Ohki M, et al. Expression profiling in ovarian clear cell carcinoma: identification of hepatocyte nuclear factor-1 beta as a molecular marker and a possible molecular target for therapy of ovarian clear cell carcinoma. Am J Pathol. 2003 Dec;163(6):2503–12.

78. Sharrocks AD. The ETS-domain transcription factor family. Nat Rev Mol Cell Biol. 2001;2(11):827–37.

79. Seth A, Watson DK. ETS transcription factors and their emerging roles in human cancer. Eur J Cancer. 2005 Nov;41(16):2462–78.

80. Sato N, Tsunoda H, Nishida M, Morishita Y, Takimoto Y, Kubo T, et al. Loss of heterozygosity on 10q23.3 and mutation of the tumor suppressor gene PTEN in benign endometrial cyst of the ovary: possible sequence progression from benign endometrial cyst to endometrioid carcinoma and clear cell carcinoma of the ovary. Cancer Res. 2000 Dec 15;60(24):7052–6.

81. Yamamoto S, Tsuda H, Takano M, Tamai S, Matsubara O. Loss of ARID1A protein expression occurs as an early event in ovarian clear-cell carcinoma development and frequently coexists with PIK3CA mutations. Mod Pathol. 2011 Dec 9;25(4):615–24.

82. Yamamoto S, Tsuda H, Takano M, Iwaya K, Tamai S, Matsubara O. PIK3CA mutation is an early event in the development of endometriosis-associated ovarian clear cell adenocarcinoma. J Pathol. 2011 Oct;225(2):189–94.

83. Ishikawa F. Telomere Crisis, the Driving Force in Cancer Cell Evolution. Biochem Biophys Res Commun. 1997 Jan;230(1):1–6.

84. Campbell PJ. Telomeres and cancer: from crisis to stability to crisis to stability. Cell. 2012 Feb 17;148(4):633–5.

85. Singh AM, Reynolds D, Cliff T, Ohtsuka S, Mattheyses AL, Sun Y, et al. Signaling network crosstalk in human pluripotent cells: a Smad2/3-regulated switch that controls the balance between self-renewal and differentiation. Cell Stem Cell. 2012 Mar 2;10(3):312–26.

86. Dubrovska A, Kim S, Salamone RJ, Walker JR, Maira S-M, García-Echeverría C, et al. The role of PTEN/Akt/PI3K signaling in the maintenance and viability of prostate cancer stem-like cell populations. Proc Natl Acad Sci U S A. 2009 Jan 6;106(1):268–73.

87. Li H, Gao Q, Guo L, Lu SH. The PTEN/PI3K/Akt pathway regulates stem-like cells in primary esophageal carcinoma cells. Cancer Biol Ther. 2011.

88. Bleau A-M, Hambardzumyan D, Ozawa T, Fomchenko EI, Huse JT, Brennan CW, et al. PTEN/PI3K/Akt pathway regulates the side population phenotype and ABCG2 activity in glioma tumor stem-like cells. Cell Stem Cell. 2009 Mar 6;4(3):226–35.

89. Lin Y, Yang Y, Li W, Chen Q, Li J, Pan X, et al. Reciprocal regulation of Akt and Oct4 promotes the self-renewal and survival of embryonal carcinoma cells. Mol Cell. 2012 Nov 30;48(4):627–40.

90. Kang SS, Kwon T, Kwon DY, Do SI. Akt protein kinase enhances human telomerase activity through phosphorylation of telomerase reverse transcriptase subunit. J Biol Chem. 1999 May 7;274(19):13085–90.

91. Bellon M, Nicot C. Central role of PI3K in transcriptional activation of hTERT in HTLV-I-infected cells. Blood. 2008 Oct 1;112(7):2946–55.

92. Heeg S, Hirt N, Queisser A, Schmieg H, Thaler M, Kunert H, et al. EGFR overexpression induces activation of telomerase via PI3K/AKT-mediated phosphorylation and transcriptional regulation through Hif1-alpha in a cellular model of oral-esophageal carcinogenesis. Cancer Sci. 2011 Feb;102(2):351–60.

93. Yang K, Zheng D, Deng X, Bai L, Xu Y, Cong Y-S. Lysophosphatidic acid activates telomerase in ovarian cancer cells through hypoxia-inducible factor-1α and the PI3K pathway. J Cell Biochem. 2008 Dec 1;105(5):1194–201.

94. Hakin-Smith V, Jellinek DA, Levy D, Carroll T, Teo M, Timperley WR, et al. Alternative lengthening of telomeres and survival in patients with glioblastoma multiforme. Lancet. 2003 Mar 8;361(9360):836–8.

Curriculum Vitae

Ren-Chin Wu, MD, PhD candidate
Graduate Program in Pathobiology
Johns Hopkins University School of Medicine
Email: rwu11@jhmi.edu
Address: 1550 Orleans St, CRB-II, Room 376, Baltimore, MD 21231

EDUCATION AND TRAINING

Year	Degree	Institution	Discipline
1993-2000	M.D.	Chang Gung University	Medicine
2000-2005	Resident	Chang Gung Memorial Hospital	Pathology
2009-2014	Ph.D	Johns Hopkins University	Pathobiology

PROFESSIONAL EXPERIENCE

2000-2005 Resident Pathologist, Department of Pathology
Chang Gung Memorial Hospital, Taoyuan, Taiwan
2004-2005 Chief Resident, Department of Pathology
Chang Gung Memorial Hospital, Taoyuan, Taiwan
2005-2009 Attending Pathologist, Department of Pathology
Chang Gung Memorial Hospital, Taoyuan, Taiwan
2005-2009 Instructor, Department of Pathology
Chang Gung University, Taoyuan, Taiwan
2006-2009 Medical Director, Department of Clinical Pathology
Chang Gung Memorial Hospital, Taipei, Taiwan

Teaching Experience

Instructor of undergraduate courses
Chang Gung University, Taiwan
Laboratory medicine (2006 - 2009)
Problem based learning in medicine (2005 - 2009)
Pathology (2004 - 2009)
Pathology laboratory (2003 - 2009)
Clinical instructor
Chang Gung Memorial Hospital, Taoyuan, Taiwan
Training Residents in a clinical setting (2005 - 2009)
Teaching Interns and clerks in a clinical setting (2004 - 2009)

CERTIFICATION

2000 Licensed Medical Doctor, Taiwan
2004 Board certification in Anatomic Pathology, Taiwan
2005 Board certification in Clinical pathology, Taiwan

HONORS & AWARDS

Scholar-in-Training Award
American Association for Cancer Research
May 2013 (AACR Chromatin and Epigenetics in Cancer Special Conference)

Excellence in Translational Research Award
Johns Hopkins Pathology Young Investigator's Day
April 2014

PUBLICATIONS

1. Guan B, Suryo Rahmanto Y, **Wu RC**, Wang Y, Wang Z, Wang TL, Shih IM. Roles of deletion of Arid1a, a tumor suppressor, in mouse ovarian tumorigenesis. J Natl Cancer Inst. 2014 Jun;106(7).
2. Liu YC, Tu YL, **Wu RC**, Huang JL, Yao TC. Life-threatening pneumonitis complicating low-dose methotrexate treatment for juvenile idiopathic arthritis in a child. Pediatr Emerg Care. 2014 Jun;30(6):415-7.
3. **Wu RC**, Wang TL, Shih IM. The emerging roles of ARID1A in tumor suppression. Cancer Biol Ther. 2014 Jun;15(6):655-664
4. **Wu RC**, Ayhan A, Maeda D, Kim KR, Clarke BA, Shaw P, Chui MH, Rosen B, Shih IeM, Wang TL. Frequent somatic mutations of the telomerase reverse transcriptase promoter in ovarian clear cell carcinoma but not in other major types of gynecological malignancy. J Pathol. 2014 Mar;232(4):473-81.
5. Gao M, **Wu RC**, Herlinger AL, Yap K, Kim JW, Wang TL, Shih IeM. Identification of the NAC1-regulated genes in ovarian cancer. Am J Pathol. 2014 Jan;184(1):133-40.
6. Yap KL, Sysa-Shah P, Bolon B, **Wu RC**, Gao M, Herlinger AL, Wang F, Faiola F, Huso D, Gabrielson K, Wang TL, Wang J, Shih IeM. Loss of NAC1 Expression Is Associated with Defective Bony Patterning in the Murine Vertebral Axis. PLoS One. 2013 Jul 26;8(7):e69099.
7. Allo G, Bernardini MQ, **Wu RC**, Shih IM, Kalloger S, Pollett A, Gilks CB, Clarke BA. ARID1A loss correlates with mismatch repair deficiency and intact p53 expression in high-grade endometrial carcinomas. Mod Pathol. 2014 Feb;27(2):255-61.
8. Wallace CG, Yen CH, Yang HC, Lin CY, **Wu RC**, Huang WC, Lin JY, Wei FC. Vascularized composite allograft rejection is delayed by intrajejunal treatment with donor splenocytes without concomitant immunosuppressants. Clin Dev Immunol. 2012;2012:704063.
9. Cope L, **Wu RC**, Shih IeM, Wang TL. High level of chromosomal aberration in ovarian cancer genome correlates with poor clinical outcome. Gynecol Oncol.

2013 Mar;128(3):500-5.

10. Kuhn E, **Wu RC***, Guan B, Wu G, Zhang J, Wang Y, Song L, Yuan X, Wei L, Roden RB, Kuo KT, Nakayama K, Clarke B, Shaw P, Olvera N, Kurman RJ, Levine DA, Wang TL, Shih IeM. Identification of molecular pathway aberrations in uterine serous carcinoma by genome-wide analyses. J Natl Cancer Inst. 2012 Oct;104(19):1503-13. **(*co-first author)**.
11. Thiaville MM, Stoeck A, Chen L, **Wu RC**, Magnani L, Oidtman J, Shih IeM, Lupien M, Wang TL. Identification of PBX1 target genes in cancer cells by global mapping of PBX1 binding sites. PLoS One. 2012;7(5):e36054.
12. Yeh CY, Chiang JM, Hsieh PS, Tsai WS, Tang R, Changchien CR, Chen JS, Wang JY, **Wu RC**, Hung HY. Immunohistochemical study of vascular endothelial growth factor (VEGF) and matrilysin (MMP-7) in T1 adenocarcinoma of the colon and rectum to predict lymph node metastases or distant metastases. Hepatogastroenterology. 2011 Nov-Dec;58(112):1943-6.
13. Liu KS, Liu SJ, Chen HY, Huang YK, Peng YJ, **Wu RC**, Ueng SW. Steady antibiotic release from biodegradable beads in the pleural cavity: an in vitro and in vivo study. Chest. 2012 May;141(5):1197-202.
14. Chang HC, Huang SC, **Wu RC**, Yu MC. Duodenal duplication cyst: a rare cause of geriatric gastrointestinal bleeding. J Chin Med Assoc. 2011 May;74(5):233-6.
15. Chen TH, Lin CJ, **Wu RC**, Ho YP, Hsu CM, Lin WP, Tseng YP, Chen CH, Chiu CT. The application of miniprobe ultrasonography in the diagnosis of colorectal subepithelial lesions. Chang Gung Med J. 2010 Jul-Aug;33(4):380-8.
16. Liu SJ, Kau YC, Chou CY, Chen JK, **Wu RC**, Yeh WL. Electrospun PLGA/collagen nanofibrous membrane as early-stage wound dressing. J Membr Sci. 2010 June;355(1-2):53-9.
17. Lee CW, **Wu RC**, Hsu JT, Yeh CN, Yeh TS, Hwang TL, Jan YY, Chen MF. Isolated pancreatic metastasis from rectal cancer: a case report and review of literature. World J Surg Oncol. 2010 Apr 7;8:26.
18. Chen JS, Hsieh PS, Chiang JM, Yeh CY, Tsai WS, Tang R, Changchien CR, **Wu RC**. Clinical outcome of signet ring cell carcinoma and mucinous adenocarcinoma of the colon. Chang Gung Med J. 2010 Jan-Feb;33(1):51-7.
19. Kuo CJ, Lin CH, Liu NJ, **Wu RC**, Tang JH, Cheng CL. Frequency and risk factors for Barrett's esophagus in Taiwanese patients: a prospective study in a tertiary referral center. Dig Dis Sci. 2010 May;55(5):1337-43.
20. Tsou YK, **Wu RC**, Hung CF, Lee CS. Intrahepatic sarcomatoid cholangiocarcinoma: clinical analysis of seven cases during a 15-year period. Chang Gung Med J. 2008 Nov-Dec;31(6):599-605.
21. Hsu JT, Chen HM, **Wu RC**, Yeh CN, Yeh TS, Hwang TL, Jan YY, Chen MF. Clinicopathologic features and outcomes following surgery for pancreatic adenosquamous carcinoma. World J Surg Oncol. 2008 Sep 3;6:95.

22. Tsou YK, Liu NJ, **Wu RC**, Lee CS, Tang JH, Hung CF, Jan YY. Endoscopic retrograde cholangiography in the diagnosis and treatment of mucobilia. Scand J Gastroenterol. 2008;43(9):1137-44.

23. Wang AC, **Wu RC**, Lin CT, Chen MC. A microbiological and immunohistochemical analysis of periurethral and vaginal tissue in women with de novo urge symptoms after mid-urethral sling procedures--a prospective case-controlled study. Int Urogynecol J Pelvic Floor Dysfunct. 2008 Aug;19(8):1145-50.

24. **Wu RC**, Hsieh YY, Chang YC, Kuo TT. Cellular neurothekeoma with melanocytosis. J Cutan Pathol. 2008 Feb;35(2):241-5

25. Huang SF, **Wu RC**, Chang JT, Chan SC, Liao CT, Chen IH, Yeh CN. Intractable bleeding from solitary mandibular metastasis of hepatocellular carcinoma. World J Gastroenterol. 2007 Sep 7;13(33):4526-8.

26. Liu EH, Chen MF, Yeh TS, Ho YP, **Wu RC**, Chen TC, Jan YY, Pan TL. A useful model to audit liver resolution from cirrhosis in rats using functional proteomics. J Surg Res. 2007 Apr;138(2):214-23.

27. Shen SC, Wu CC, Ng KF, **Wu RC**, Chen HM, Chen TC. Follicular dendritic cell sarcoma mimicking giant cell carcinoma of the pancreas. Pathol Int. 2006 Aug;56(8):466-70.